Optimisation of ExoCounter Technology for use in Cerebrospinal Fluid and Investigation of Placenta-Derived Exosomes Within Cerebrospinal Fluid.

Report submitted for M.Sc. by Research (October 2023)

Bryony Davies

Wolfson College

Nuffield Department of Women's and Reproductive Health

Supervised by Professor Manu Vatish and Dr Wei Zhang

Word count: 27,771

Thank you so much to Professor Manu Vatish, Dr Wei Zhang, Emily Mazey, Dr Gabe Jones, Emily Hyde, Dr Will Cooke, Dr Sarah Hutchinson, Michella Ma, Dr Faheem Seedat, Dr Catarina Palma dos Reis, Dr Angga Lokeswara, Qian Chen, Dr Neva Kandzija, Dr Prassana Logenthiran, Morganne Wilbourne, Dr Maryam Rahbar, Dr Shuhan Jiang, Magdalena Bachmann, and my friends at Wolfson College: Aneesh, Atticus, Elias, Oscar, Johannes, Anwen, Cris, and Jake.

Abstract

Pregnancy is associated with neurological changes and increased risk of certain neurological pathologies. The mechanisms and causes of these changes are not entirely clear. Placenta-derived exosomes are small vesicles released from the placenta into maternal circulation. Research suggests that these exosomes are bioactive and can affect cells and tissues they encounter. There is evidence that exosomes of non-placental origin can cross the blood-brain barrier and be taken up by central nervous tissues, and that placenta-derived exosomes may increase the permeability of the blood-brain barrier. At the time of writing, no human studies have addressed the possibility that placenta-derived exosomes may cross the blood-brain barrier and affect neurological tissues. This project used a novel technology for exosome quantification, the ExoCounter assay, to analyse placenta-derived exosomes in matched cerebrospinal fluid and plasma samples from normotensive, preeclamptic and eclamptic pregnant women. This project did not find evidence that placenta-derived exosomes are present in cerebrospinal fluid. No difference was seen in plasma or cerebrospinal fluid counts between the three clinical groups, but this was affected by small samples sizes and unmatched gestational age between groups. In addition to work on the samples, this project assessed performance of the ExoCounter assay, and found high linearity, high repeatability, and dependence of the assay on intact exosome membranes. The impact of human/pipetting error and human anti-mouse antibodies was assessed, with no evidence found of interference by either factor.

Table of Contents

List of Figures

List of Tables

List of Abbreviations

ANOVA = Analysis of variance

BBB = Blood brain barrier

BC = Before Christ

BCA = Bicinchoninic assay

BMI = Body mass index

CNS = Central nervous system

CP = Choroid plexus

CSF = Cerebrospinal fluid

d.p. = Decimal points

DLS = Dynamic light scattering

DNA = Deoxyribonucleic acid

ELISA = Enzyme-linked immunosorbent assay

EOPE(T) = Early onset preeclampsia

ESCRT = Endosomal sorting complexes required for transport

FGR = Foetal growth restriction

HAMA = Human anti-mouse antibody

HELLP = Haemolysis, elevated liver enzymes, low platelets

HIV = Human immunodeficiency virus

HUVEC = Human umbilical vein endothelial cell

ICH = The International Council for Harmonisation of Technical Requirements for Registration of Pharmaceuticals for Human Use

ICU = Intensive care unit

IFNγ = Interferon gamma

IL10 = Interleukin 10

IUGR = Intrauterine growth restriction

LOPE(T) = Late onset preeclampsia

LPS = Lipopolysaccharide

MHC = Major histocompatibility complex

mmHg = Millimetres of mercury

(m, μ, n) + (m, l, g) = (milli, micro, nano) + (metres, litres, grams)

MRI = Magnetic resonance imaging

NDOG2 = Nuffield Department of Obstetrics and Gynaecology 2

NK = Natural killer

NTA = Nanoparticle tracking analysis

OCCU = Obstetric critical care unit

PBMC = Peripheral blood mononuclear cells

(f)PBS(T) = (Filtered) phosphate-buffered saline (with Tween-20)

PCR = Polymerase chain reaction

PD-L1 = Programmed cell death ligand 1

PlGF = Placental growth factor

pH = Potential of hydrogen

PLAP = Placental alkaline phosphatase

pMSC = Placental mesenchymal stromal cells

(m, mi)RNA = (messenger, micro) ribonucleic acid

ROUT = robust regression followed by outlier identification

Rpm = Revolutions per minute

s.f. = Significant figures

SEM = Scanning electron microscopy

sFlt1 = Soluble Fms-like tyrosine kinase-1

TBS(T) = Tris-buffered saline (with Tween20)

TEER = Transendothelial electrical resistance

TEM = Transmission electron microscopy

TGFβ = Transforming growth factor β

TNF(α) = Tumour necrosis factor (α)

UK = United Kingdom

VEGF = Vascular endothelial growth factor

Chapter 1 – Introduction and Literature Review

Introduction

The neurological system is highly involved in pregnancy and can drive pathology. Causes and mechanisms of healthy and pathological changes are not entirely clear. Research has revealed biological activities of exosomes, small membrane-bound vesicles released from cells, in many contexts. This includes exosomes derived from the placenta, which have established in vitro effects on multiple biological pathways, and have been implicated in diseases of pregnancy.

At the time of writing, there are no published studies investigating the possibility that placenta-derived exosomes reach and affect the central nervous system in humans. This project aims to fill this gap, using a novel technology for exosome quantification. In brief, this project will characterise and optimise the performance of the ExoCounter assay, particularly for use in cerebrospinal fluid. Placenta-derived exosomes in matched plasma and cerebrospinal fluid samples will then be analysed by ExoCounter.

To provide more context for the experimental work of this project, the introductory section will give a summary of research in relevant topics. This will include an overview of neurological changes in pregnancy, preeclampsia and eclampsia, and exosomes, particularly placenta-derived exosomes, and methods of exosome quantification.

The brain and its changes in pregnancy

Part of the rationale for this project stemmed from observations of neurological changes in pregnancy. This section will outline research showing pregnancy-related changes in the brain and its functions.

1.1 Brain structure and cellular composition

To understand some of the later-discussed brain changes associated with pregnancy, it is useful to have an overview of the brain. The brain is a complex organ responsible for regulation of internal physiological processes, interaction with the external world, and complex cognitive functions that give us consciousness and awareness. The brain is enclosed within the skull, but separated by membranous coverings called the meninges, which provide protection and support. The three membranes (from outermost inwards) are the dura mater, arachnoid mater, and pia mater[1].

The brain is divided into a right and left hemisphere, joined by a band of nerve fibres (the corpus callosum). Each hemisphere is divided into lobes, which are associated with specific functions.

- The frontal lobe, at the front of the head, is associated with complex human skills[2], including abstract reasoning, voluntary movement, personality, and executive function (high-order processes that regulate and organise behaviour towards a particular goal[3]). The frontal lobe contains the prefrontal cortex, which is involved in executive functions, memory, language, and intelligence[4].
- The parietal lobe, in a central position, integrates sensory information, including spatial relationships, proprioception, object identification, and information on touch, taste, and temperature. The parietal lobe may contribute to language processing and production, but this is disputed[5].
- The occipital lobe, at the back of the brain, is the visual processing centre. Functions include colour determination, visuospatial information processing, depth and distance perception, and visual memory[6].

- The temporal lobe, located at ear level, is multifunctional. It has roles in speech perception and production, hearing, episodic memory, social behaviour, and visual processing (via the temporo-occipital junction). The temporal lobe contains the hippocampus and amygdala. The hippocampus is important for memory and the amygdala is involved in the reward system and motivation, and emotional processing and responses, particularly those relating to fear[7].

The four lobes form the cerebrum. The remaining brain structures include the hypothalamus, pituitary gland, cerebellum, and brainstem. The pituitary gland and hypothalamus have central roles in endocrine regulation, and oversee functions including sleep, sexual behaviour, and body temperature[8]. The cerebellum is associated with balance and motor control, with possible involvement in cognitive, emotional, and social processes[9]. The brainstem connects to the spinal cord; it acts as a 'relay station'[10], communicating between body parts and the brain. Separate structures in the brainstem – the midbrain, pons, and medulla – have distinct functions. The midbrain is important for auditory and visual information. The pons coordinates eye and facial movement, balance, and hearing. The medulla controls breathing, heart rhythms, blood gas levels, blood pressure and reflexive activities[10–12].

At the centre of the brain, there are four interconnected cerebrospinal fluid (CSF)-filled cavities forming the ventricular system. The ventricles are connected by channels called 'foramina' (sing. foramen). The ventricular system is continuous with the CSF-filled central canal of the spinal cord. The ventricular system and central canal are lined with specialised neuroepithelium, called ependyma. This comprises a continuous monolayer of ependymal cells and serves as a 'CSF-brain' barrier. As well as its role in circulation of CSF, the ventricular system protects the brain by providing buoyancy and buffering against physical trauma[13].

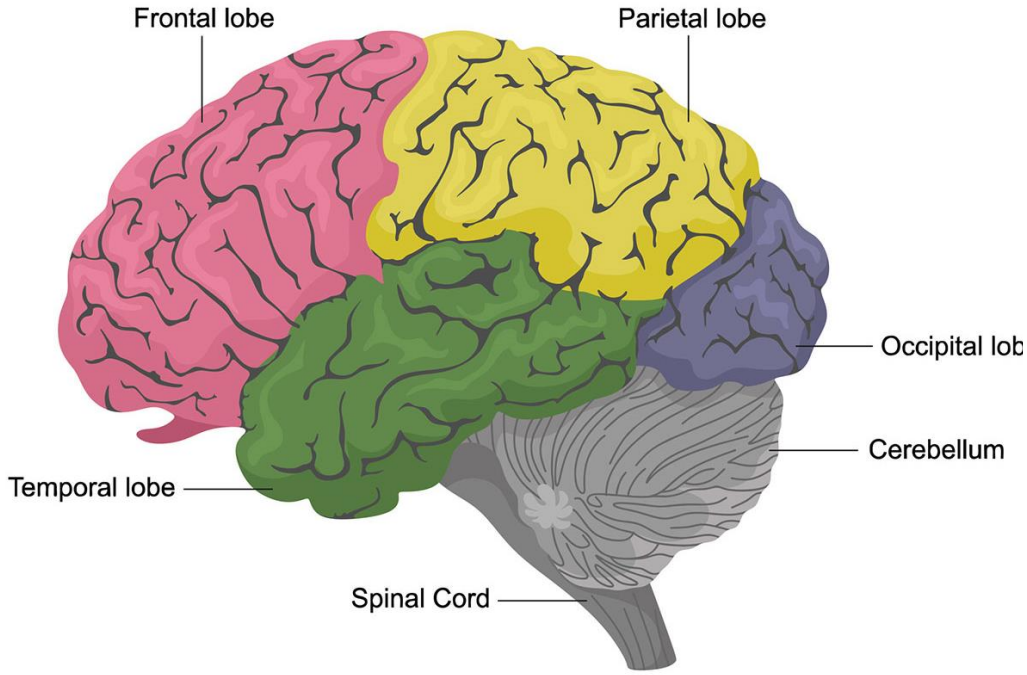

Figure 1: Sagittal diagram of brain showing the four lobes, spinal cord, and cerebellum. This diagram is taken from Johns Hopkins Medicine's web page 'Brain Anatomy and How the Brain Works'[14].

Cells in the brain are divided into two main categories: neurons and glial cells. Neurons are responsible for transmission of information via electrochemical signals. The typical model of a neuron is composed of a cell body, an axon, which transmits signals, and dendrites, which receive afferent signals via synapses with other neurons[15], however structure can vary between neuron types[16]. Neurons form two types of 'matter' within the brain: grey and white. Grey matter is formed mainly by neuron cell bodies, dendrites, unmyelinated axons, and axon terminals. White matter mostly consists of long-range

myelinated axons, used for global communication, and contains few cell bodies[17]. Although simplified, grey matter can be thought of as the place where processing is completed, and white matter communicating between grey matter areas and the rest of the body[17].

Glial cells encompass any non-neuronal cells that provide support, nutrition, homeostatic functions etc[10]. Astrocytes are the most abundant glial cells, occupying ~25% of the total brain volume[18]. During development, astrocytes guide migration of developing axons[19] and are likely involved in formation and function of synapses[20]. Astrocytes regulate blood flow within the central nervous system (CNS) according to synaptic activity[21], maintain interstitial fluid pH and ion concentrations, neurotransmitter homeostasis, alter neuronal excitability[22], and contribute to BBB function[23,24]. Oligodendrocytes are myelin-producing glial cells needed for insulation of axons and efficient conduction of signals[25]. Microglia are the primary resident immune cells of the brain[26], mirroring tissue-resident macrophages, and support cognitive processes and homeostasis. Mice depleted of microglia show deficits in learning tasks[27,28], demonstrating extra-immune functions.

1.2 Cerebrospinal fluid

CSF is a clear fluid occupying the ventricular system, perivascular space (space surrounding small blood vessels in the brain[29]), and space between the arachnoid mater and pia mater. It consists of water, proteins in low concentrations, ions, neurotransmitters, and glucose. Human adults have ~150mL of CSF which is renewed 2-3 times a day[30]. CSF provides hydromechanical protection by acting as a shock absorber and enabling buoyancy. It provides and circulates nutrients and removes waste products which interfere with neuronal function[31].

The traditional hypothesis of CSF production is continual CSF production by the choroid plexus (CP), a monolayer of specialised epithelial cells within a network of capillaries in the ventricles of the brain[30,32]. The epithelial cells in the CP are connected by tight junctions, restricting paracellular diffusion of substances, whereas underlying capillaries are leaky. A plasma ultrafiltrate passes from the capillaries to the epithelial cells, where compounds in the fluid undergo passive pressure-driven filtration through the basolateral membrane. At the apical surface, compounds are actively secreted into the ventricles to form CSF. Water transport between the blood and ventricular system occurs via aquaporin-1 channels[33]. Under this model, CSF is considered a highly regulated ultrafiltrate of the plasma, and therefore has different concentrations of substances compared to plasma (see table below).

A second hypothesis of CSF production opposes the traditional model. There are various lines of clinical and animal-based evidence that suggest that the CP is not the only site for CSF production, and that other sites can produce a comparable fluid[33–37]. As an alternative to sole choroid plexus-based production, this model suggests that CSF is permanently produced along the entire CSF system by filtration through cerebral capillary walls into the interstitial fluid of surrounding brain tissue, and that fluid is simultaneously reabsorbed into vessels of lower hydrostatic pressure, leading to a continuous exchange between plasma and interstitial fluid/CSF [34,38]. It is typically considered that both the choroid plexus and extrachoroidal sites contribute to CSF production, but the main site of production remains contested.

	CSF	Blood plasma
pH	7.28-7.33[39]	7.35-7.45(arterial)[40]

Osmolality (mOsm/Kg)	283-296[41]	275-295[42]
Protein content (mg/ml)	0.16-0.38[43,44]	63-85[43,44]
Sugar content (mg/ml)	0.45-0.8[43,44]	0.8-1.2[43,44]
K+ (mmol/kg)	2.86[44,45]	4.63[44,45]
Ca^{2+} (mmol/kg)	1.14[44,45]	2.35[44,45]
Na+ (mmol/kg)	147[44,45]	150[44,45]
Mg^{2+} (mmol/kg)	1.1[44,45]	0.8[44,45]
Cl^- (mmol/kg)	113[44,45]	99[44,45]
HCO_3^- (mmol/kg)	23.3[44,45]	26.8[44,45]
Inorganic phosphate (mg/100ml)	3.4[44,45]	4.7[44,45]

Table 1: Comparing plasma and CSF constituents. Exact values for concentration of ions and other substances varies between papers; these values are largely taken from Hladky and Barrand (2014).

Being near neurological tissues, the CSF proteome is an indicator of neurological health with relevance in many neurological diseases e.g. Alzheimer's and Huntington's disease[46]. As a result, it has been desirable to characterise both normal and pathological proteomes of the CSF, to identify biomarkers or clues about underlying pathology[47].

Several studies investigate the protein composition of CSF, using various methodologies[46–53]. In studies which drew comparisons with the plasma proteome, many proteins were seen within the CSF dataset that were not found in the plasma dataset, and vice versa, demonstrating the selective nature of protein transfer between the two fluids, and suggesting contribution from neurological tissues[53]. The main fraction of proteins in

the CSF are blood-derived, for example albumin which constitutes ~35-80% of total CSF protein, and immunoglobulins, which are present in low concentrations. Approximately 20% of CSF proteins are brain-derived, but not necessarily brain-specific[50,51]. Studies find significant inter-individual differences, suggesting a high degree of variation in the population[48,51]. The CSF proteome is also altered by pregnancy, with an enrichment of proteins associated with pregnancy in other tissues e.g. prolactin[48].

1.3 The Blood-Brain Barrier

The blood-brain barrier (BBB) is a selective interface within CNS vasculature that separates blood from the brain. It has an important role in maintaining the environment around the CNS and preventing entry of pathogens, toxins, non-neurological immune cells. Furthermore, the BBB protects against ion dysregulation[54]. To carry out this function, CNS vessels have properties that allow tight regulation of substances moving between blood and the CNS. The BBB is composed primarily of endothelial cells, glial cells and pericytes. The endothelial cells of the BBB have properties that distinguish them from non-BBB endothelial cells, and support their role in the BBB. These properties include high expression of tight junctions between adjacent cells to limit paracellular movement of solutes, and lower rates of transcytosis to reduce vesicle-mediated transcellular movement of compounds[45,55].

Unregulated diffusion of substances across the cell membrane is restricted by the presence of efflux transporters for lipophilic molecules. Additionally, CNS endothelial cells have nutrient transporters that enable entry of nutrients into the CNS and removal of waste products into the bloodstream. CNS endothelial cells have low expression of leukocyte adhesion molecules, to limit immune cells entering the CNS[56].

Pericytes cover the endothelial walls of the microvasculature and are embedded in the vascular basement membrane. The microvasculature of the CNS has the highest known pericyte coverage of any tissue. Evidence in mice suggests that pericyte deficiency increases BBB permeability to water and tracer compounds via endothelial transcytosis, potentially by altering the protein expression profile of associated endothelial cells[57]. The basement membrane also has a role in BBB permeability by connecting cells, regulating intercellular communication, and providing an additional barrier[55].

Astrocytes are the primary glial cell associated with the BBB. Astrocytes are important in inducing the CNS-specific properties of endothelial cells and regulate water homeostasis[56,58–60]. Furthermore, astrocytes regulate contraction and dilation of vascular smooth muscle cells and pericytes surrounding arterioles and capillaries in response to neuronal activity. Astrocyte-derived factors may also influence BBB function[61]. Microglia may also be important in BBB integrity and tight junction expression[56,62].

1.4 Structural Changes Associated with Pregnancy

It is well documented that pregnancy is associated with structural changes in the brain. 20th century neurological studies using autopsies of deceased pregnant women identified enlargement of the pituitary gland[63]; these findings are now supported my magnetic resonance imaging (MRI) images[64]. A 2022 review of neuroimaging studies identified other changes observed in pregnancy, including decreased total brain size, decreased cortical thickness, increased sulcal width, decreased sulcal depth and length, decreased grey matter volume, and increased ventricle size. These changes are suggestive of neurological tissue loss during pregnancy[65].

Subsequent studies confirmed grey matter volume losses in consistent brain regions, with the largest functional overlap seen in areas associated with theory of mind tasks, rest, and higher-level cognitive tasks[66]. Another study associated grey matter reductions with areas involved in social cognition[67]. Areas that have been linked to pregnancy-related tissue changes include the amygdala, temporal lobe, hippocampus, hypothalamus, and medial prefrontal region, but there is variation between studies, and this is not an exhaustive list[68]. White matter microstructure, however, seems unaffected by pregnancy[66]. Connectome analyses suggest that structural changes are accompanied by changes in the functional brain network[69]. Murine studies support the notion that structural and functional changes are translated into altered behaviour, particularly the onset of maternal behaviours[70,71]. The next section will expand on behavioural changes further.

1.5 Behavioural and Cognitive Changes in Pregnancy

Behavioural and cognitive changes during pregnancy are consistently observed in human studies and animal models. A review of behavioural changes identified mood, sleep, diet and sexual behaviour as areas that are all potentially affected by pregnancy. Reported cognitive deficits include poor concentration, memory issues, and executive impairment. Importantly, some behavioural changes may be the result of lifestyle changes during pregnancy, such as smoking cessation, eating a healthier diet and prioritising sleep, but this is unlikely to account for all behavioural changes. This section will briefly outline important findings related to these topics.

Increased caloric intake is often observed in pregnant women to meet the needs of a growing foetus[72]. There is evidence that this is partly achieved by decreasing the sensitivity of the hypothalamus to leptin (an appetite-suppressing hormone)[73,74]. Increased appetite may be affected by nausea and morning sickness, which are common

experiences in pregnancy[75]. Another diet-related change that is occasionally observed is pica (consumption of non-food items)[72]. Causes of pica are not entirely clear, but theories suggest it may function as a coping mechanism or be due to mineral deficiencies[76]. In one study, 32% of pregnant women with pica stated reduced stress and anxiety as their reason, 16% to satisfy cravings and 4% to reduce nausea. 40% of women could not give a reason[77].

Research suggests that rates of depression and anxiety are significantly increased in pregnant women compared to nonpregnant women[78]. Somewhat conversely, hormonal responses to stress are suppressed in pregnancy and lactation, possibly to prevent detrimental exposure of the foetus to glucocorticoids. This may be mediated by increased activity of neurological pathways that inhibit the hypothalamus-pituitary-adrenal axis, which regulates stress responses[74,79]. Self-reports suggest that pregnant women experience emotions at extreme ends of the scale more frequently (euphoria, rage etc.) and show increased mood instability, manifesting in 'mood swings'[80]. Irritability and anger were also reported by 13.9% and 18.8% of women respectively[80]. Overall, there is a lot of variation in mood changes experienced in pregnancy, which is likely influenced by environmental factors, preexisting emotional health and different life experiences.

Sexual behaviours are often altered in pregnancy, with reported changes in frequency of sexual activity, arousal, and satisfaction. These changes may also relate to changing body image, discomfort, and anxiety about pregnancy[81,82]. Pregnancy is also associated with sensory changes, particularly related to taste, with more than 90% of women reporting taste changes in one study[83,84]. Finally, sleep is affected during pregnancy. A meta-analysis of studies on sleep quality in pregnancy found that 46% of women report poor sleep, and sleep quality worsens from the second to third trimester[85]. Again, this may also relate to discomfort and anxiety about impending parenthood.

Moving on to cognitive changes, a meta-analysis by Davies et al found that general cognitive function was worse in pregnant than non-pregnant women, but only in the third trimester[86]. General cognitive functioning was defined to include memory, attention, executive functions, verbal and visuospatial abilities, and processing speed. A small number of individual studies also found changes in the first and second trimester[86,87]. Interestingly, one study found that women pregnant with boys outperform women pregnant with girls[87].

Memory changes are frequently self-reported in pregnancy. This includes 'memory fog', a chronic feeling of memory impairment or memory fatigue, including a general sense of confusion and disorientation and reduced ability to focus[80]. Pregnant women also report short term memory lapses occurring intermittently and noticeably[80]. Some studies report objective differences in memory performance between pregnant and nonpregnant women[88–90],while others find no effect[91,92], and some show mixed results[93]. One meta-analysis suggested that pregnancy has a negative effect on subjective memory, free recall, working memory, prospective memory, and a positive effect on recognition memory tasks[94]. It is important to note that performance on memory tests may not accurately reflect real-life memory function, and studies focus on different points during pregnancy, which may explain varied effects. For clarity, some terms are explained in the table below.

Memory-related terms	*Meaning in psychology*
Free recall	A common memory task in which participants study a list of items and then attempt to remember the items in any order[95].
Working memory	A form of short-term memory that retains information for a very brief period to be used in cognitive tasks[96,97].
Prospective memory	A form of memory that focuses on the intention to act in the future aka. remembering to complete a planned action[98].
Recognition tasks	Tasks which test recognition memory: the ability to recognise objects, people and events that were encountered previously[99,100].

Table 2: Explaining memory terminology

1.6 Long-Term Neurological Changes

Human and animal studies[101,102] suggest that structural changes associated with pregnancy are not fully reversed in the postpartum period and can be identified long after birth. Using high-resolution brain scans, Hoekzema et al identified a consistent pattern of cortical grey matter reductions in recently postpartum women that was not observed in nulliparous controls. This reduction was still observed two years after birth, except partial recovery of a left hippocampal cluster. Grey matter changes were so consistent that a classification algorithm could accurately distinguish between parous and nulliparous women based on grey matter[67]. However, in a second study by Hoekzema et al, partial

restoration of grey matter was observed between early postpartum (~100 days) and later postpartum (~400 days), suggesting there is some rejuvenation effect[66].

Longer term studies also suggest eventual recovery from grey matter reductions. The Rotterdam prospective cohort study has investigated multiple health parameters in ~1800 participants since 1990. Brain MRI imaging was added to the study in 2005 and >12,000 scans have been processed (as of January 2022), of which 2392 are parous women. The time difference between first birth and first MRI scan was roughly 30-40 years. This data found an association between increased global grey matter volume and previous pregnancy; this association persists after adjustment for relevant parameters[103]. This may suggest that there is long term correction or even overcorrection for changes in the peri- and postpartum period.

Notably, there is variation in postpartum findings relating to grey matter[104], and this variation is maintained even in studies many years after birth, as will be described later. Small sample sizes, different time points for measurement and different imaging and analysis techniques may contribute to differing results, or it may reflect a true variation in the ability of female brains to 'bounce back' post-pregnancy. The extent of recovery after pregnancy may be affected by external factors: evidence from rodents suggests that stress exposure affects postpartum brain volume[105].

Overall, evidence is rather limited regarding long-term brain changes due to pregnancy. There is a more research done on animal models, which have limited use when extrapolating to humans[106]. It is difficult to separate the effects that raising a child has on the brain from those associated with pregnancy. A comparative study between adoptive and biological mothers may address this issue. However, the available evidence does

suggest that there are observable changes which persist into the postpartum period and beyond.

1.7 The Blood-Brain Barrier in Pregnancy

During pregnancy, the BBB must adapt to physiological changes. As well as changes in blood flow distribution, pregnancy leads to the release of vasoactive factors into the bloodstream which have the potential to increase BBB permeability. However, vasogenic brain oedema is not observed in normal pregnancy, suggesting that adaptation of the BBB counteracts systemic changes to protect the neurological system. As will be described further in the next section (Preeclampsia and eclampsia), failure of cerebral vasculature and the BBB to correct for these changes has been implicated in disease[107].

The exact nature of this adaptation is not entirely clear, due to difficulty in studying the BBB in humans. In vivo animal studies and in vitro studies suggest that pregnancy may be associated with increased BBB permeability to certain solutes, but there is conflicting evidence[107–110]. In rats, there is no difference between tight junction protein expression in pregnant and non-pregnant BBBs, suggesting no increase in paracellular permeability[107]. It is not clear how these findings would translate to human pregnancy. Overall, it is logical that the BBB must adapt to physiological changes to preserve a healthy neurological environment in pregnancy, but evidence is limited, particularly in human subjects.

Preeclampsia and eclampsia

2.1 Symptoms, Complications, and Risk factors

Preeclampsia and eclampsia are two related hypertensive disorders of pregnancy, which both involve multiple organ systems. Incidence of preeclampsia is estimated to affect 2-10% of pregnancies worldwide. Pre-eclampsia is characterised by sudden-onset hypertension (systolic blood pressure ≥ 140 mmHg and/or diastolic blood pressure ≥ 90 mmHg), accompanied by another associated new-onset end-organ complication. This is often proteinuria, but can also be other renal complications, liver complications, uteroplacental dysfunction (e.g. foetal growth restriction (FGR), abnormal umbilical artery Doppler analysis), haematological complications (e.g. thrombocytopenia, disseminated intravascular coagulation), or neurological complications (e.g. eclampsia (see later), stroke)[111,112].

Preeclampsia is divided into subcategories based on timing of onset. As this is difficult to determine exactly, timing of delivery is used as a proxy measure, although it is important to note evidence that this is not a perfect proxy for onset and may underestimate incidence of early onset preeclampsia[113]. The International Society for the Study of Hypertension in Pregnancy divides preeclampsia into preterm (delivery before 37 gestational weeks), term (delivery at or after 37 gestational weeks), and postpartum preeclampsia (after delivery)[114,115]. In research, preeclampsia is usually divided into early onset and late onset preeclampsia, with the cutoff being delivery at 34 gestational weeks, but this classification is not favoured clinically[115–117]. This division is based on differences in clinical presentation, complications and risk factors, as will be described later.

Preeclampsia increases the risk of many adverse health outcomes. For the foetus, preeclampsia-associated placental dysfunction leads to a higher likelihood of FGR (particularly in early onset disease), iatrogenic and spontaneous preterm birth, foetal hypoxia, placental abruption, foetal distress, and foetal death[111]. Preeclampsia can progress to seizures or coma, in which case the disease would be classified as eclampsia, which carries a high risk of mortality[115]. Severe preeclampsia can be associated with haemolysis, elevated liver enzymes and low platelet count syndrome (HELLP syndrome). Preeclampsia can also lead to non-obstetric complications, including but not limited to heart failure, pulmonary oedema, stroke, kidney damage (esp. glomerular endotheliosis) and peripartum cardiomyopathy[118].

Although symptoms resolve shortly after delivery of the placenta, a preeclamptic pregnancy has long term effects, with reduced life expectancy and increased lifetime risk of diabetes, stroke, and cardiovascular disease for the mother[115]. For the baby, there is an increased risk of neurodevelopmental, cardiovascular, and metabolic aberrances as an adult. As of 2012 it was estimated that over 300 million women and children worldwide are at increased risk of chronic health issues because of preeclampsia exposure[119]. An analysis of Danish health records showed that offspring exposed to preeclampsia, eclampsia and hypertension in pregnancy had a 29%, 188% and 12% increased risk of all-cause mortality than non-exposed offspring over a 41-year follow-up period. For preeclampsia, risk of mortality increased with disease severity[120].

Several risk factors have been identified for preeclampsia, with minor variation between factors listed by different organisations[115]. Evidence suggests different risk factors are at play in early onset and late onset preeclampsia, potentially indicating different pathological mechanisms. A multivariate approach identified factors associated with early onset and late onset preeclampsia in a >8000 sample set. For both groups, previous

pregnancy without preeclampsia reduced risk, while previous pregnancy with preeclampsia increased it. History of chronic hypertension was associated with early onset preeclampsia. Risk of late onset preeclampsia was increased if the woman's mother had preeclampsia. Use of ovulation induction, but not in vitro fertilisation, was associated with risk of early onset preeclampsia[121].

Ethnicity affected the likelihood of preeclampsia development, with black women at higher risk of preeclampsia, and mixed and Indian/Pakistani women at higher risk of late onset preeclampsia only[121]. A large cohort study in the UK supports a role for race in risk. It found that black women are at higher risk of preeclampsia than white women, and that South Asian women have higher risk than white women for preterm preeclampsia only[122]. This association remains after accounting for social deprivation[123–125] and ethnicity-associated differences in incidence of chronic hypertension and cardiovascular disease[126,127].

Preexisting medical conditions are associated with increased preeclampsia risk, particularly chronic hypertension, which causes a fivefold risk increase compared to normotension[128]. A body mass index (BMI) >30 kg/m^2 (The International Society for the Study of Hypertension in Pregnancy and National Institute for Health and Care Excellence) or 35 kg/m^2 (American College of Obstetricians and Gynaecologists) is listed as a risk factor. Pre-pregnancy diabetes mellitus, chronic kidney disease and thyroid dysfunction are also risk factors[115]. There is some evidence for a role of gut dysbiosis, but more research is needed, particularly as dysbiosis is associated with other risk factors, such as obesity and metabolic disorder[129,130].

Obstetric history is relevant when considering preeclampsia risk. Primiparity is linked with a threefold increase in preeclampsia incidence[131]. In multiparous mothers, longer

intervals between pregnancies increase risk, which reaches that of primiparity after a 10-year interval[132]. A subsequent pregnancy has the same risk as a primiparous pregnancy where the pregnancy involves exposure to new paternal antigens[133]. Multiple pregnancies, e.g. twins, carry a greater preeclampsia risk, with increasing risk for each extra foetus present[131]. As mentioned earlier, previous preeclamptic pregnancies increase risk substantively, as do previous pregnancies complicated by FGR, placental abruption, and stillbirth, particularly when associated with placental malperfusion[115].

Maternal age at both extremes is associated with increased preeclampsia risks. Both age categories are also linked with other risk factors. In mothers of advanced age (≥35 years), there is increased use of artificial reproductive technologies, multiple pregnancies, and a higher incidence of preexisting cardiometabolic issues. However, risk still increases with every year after 32 if confounding factors are accounted for[121,134]. In young mothers (<20 years), socioeconomic factors and increased primiparity influence risk. Maternal age below 20 years is associated with late onset disease rather than early onset[135]. Environmental factors have also been implicated, including air quality and exposure to pollution[136]. High altitude (>2,700m) pregnancies have higher rates of preeclampsia, which is particularly pronounced in immigrants as compared to multigenerational high-altitude inhabitants[136]. Diet may also influence preeclampsia risk[137].

2.2 Pathology

The multisystemic nature of preeclampsia is well-established but presents issues when explaining pathology. There is no general consensus on the pathogenesis of preeclampsia, with different models placing different systems at the core of the disease. Furthermore, it is not clear if variations in clinical presentation represent different disease pathogenesis

or variations in susceptibilities of the affected women. Differences seen in early versus late onset preeclampsia cases give some weight to the idea that the diagnosis of preeclampsia may include related but distinct disease states with different causes and complications.

Research into preeclampsia pathogenesis has not been able to reach a consensus on the order of causation. Feedback between different systems complicates the research further. The most common working model will be described below, along with other relevant lines of discussion about preeclampsia pathology.

2.3 Pathogenesis

The two-stage model of preeclampsia proposes that the disease initiates due to syncytiotrophoblast stress (stage I), which leads to maternal symptoms (stage II). The syncytiotrophoblast stress seen in preeclampsia is thought to be linked to poor placentation (this is expanded upon below). There is consistent evidence to show that the placenta and its function is central to preeclampsia[138,139]. Many questions remain regarding the exact details of the two-stage model, particularly the underlying causes of poor placentation and syncytiotrophoblast stress, and the mechanism of linkage between placental stress and maternal symptoms. There is evidence for involvement of many biological pathways and systems, which show aberrances that may be causative or reactive in disease pathology.

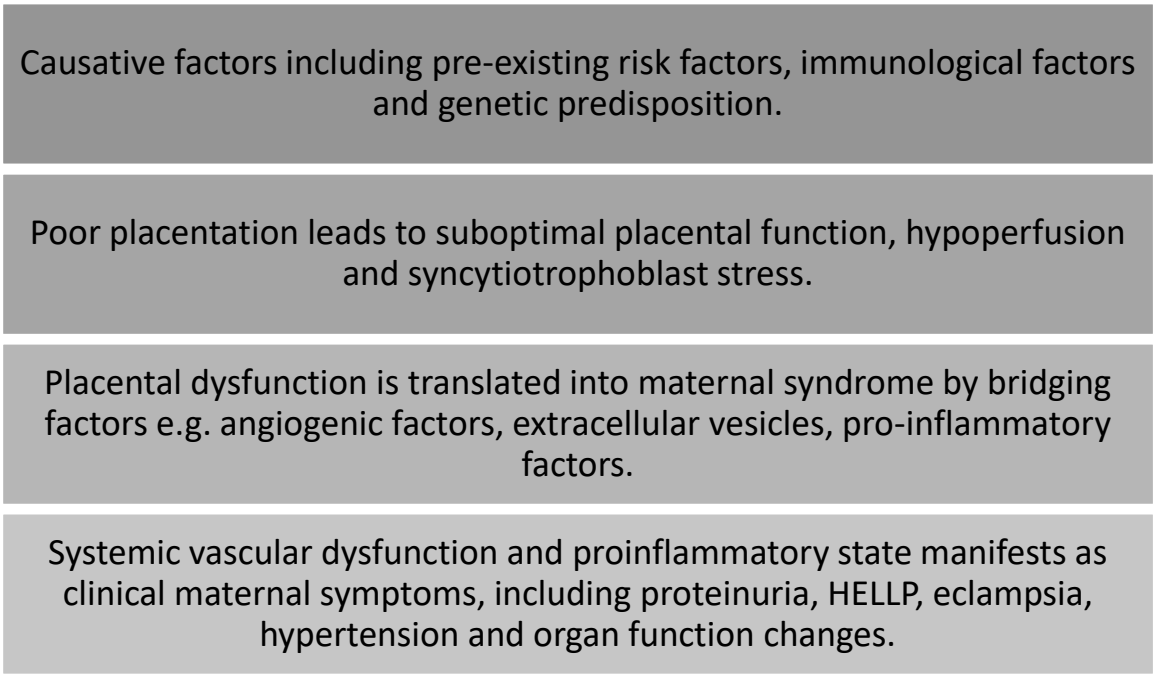

Proposed Model of Preeclampsia Pathogenesis

As seen in the chart above, a central issue in preeclampsia pathology is poor placentation, the process by which the placental develops and embeds itself in the uterus. In normal placentation, the fertilised ovum develops into a blastocyst (cluster of dividing cells), which will develop into the foetus and foetal portion of the placenta. The blastocyst has an outer layer of trophoblast cells. The blastocyst implants into the uterus and contact between the trophoblast cells and endometrium triggers development of a multinucleated outer layer of syncytiotrophoblasts and inner layer of cytotrophoblasts. The syncytiotrophoblast layer sends out projections which penetrate maternal tissues, while cytotrophoblasts secrete enzymes to assist syncytiotrophoblast invasion of the endometrial wall. This also triggers formation of a specialised tissue called decidua from the endometrium[140,141].

Projections of cytotrophoblasts grow into the syncytiotrophoblast layer, forming primary chorionic villi. The villi are important structures for providing nutrients to the foetus and removing waste. They are surrounded by intervillous space, where maternal blood

provides nutrients and other substances e.g. dissolved gases[140,141].Some villi, termed anchoring villi, are connected to the decidua through the cytotrophoblast shell. Later, a central core of loose connective tissue and blood vessels will form, marking development into secondary and then tertiary villi respectively. Some villi ('branching villi') grow laterally within the intervillous space to provide a large surface area for substance exchange between mother and foetus[140,141].

As the primary chorionic villi are forming, spaces called lacunae form within the syncytiotrophoblast layer. Erosion of maternal tissues connects the uterine spiral arteries to the lacunae network, establishing circulation between maternal and foetal tissues. The maternal spiral arteries undergo remodelling into lower resistance vessels to meet the high circulation demands of the growing foetus. The spiral arteries become significantly dilated, lose endothelium, smooth muscle cells and inner elastic lamina, and lose their ability to constrict in response to neural and hormonal signals at their terminal ends[140,141]. Cytotrophoblasts invade the spiral arteries and replace lost cells. Factors produced by both the decidua and placenta promote the remodelling process[142]. Maternal immune cells contribute to the remodelling process, for example uterine natural killer cells and macrophages. Maternal spiral artery remodelling is a crucial process for pregnancy outcomes, as it affects blood (and therefore nutrient) flow to the developing foetus[140,141].

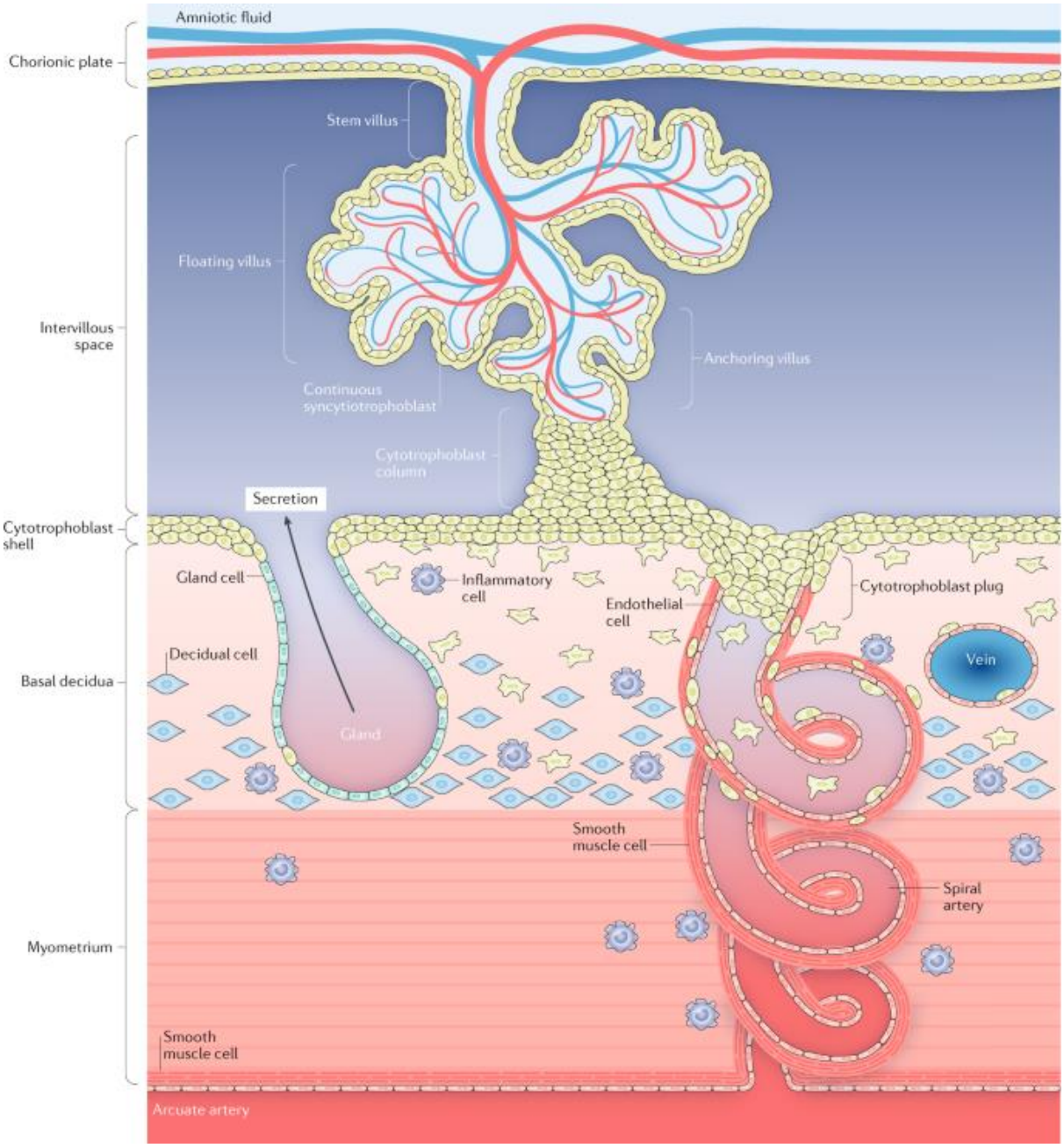

Figure 2: Illustration showing the structure of the first trimester placenta, from Aplin et al 2020[143].

Spiral artery remodelling is implicated in preeclampsia pathogenesis. There is evidence of limited remodelling in preeclamptic deciduae, with both reduced diameter of remodelled spiral arteries and depth of remodelling in preeclamptic placentas compared to normal placentas[144–146]. In preeclampsia, remodelling of the spiral arteries is commonly restricted to the decidua, while in normal pregnancy it extends into the myometrium[145].

Notably, abnormal uterine Doppler findings are more common in early onset preeclampsia than late onset preeclampsia[147]. Traditionally, poor spiral artery remodelling was assumed to cause placental hypoperfusion and chronic hypoxia. A 2009 model by Burton et al.[144,148] suggests that the effect on flow volume is minimal, but that flow has increased pulsatility and pressure. This is partly attributed to the persistence of smooth muscle cells in the spiral arteries is preeclampsia that would ordinarily be replaced, meaning that the spiral arteries retain contractility in preeclampsia. This pulsatile flow may lead to ischaemia-reperfusion injury and oxidative stress rather than chronic hypoxia[148].

Whether due to placental hypoxia or ischaemia-reperfusion injuries, the result is adverse placental function and syncytiotrophoblast stress. This leads to release of inflammatory and stress-signalling factors, which cross into maternal circulation and can affect multiple biological pathways and systems. The exact nature of these bridging factors is not known, and there are likely multiple factors involved. Several candidates have been identified including syncytiotrophoblast-derived extracellular vesicles, (anti)angiogenic factors, free foetal haemoglobin[149], and reactive oxygen species[115,150].

Abnormal histopathological findings have been reported in preeclamptic placentae, including atherosis, syncytial knots, increased cytotrophoblast proliferation, accelerated villus branching, small sclerotic villi, and thickening of the trophoblast membrane[115,151]. However, there is a large overlap between histopathology observed in preeclamptic placentas and those seen in FGR[152], suggesting extra factors are at play in preeclampsia initiation. Furthermore, while abnormal histological placental findings are common in preeclampsia, pregnancies with severe preeclamptic symptoms can still have normal histological findings, and normal placental histology cannot be used to exclude disease[152]. Abnormal histological findings are more common in preterm preeclampsia, as opposed

to term, suggesting differences in pathological mechanisms[115,152]. Abnormal placentation is also less associated with late onset preeclampsia [150].

A less-cited theory of preeclampsia pathogenesis places the maternal cardiovascular system at the centre of disease initiation. This theory has significantly less traction than placenta-oriented models but is worth mentioning. Briefly, this theory states that placental dysfunction is preceded by maternal cardiovascular maladaptation to pregnancy. Evidence given for a primary cardiovascular role include the higher risk of cardiovascular disease persisting decades post-preeclampsia, and the predominance of cardiovascular symptoms in preeclampsia, particularly hypertension[153,154]. The two theories are not mutually exclusive, as a vicious cycle where placental stress aggravates peripheral cardiovascular function and suboptimal cardiovascular function worsens placental stress may form.

There is evidence for a causative immune component to preeclampsia, with one theory stipulating that preeclampsia is due to inadequate tolerance of the maternal immune system to paternally inherited antigens in the foetus[115]. There are many lines of evidence suggesting that exposure to paternal antigens reduces preeclampsia risk. Pre-conception use of barrier contraception (e.g. condoms) compared to non-barrier methods (e.g. hormonal pill, intra-uterine device) is associated with higher preeclampsia risk[155,156], although this has not been entirely consistent across studies, with some showing no risk change[157]. A higher incidence of preeclampsia is observed in subsequent pregnancies where paternity has changed[158], pregnancies after a long inter-pregnancy interval[159], pregnancies conceived with donor sperm[160] and primiparous pregnancies[161]. Oral sex practices are associated with lower preeclampsia risk, particularly when semen is ingested[162]. These observations suggest that a lack of maternal tolerance to paternal antigens may contribute to preeclampsia pathology.

Furthermore, normal placentation is characterised by a T cell and cytokine profile biased towards type 2 helper T cells and anti-inflammatory cytokines e.g. IL10. Preeclamptic T cell profiles lean towards type 1 helper T cells and associated pro-inflammatory cytokines e.g. TNF and IFNγ[163,164]. Preeclampsia may also be associated with increased complement activation[165]. More aggressive macrophage phenotypes are observed in preeclamptic placentae[166]. A mechanism for immune involvement in pathogenesis would be that a more aggressive, pro-inflammatory immune response against paternal antigens expressed on trophoblasts would impede invasion of the endometrial tissues and growth of cytotrophoblasts into the spiral arteries, therefore reducing depth and success of placentation.

To summarise, the pathogenesis of preeclampsia is still unclear and different theories emphasise different systems. Typically, the placenta is considered essential for pathogenesis. Deficient spiral artery remodelling is observed in preeclampsia, resulting in syncytiotrophoblast stress due to hypoxia and/or ischaemia-reperfusion injury. There is evidence of abnormal placental morphology in preeclampsia, but there is a large overlap with FGR. The underlying causes of poor placentation and spiral artery remodelling are not clear, but likely involve predisposing risk factors and immune intolerance to paternal antigens. In the two-stage model, placental issues (stage I) are translated into maternal symptoms (stage II) by bridging factors, which may include syncytiotrophoblast-derived extracellular vesicles, (anti)angiogenic factors, and other bioactive molecules.

2.4 Endothelial Dysfunction in Preeclampsia Pathology

Widespread endothelial dysfunction, driven by factors released from the stressed placenta, is thought to underlie other organ dysfunction seen in preeclampsia. Arterial stiffness, an indicator of endothelial dysfunction, has been observed in preeclamptic women and increases with disease severity[149,167]. Endothelial dysfunction may lead to reduced blood flow to important organs, including the heart and kidney, and increased venous congestion. This can induce reflex constriction of arteries, driving hypertension. Early endothelial dysfunction, particularly linked to the placenta, is especially associated with early onset preeclampsia.

Placental release of angiogenic factors is implicated in preeclampsia development and can have effects on the vascular system. Serum soluble Fms-like tyrosine kinase-1 (sFlt1) is increased, and placental growth factor (PlGF) decreased approximately 5 weeks before preeclampsia onset. sFlt1 is an antiangiogenic factor and PlGF is an angiogenic factor[168]. The ratio of sFlt1 and PlGF is used in preeclampsia diagnosis and early prediction, as it is significantly raised in many preeclampsia patients[115,168]. Again, while increased sFlt1:PlGF ratio is strongly associated with preeclampsia, it is not uniformly observed in all established cases, highlighting heterogeneity.

sFlt1 can bind both PlGF and vascular endothelial growth factor (VEGF), reducing biologically available PlGF and VEGF, which are potent angiogenic factors. One theory states that when sFlt1 levels reach a certain threshold, the associated reduction in angiogenic factors leads to widespread angiogenic dysfunction and clinical preeclampsia[169,170]. In women with preexisting endothelial issues, such as those seen in hypertension or obesity, this threshold is lower, so that clinical symptoms manifest at lower sFlt1 levels[171,172]. In this case, the normal sFlt1 rise seen in non-preeclamptic

pregnancies may be sufficient to cause preeclampsia in highly susceptible women, potentially explaining why increased sFlt1 is not seen in every preeclampsia case[173].

There is evidence that sFlt1 levels may promote clinical preeclampsia symptoms, particularly relating to endothelial dysfunction. In rat models, excess adenoviral expression of sFlt1 produces a preeclampsia-like syndrome, including proteinuria, hypertension, and glomerular endotheliosis[169,173]. Furthermore, serum from healthy pregnant women, but not preeclamptic women, can induce endothelial tube formation of human umbilical vein endothelial cells (HUVECs)[169]. Addition of exogenous sFlt1 to healthy serum inhibits tube formation, while addition of VEGF and PlGF to preeclamptic serum enables tube formation. Additionally, pilot studies of extracorporeal reduction of sFlt1 by apheresis may bring clinical benefits by increasing duration of pregnancy[174,175].

2.5 Differences in Late and Early Onset Pathology

As alluded to in the sections above, differences have been identified between late and early onset preeclampsia. Early onset preeclampsia is associated with worse neonatal outcomes, including prematurity, foetal growth restriction and perinatal morbidity and mortality. Early onset preeclampsia also carries a higher risk of future cardiovascular disease for the mother, possibly due to the increased severity associated with early onset disease. Late onset preeclampsia is still dangerous, with 20% of HELLP syndrome and 55% of eclampsia cases presenting on or after 37 gestational weeks[116]. There are differences in risk factors associated with early and late onset preeclampsia. Furthermore, early onset preeclampsia shows significant association with angiogenic biomarker patterns, while this is not observed in late onset preeclampsia[115]. As a result, angiogenic biomarker ratios have limited diagnostic use in late onset disease.

It has been suggested that early and late onset preeclampsia have different mechanisms of pathogenesis and may even be distinct diseases, rather than subtypes of preeclampsia[117]. An often-cited theory proposes that early onset preeclampsia is the result of poor placentation while late onset disease relates to pre-existing maternal endothelial dysfunction or an abnormal reaction to normal factors shed from a healthy placenta[117,176–178]. Abnormal histopathological findings are less common in late onset placentas compared to early onset[115], supporting this theory. This theory is consistent with lower likelihood of FGR in late onset preeclampsia.

A second theory posits that both categories of preeclampsia begin in the placenta. In this model, early onset preeclampsia starts in early placental development with shallow and/or abnormal placentation and limited spiral artery remodelling. In late onset preeclampsia, initial placentation is normal but there is intrinsic placental dysfunction in later gestation, as the maturing placenta outgrows the capacity of the uterus and other maternal systems. This leads to placental hypoperfusion. In both early onset and late onset, the placental issues then lead to the same syncytiotrophoblast stress, only with different timings[116]. However, machine learning approaches using data on systolic blood pressure, urinary protein, serum urea nitrogen, potassium and calcium levels, creatinine, platelet, and white blood cell counts from >11,000 pregnant women could predict late-onset preeclampsia in the early second trimester[179]. This suggests that late onset preeclampsia cases diverge from normal pregnancies at an earlier gestational age than is often assumed[116], and that 'late onset' may be a misleading term for what is really 'late presenting' disease.

Overall, differences are consistently seen in the presentation, risk factors and outcomes of women with early and late onset preeclampsia. It has been suggested that this is a result of different underlying mechanisms. Proposed mechanisms for late onset preeclampsia place either the maternal endothelial system or the placenta at the initiation of disease.

2.6 Treatment

Currently the only effective treatment for preeclampsia is delivery of the placenta. In early onset preeclampsia, there is a need to balance the risks of preterm birth with those of a preeclamptic pregnancy. Therapeutics are focused on attenuating symptoms but do not address underlying causes. Antihypertensive medications are used to manage blood pressure and associated complications while magnesium sulphate reduces risk of eclampsia onset. The main aim of these treatments is to prolong pregnancy and thus minimise the adverse effects of preterm birth[115,180].

Some novel therapeutic strategies are being investigated[180]. As mentioned above, there has been some success in prolonging pregnancy in preterm preeclamptic women by reducing sFlt1 using an extracorporeal dextran-sulphate apheresis column[175]. There are issues as these columns are not selective and remove other blood components that may be important during pregnancy[180]. Recombinant or adenovirus-carried PlGF or VEGF treatment improves blood pressure and sFlt1 levels in rodent models[180–183]. PlGF has also been trialled in primate models of preeclampsia with positive effects[180,184,185]. Small interfering RNAs have been used in baboon models of preeclampsia to lower sFlt1 levels, with success in lowering blood pressure and proteinuria[186].

There has been more progress in development of prophylactic treatments. One of the earliest suggestions for prophylaxis was aspirin. A 1985 trial showed that prophylactic aspirin treatment reduced preeclampsia, FGR and stillbirth in high-risk women[187]. Studies of aspirin use in preeclampsia have since been plagued with variations in dosage and timing of treatment onset[115]. However, evidence from a meta-analysis confirms that aspirin is effective in preventing preterm preeclampsia if given to high-risk women before 16 gestational weeks[115,188]. The best dosage for prevention is yet to be determined. Meta-

analyses have identified that low-dose calcium supplements reduce preeclampsia risk in high-risk women with low dietary calcium intake, and that exercise can also reduce risk[180,189,190]. Treatment of pre-existing hypertension before or in early pregnancy also reduces risk of preeclampsia development[180,191].

2.7 The Neurological System in Preeclampsia and Eclampsia

As early as 400BC, Hippocrates noted that headaches preceded 'fits' in pregnancy[192]. The most obvious indicator of neurological involvement in preeclampsia is seizure, but there are other associated neurological complications, including cortical blindness, ischaemic stroke, subarachnoid and intracerebral haemorrhage[115,193]. It is estimated that neurological complications are a direct cause in 30-70% of preeclamptic deaths, often due to intracerebral haemorrhage or cerebral oedema[193–197].

The underlying causes of neurological dysfunction, particularly seizure, in preeclampsia are not entirely clear[115]. Autoregulation of cerebral blood flow has been implicated. In normal conditions, arterioles react to systemic blood pressure changes to ensure constant cerebral flow and prevent hyper- and hypoperfusion injuries. Two theories of eclamptic seizure hinge on this system, with one suggesting that overcorrection for increased pressure results in cerebral ischaemia, and another contrarily suggesting that rapid hypertension exceeds the autoregulatory capacity and results in vasogenic oedema (extracellular accumulation of fluid[198]) and BBB dysfunction. Notably, the reversibility of symptoms postpartum is inconsistent with ischaemic injury and there is significant overlap between clinical presentation of eclampsia and other cases of hypertension-related cerebral oedema, lending more weight to the second theory.

However, studies find little correlation between hypertension and eclamptic seizure, with ~40% of eclamptic seizures occurring at normotension. It is possible that the autoregulatory system may independently go awry. Indeed, abnormalities in autoregulation have been observed in preeclampsia and chronic hypertension[199–202], although there is some contradictory evidence[203]. As described earlier, preeclampsia (and eclampsia) is associated with widespread endothelial dysfunction, and it is possible that endogenous disruption of the cerebral autoregulatory system is also a function of endothelial dysfunction. This would also suggest that some bridging factors from the stressed placenta are able to reach and affect neurological tissues.

Biological activity of placenta-derived factors in neurological tissues would require the BBB to be crossed. Increased BBB permeability is observed in several animal models of preeclampsia and incidences of cerebral oedema in eclamptic women is also consistent with this. Furthermore, increased CSF to plasma albumin ratio has been observed in eclamptic and preeclamptic women, suggesting BBB injury[204]. In a rodent model, circulating factors in maternal plasma were suggested to inhibit efflux transporters in the BBB, which was then associated with increased hippocampal sensitivity to seizure[205].

The underlying causes of BBB dysfunction are not clear. Damage due to defects in the autoregulatory system has been implicated, as well as inflammation and extracellular vesicles. In a rat model of preeclampsia, pro-inflammatory cytokines increase BBB permeability[206]. Given the association with preeclampsia and a pro-inflammatory state, pro-inflammatory cytokines are a likely candidate for causing BBB issues. Leon et al 2021 found that exposure to placental extracellular vesicles in in vivo and in vitro models disrupted BBB function[207]. This paper is discussed in more depth in Section 3.2.f.

2.8 Long-Term Consequences

Although acute symptoms generally resolve postpartum, preeclampsia and eclampsia have long-term implications on neurological health. Multiple studies find that women exposed to preeclamptic pregnancy show higher risk of all-cause dementia and Alzheimer's disease after adjustment for multiple variables[208–210]. Studies of brain structure showed reduced cortical grey matter volume in previously preeclamptic women compared to previously normotensive pregnant women[211]. The preeclamptic group also showed increased white matter lesions in the temporal lobe and altered microstructural integrity in the temporal, occipital and parietal lobes[211,212], a feature that is associated with cerebrovascular damage[213]. Importantly, white matter lesions are also associated with risk of dementia and stroke[213]. Some studies find poorer performance in various measures of cognitive function in previously preeclamptic women[214–216], although another study suggested that this may be mediated by confounding factors, including BMI, depression, and education level[217].

2.9 Summary

Research into preeclampsia and eclampsia has identified widespread physiological dysfunction, but less progress has been made in understanding the mechanisms of this dysfunction. There is still debate about the central causes of preeclampsia, and variations in clinical presentation and research findings has led researchers to question whether all preeclampsia cases are even the same disease. Working models of preeclampsia pathology are disputed and leave many questions unanswered. Limited understanding of preeclampsia is an issue when looking for therapeutic strategies. Current treatment

options for preeclampsia are limited and focus on symptom attenuation, rather than targeting core mechanisms.

Preeclampsia is associated with acute and long-term neurological consequences. Acute complications include seizure, cortical blindness and cerebrovascular issues, including stroke and haemorrhage. Long-term risks include association with dementias, structural brain changes, and possible impact on cognitive function. Again, there is no consensus on the mechanisms that underlie this and variation in clinical findings further complicate the research.

Exosomes

3.1 Extracellular Vesicles

Extracellular vesicles are lipid-bound particles that are secreted by cells into extracellular space. Within the lipid membrane, extracellular vesicles can contain biologically active cargo, e.g. nucleic acids and proteins. When they encounter recipient tissues or cells, extracellular vesicles interact via receptor molecules and ligands and can be internalised by micropinocytosis and phagocytosis. The cargo of extracellular vesicles can influence the behaviour and function of recipient cells. In this way, extracellular vesicles provide a system by which biological messages about cell and tissue health can be delivered to physiologically distant tissues, and may alter the function of those tissues in a pathological or healthy adaptive manner[218,219].

Extracellular vesicles can be broadly classified as microvesicles, exosomes and apoptotic bodies. The main distinction between classifications is route of formation, but there are also differences in vesicle size and protein content[218]. The size ranges given for different

vesicle classifications are rough and differ between papers. This may reflect differences in vesicle populations from various origin tissues[220], effects of isolation, freezing and storing[221,222], or variable results from different methods of measurement.

Microvesicles range from 100nm to 1μm in diameter and form by direct budding and pinching from the plasma membrane. They contain mostly cytosolic- and plasma membrane-associated proteins, such as tetraspanins, cytoskeletal proteins and integrins[223]. Apoptotic bodies are between 1 and 5μm in diameter and form as products of apoptotic cell death[224,225]. Under normal physiology, they are considered relatively inactive and have markers that promote their removal by immune cells. However, there is evidence that apoptotic bodies can modulate immune responses, and defective apoptotic body clearance is implicated in autoimmune disease[224]. Exosomes will be described in the sections below.

Research into extracellular vesicles can roughly be divided into three main aims: identifying changes in vesicle numbers or markers for use in diagnosis, identifying the contribution of vesicles to disease pathology, and use of vesicles as a therapeutic delivery system. Several fields of medical research have had success in using extracellular vesicles for these purposes[226–231], and significant efforts are underway to better understand extracellular vesicles in the context of pregnancy, so that they can be integrated into therapeutic and diagnostic approaches[232].

3.2 Exosomes

This project focuses on exosomes, and these will therefore be discussed in more detail than other extracellular vesicle types. Exosomes are the smallest category of extracellular vesicle at 30-150nm diameter[218,220,233]. As with other vesicle types, this size range is

variable, and the diameter of exosomes can also be affected by handling and storage[220–222]. There are also differences in the production routes and cargo of exosomes compared to other extracellular vesicle types. These will be discussed in this section.

3.2.a Production

The main route for exosome production begins in the endosomal system – part of a dynamic, intracellular sorting and transport system for cell components. Endosomes are membrane-bound cytosolic organelles which are part of the endocytic pathway. This pathway regulates recycling, sorting, storage, transport and trafficking of proteins and lipids between various organelles[234]. Early endosomes mature into late endosomes then multivesicular bodies. During this process, inward budding of the lipid endosomal membrane forms intraluminal vesicles, the precursor to exosomes, which accumulate in the lumen of the multivesicular body. Some multivesicular bodies will be transported to lysosomes for degradation, while some will be fused with the cell's plasma membrane. It is not entirely clear what signals regulate this decision. However, if the multivesicular body fuses with the cell membrane, it releases intraluminal vesicles into the extracellular space as exosomes[218–220,233].

3.2.b Composition and Cargo

As mentioned previously, exosomes are enclosed by a lipid bilayer membrane. Exosome cargo varies depending on origin. The cargo of exosomes can include proteins, nucleic acids (both DNA and RNA in many forms), amino acids and metabolites. Exosome cargo does not perfectly reflect the contents of the parent cell, as regulated protein sorting and

overrepresentation of proteins relevant to exosome biogenesis skew the contents. The 'Endosomal Sorting Complexes Required for Transport' (ESCRT) proteins are considered important in regulating exosome biogenesis, and therefore can be found in exosome cargo. These include the proteins Alix, TSG101, and HSC70, which are often used as exosome markers. Importantly, there is some evidence for an ESCRT-independent mechanism of exosome biogenesis, as cells depleted of ESCRT proteins are still able to produce exosomes[235–237]. The protein cargo of exosomes is also influenced by posttranslational modifications on proteins, such as ubiquitination[238,239].

Exosomes contain tetraspanins, particularly CD63, CD9 and CD81. Tetraspanins are membrane-spanning proteins with a role in cell membrane structure[240]. These were once considered a specific marker for exosomes, but they have also been identified in microvesicles and apoptotic bodies[218]. In this project, the tetraspanin CD63 is used to immobilise exosomes. Other membrane proteins frequently present in exosomes include ligands, receptors, MHC molecules, integrins and flotillins[219]. As with proteins, nucleic acid content of the exosome is regulated, and some RNA subtypes are differentially represented in exosomes compared to the parent cell. Certain miRNAs are preferentially included in exosomes[239,241] and general miRNA content is higher in exosomes than host cells[239,242].

3.2.c Placenta-Derived Exosomes

During pregnancy, the placenta releases extracellular vesicles, including exosomes, into maternal circulation. In this project, these are called placenta-derived extracellular vesicles, but they are also referred to as syncytiotrophoblast extracellular vesicles in literature[149]. Placental alkaline phosphatase (PLAP) is used as a marker for these

vesicles[243,244]. Using this marker, placenta-derived exosomes are first observed in the first trimester of pregnancy, and their numbers increase with gestational age[244]. Several studies have suggested that these exosomes may be biologically active and influence pathways relevant to both healthy and pathological pregnancies. This will be expanded upon below.

3.2.d Role of Placenta-Derived Exosomes in Pregnancy

Placenta-derived exosomes are implicated in many processes of normal pregnancy. Perhaps the most-studied area is exosome-mediated immune modulation, as maternal tolerance is essential for preventing rejection of the foetus and enabling healthy pregnancy[245]. Many immune cells are involved in the maternal immune response, primarily natural killer (NK) cells, macrophages, and T cells. NK cells and macrophages are highly abundant in the decidua, with lesser T cell presence and near-absence of B cells and dendritic cells[246,247]. In vitro evidence suggests that both NK cells and monocytes can internalise placenta-derived exosomes[166,248–250], although there is some in vitro evidence that monocytes (a precursor to macrophages) preferentially interact with placenta-derived exosomes over NK cells[250]. Notably, this experiment was performed using cells isolated from peripheral blood, so it is not clear how this translates into an in vivo decidual setting.

Studies suggest that placental exosomes modulate the behaviour of macrophages and their precursors, monocytes. Transcriptomics of monocytes incubated with placenta-derived exosomes found a more tolerogenic and immunosuppressive phenotype than in non-exposed monocytes. The analysis showed enrichment of the anti-inflammatory IL10 pathway and suppression of genes involved in antigen presentation. Exosomes may promote expansion of a monocyte subset with potent immunosuppressive capabilities,

that is increased in the peripheral blood of pregnant women as compared to non-pregnant controls[250].

Incubation of T cells with exosome-exposed monocytes reduces general T cell proliferation but promotes formation of regulatory T cells[250], a T cell subset that suppresses exaggerated or deleterious immune responses[251]. Regulatory T cell populations expand during pregnancy, particularly regulatory T cells with specificity for foetal antigen, and mouse studies suggest that they are required for foetal survival[252–255]. Therefore, changes seen in T cell populations are consistent with those seen in healthy pregnancy and upregulation of regulatory T cells by exosome-exposed monocytes may contribute to pregnancy success.

Incubation of monocytes with placenta-derived exosomes upregulates programmed cell death ligand-1(PD-L1), which promotes tolerance by suppressing T cell proliferation and activation[250,256]. Cytokine profiling of medium from exosome-exposed monocyte and T cell co-culture showed reduced cytotoxic cytokines. There is also evidence that extracellular vesicles of pregnant women carry immunosuppressive cargo (the cytokines TGF-β1 and IL10), but the extracellular vesicles were not tested for placental origin[249]. Placenta-derived exosomes have also been demonstrated to carry PD-L1[246].

A murine study of placenta-derived exosome uptake by macrophages suggested that placenta-derived exosomes are preferentially targeted to the lungs and liver and are frequently internalised by pulmonary macrophages[246,257]. It is not clear if this translates to humans or what the physiological implications would be, but this demonstrates that the effects of placenta-derived exosomes may be wide-reaching.

There is evidence for a role of placenta-derived exosomes in the endothelial system. One study showed that placenta-derived vesicles transfer functional miRNAs into endothelial

cells[258]. Exosomes isolated from peripheral blood of pregnant women promote HUVEC migration, with a decreasing effect with increasing trimester[259]. Furthermore, there is evidence that exosomes isolated from trophoblast cell lines can promote vascular smooth muscle migration[260].

Exosomes derived from isolated placental mesenchymal stromal cells can stimulate angiogenesis and endothelial cell migration, as measured using endothelial tube formation assay, cell migration assays and mouse model of ischaemic injury. This study suggests that, despite the focus on syncytiotrophoblast-derived vesicles, vesicles from other placental cell types may be biologically active[261]. An effect of exosomes on the endothelial system and angiogenesis is particularly relevant given the established importance of artery remodelling in pregnancy success.

When considering the role of placenta-derived exosomes in normal pregnancy, it is important to note that many studies are performed ex vivo or in murine models, so it is not clear how they translate into a human in vivo context. There are many other pregnancy-associated physiological and hormonal changes that have effects alongside placenta-derived exosomes. To the best of my knowledge, no papers have addressed the relative contributions of placenta-derived exosomes and other relevant factors to changes in pregnancy, so it is difficult to estimate how biologically significant the effects of placenta-derived exosomes are.

3.2.e Role of Placenta-Derived Exosomes in Preeclampsia

Total exosome load in the plasma is increased in pregnancy, and there is evidence that this increase is even larger in preeclamptic pregnancy[262]. Several studies have found increased levels of placenta-derived extracellular vesicles and/or exosomes in the plasma

of preeclamptic women, compared to normotensive pregnant women[262–265]. However, the increase in total exosomes is often observed to be greater than the increase in placenta-derived exosomes, meaning that the proportion of placenta-derived exosomes may be effectively decreased or unchanged in the peripheral plasma[262,266]. A study of extracellular vesicles isolated by placental perfusion found that expression of PLAP per vesicle was reduced in preeclampsia compared to normal pregnancy. The implications of this are not entirely clear, but may suggest that measurements and comparisons between preeclampsia and normal pregnancy are being affected by different expression of markers, or may reflect a lower proportion of placenta-derived extracellular vesicles[267]. Other studies find differences between early and late onset preeclampsia, with early onset preeclampsia being associated with higher levels of placenta-derived vesicles[263,266].

The cargo of placenta-derived exosomes and other extracellular vesicles is different in preeclamptic pregnancies[266]; there is evidence of different lipid profiles in preeclamptic and normal placenta-derived vesicles[166,268]. Exosome cargo relating to angiogenesis/endothelial function, inflammation and cellular stress have been studied most extensively, because of links to pathology[138,266,269], however there is evidence of differentially expressed cargo relevant to other processes. A 2015 proteomics analysis of syncytiotrophoblast-derived extracellular vesicles from placental explants found almost 200 differentially expressed proteins in preeclamptic vesicles compared to normal. The main biological processes of these proteins included cellular processes, single-organism processes, and metabolic processes[270]. Interestingly, the most upregulated protein in preeclamptic vesicles, siglec-6, is suspected to suppress trophoblast invasiveness, and therefore has clear links to preeclampsia pathology[270,271].

Differential expression of compounds relating to endothelial and vascular function have been reported. Increased exosomal expression of sFlt1 and soluble endoglin has been

observed in preeclampsia[272,273]. Furthermore, placenta-derived exosomes show reduced levels of endothelial nitric oxide synthase in preeclampsia versus normal pregnancy. Nitric oxide synthase produces nitric oxide, which is a potent vasodilator, suggesting that reduced nitric oxide availability from vesicles may contribute to endothelial dysfunction[274,275]. Preeclamptic placenta-derived exosomes express neprilysin which increases blood pressure by constricting vessels and promoting sodium retention[264,276–278]. Altered expression of such compounds suggests that placenta-derived exosomes and other extracellular vesicles may be physiologically relevant in the vasculature.

There is evidence that preeclamptic placenta-derived extracellular vesicles can induce endothelial dysfunction[272]. This is highly relevant when considering that endothelial dysfunction is often implicated in preeclampsia pathology. Exposure of HUVECs to preeclamptic exosomes results in reduced cell proliferation, tube formation and cell migration, and increase permeability and apoptosis, as compared to normal pregnancy exosomes[272,279]. Exposure to preeclamptic exosomes may also decrease expression of binding proteins in HUVECs, such as VE-cadherin and occludin[279]. Vesicles from preeclamptic women but not normal pregnancy can inhibit relaxation of isolated myometrial arteries. Whole plasma did not have the same effect[280].

If pregnant mice are injected with preeclamptic or normal pregnancy exosomes, the preeclamptic exosome-injected mice develop a preeclampsia-like syndrome, including increased blood pressure and reduced foetal birth weight[272]. This may give the impression that placenta-derived exosomes have a causative effect in human preeclampsia, however it is important to remember that injection of human exosomes into mice will generate an anti-human inflammatory response[281], and changes seen in the mice may be related to an increased anti-human immune response to the preeclamptic vesicles and may not replicate the physiological effects of preeclamptic exosomes in a human setting. Furthermore, it is

not clear in the study where the site of injection was, and this is also unlikely to be physiologically representative as the tail vein is frequently used for injections in mice. Injection of extracellular vesicles is also associated with other events, particularly embolism[166].

Studies have observed immunological effects of preeclamptic exosomes. One study observed placenta-derived vesicles bound to circulating monocytes of pregnant women, suggesting that placenta-derived vesicles come into close contact with circulating immune cells. Incubation of PBMC with placenta-derived vesicles from preeclamptic placentae increases production of inflammatory cytokines, such as IL-18 and TNFα, from PBMC. Noticeably, this effect was not observed if PBMC was incubated with vesicles isolated by mechanical disruption of villous tissue, suggesting that isolation method may affect the behaviour of vesicles[282]. Furthermore, exposure to preeclamptic placenta-derived extracellular vesicles shifts macrophages towards a more inflammatory phenotype in vitro and in murine models. Preeclamptic-vesicle-exposed macrophages were capable of inhibiting angiogenesis in tube formation assays[166].

As with placenta-derived exosomes in normal pregnancy, it is not clear how extensive the contribution of exosomes is to preeclampsia pathology. It is important to keep in mind that there are many other changes observed in preeclampsia and other factors that are also associated with preeclampsia, such as products of oxidative stress and antiangiogenic factors.

3.2.f Exosomes and the Blood-Brain Barrier

There is a lot of scientific interest in the interaction between exosomes and the BBB. This section will summarise recent research that is relevant to this project, and then expand on papers that focus on the interaction between placenta-derived vesicles and the BBB.

The possibility that exosomes may cross the BBB has generated a lot of interest as it presents a possible method to deliver therapeutic substances to the CNS, which has long been an issue when developing drugs targeted to the brain[283,284]. In addition, it provides a mechanism by which peripheral cancers may metastasise to the brain[283,285]. It has been established that exosomes can cross the BBB into the CNS in both in vitro and in vivo experiments[283,284,286–290], Furthermore, CNS-derived exosomes have been identified in peripheral circulation, suggesting bidirectional passage of exosomes[290–293]. While the ability of exosomes to cross the BBB has been shown, there is limited understanding about the specific details. For example, it is not clear by which mechanisms exosomes cross, whether there is selectivity for specific exosomes, and whether disease states or other altered physiological states can affect crossing[290]. Furthermore, most evidence is in vitro [294], and in vivo studies primarily use murine models, so even less is known about human in vivo mechanisms[290,294–296].

Several potential mechanisms have been proposed for exosome crossing, and it is possible that different mechanisms apply to exosomes of different origins. The main mechanism put forward is the transcytotic mechanism, which involves transcellular transport of exosomes via membrane-bound carriers/vesicles, which then eject exosomes on the other side of the cell[286,290,294]. This is often observed in epithelial cells, and similar pathways are used by other substances to cross the BBB, such as immune cells, large proteins, and viruses[290,295–297]. Again, the evidence for transcytosis is almost entirely based on in vitro

assays[289], so it is not clear if this is representative of in vivo behaviour. There is also some evidence that paracellular transport is possible and may be upregulated in certain disease states and inflammation[283,294].

Different mechanisms of initial uptake by BBB cells are also suggested, including macropinocytosis (a non-specific internalisation process by which actin-rich structures extend from the cell-surface and collapse to form a cellular compartment, the macropinosome, which contains extracellular material[298]) and receptor-mediated endocytosis (process by which recruitment of proteins, especially clathrin to the plasma membrane followed by invagination of the membrane forms a clathrin-coated vesicle that typically fuses with a sorting endosome to release cargo)[289,299,300]. Blocking micropinocytosis or receptor-mediated endocytosis significantly decreases extracellular vesicle uptake. Neither completely prevented uptake, suggesting that a mixture of mechanisms may be used[301]. It is also possible that the contents of exosomes are released into BBB cells, repackaged, and re-released on the CNS side, allowing a transfer of cargo but not necessarily the original exosome structure itself[289]. Importantly, different exosome types cross the BBB at different rates[290], but the reasons for this are not entirely clear, and may relate to size, cargo, and markers on the exosome membrane.

Other studies also support an effect of inflammation on BBB crossing, particularly associating inflammation with increased active transport of extracellular vesicles[289,294,301]. Pre-conditioning by pro-inflammatory cytokines, e.g. IL-6 and TNF-α, has been implicated in promotion of exosome crossing, particularly the endocytosis of exosomes[302]. There is also evidence that exosomes containing inflammatory mediators themselves can disturb the BBB[303–305]. This may lead to a vicious circle where neuroinflammation leads to increased exosome crossing, and inflammatory markers in exosomes promote neuroinflammation and further exosome crossing[286,306,307].

A 2020 paper by Banks et al attempted to look more in depth at exosome uptake by the brain[290]. They found that four out of ten tested exosome types showed non-random uptake by different brain regions, with uptake increased in the olfactory bulb compared to the cerebral cortex, cerebellum, and whole brain uptake rates. This suggests that exosomes are not equally internalised by all brain regions, but that this may depend on exosome phenotype. A second study supported high uptake in the olfactory bulb of healthy brains but suggested that patterns of uptake were different in mouse models of neurological pathologies, including stroke, Parkinson's disease, autism, and Alzheimer's disease[308]. It also suggested that exosomes in pathological brains preferentially home to areas of inflammation[308]. Induction of inflammation by LPS, a major component of certain bacteria cell walls[309], also increases brain uptake of exosomes in some exosome types. Additionally, exosomes are not taken up by all cell types equally, with one study finding that exosomes were preferentially taken up by neurons in pathological brains, as compared to glial cells[308].

While there has been extensive research into the functional effects of CNS-derived vesicles within the brain, there are fewer studies looking at the effects of peripheral exosomes in the CNS[310,311]. One study found that small extracellular vesicles in milk were able to cross the BBB after consumption by mouse pups. Comparing mice fed with milk containing RNA-depleted or RNA-sufficient vesicles revealed differential expression of genes in the hippocampus, and reduced dendritic complexity in the hippocampus of the RNA-depleted-milk mice. The RNA-depleted-milk mice also performed more poorly in tests of spatial learning and memory, and showed increased severity of induced seizure compared to RNA-sufficient-milk mice[287]. Other studies suggest that peripheral exosomes can also impact glial cells[285,312]. Overall, these studies suggest that peripheral extracellular vesicles can alter brain function[310,311].

There are very few studies which look specifically at placenta-derived exosomes and the CNS, and they are primarily conducted in mouse models, which have serious physiological differences compared to humans[106].To date, there is no in vivo evidence of placenta-derived exosomes crossing the BBB. There are two main studies that address localisation of placenta-derived vesicles in mice[313,314]. Both studies had a similar design in that placenta-derived vesicles were injected via tail vein into mice. In Tong et al 2017, the vesicles were derived from human placental explants and injected into pregnant mice. In Nguyen et al 2021, the vesicles were purified from mouse plasma of pregnant and non-pregnant mice and injected into both pregnant and non-pregnant mice.

Tong et al found placental vesicles localised to the lungs, liver, and kidneys of the pregnant mice, and did not observe vesicles in the brain, thymus, heart, spleen, pancreas, skeletal muscle, or foetal-placental unit[314]. Nguyen et al observed that vesicles from pregnant mice localised to the lungs when injected into non-pregnant mice, while vesicles from non-pregnant mice did not, perhaps suggesting some affinity of pregnancy-specific vesicles for the lungs. Vesicles from both pregnant and non-pregnant were detected in the liver. In pregnant mice expressing green fluorescent protein in the placenta, endogenous placenta-derived vesicles were found in the maternal lungs[313].

Some studies find that vesicles derived from placental mesenchymal stromal cells (pMSCs) can have neurological effects[315,316]. pMSCs are a multipotent stem cell type which has been shown to secrete exosomes that could potentially enter the maternal circulation[317,318]. Barzegar et al found that injection of vesicles from human pMSCs protect the brain from ischaemic injury in a mouse model of ischaemic stroke, and Clark et al observed that vesicles from human pMSCs promoted myelin regeneration, protected oligodendrocytes, and improved motor function in a mouse model of multiple sclerosis, a disease characterised by demyelination, inflammation, and neuronal loss[319]. Neither

study investigated whether the vesicles crossed the BBB into the CNS, so it is not clear if this is due to downstream signalling effects or direct activities of vesicles in the CNS. However, these studies provide evidence that non-trophoblast-derived placental vesicles may also impact the CNS and possibly cross the BBB[315,316].

An important study that largely motivated this project is Leon et al 2021[207]. To summarise the key findings, this paper found that preeclamptic plasma increased permeability in a monolayer of female brain endothelial cells, used as a model of the BBB, to high-molecular weight dyes, and reduced transendothelial electrical resistance (TEER) in comparison to normotensive pregnancy plasma. TEER is an established method for estimating the integrity of monolayers, with particular emphasis on tight junction integrity and paracellular resistance[320,321]. Isolated small extracellular vesicles (mostly comprised of exosomes, based on average particle diameter) from preeclamptic and normotensive placental explants reduced TEER, but preeclamptic vesicles caused a greater reduction. Increased permeability was also seen after incubation with preeclamptic vesicles[207]. This study suggested that placenta-derived vesicles may increase the permeability of the BBB in vivo, and to a much greater extent in preeclamptic pregnancies.

Overall, evidence strongly suggests that exosomes can cross the BBB in both directions. The mechanisms of this are not entirely clear, but likely involve transcytosis and paracellular movement. Peripheral exosomes can be taken up by central nervous tissues and drive changes in neuronal and glial behaviour. Both uptake by neurological tissues and crossing of the BBB are influenced by the exosome phenotype and the physiological state of the tissues, particularly inflammation and pathological changes.

3.3 Quantifying Exosomes

There are several methods available for quantifying exosomes, each with its own advantages and limitations. This section will outline the available methods for exosome quantification and then introduce a new method that will be used in this project: the ExoCounter.

3.3.a Existing Methods

Electron microscopy was the first method used to identify exosomes. Transmission electron microscopy (TEM) involves passing a beam of electrons through an ultra-thin specimen. When the beam strikes the specimen, it is not all transmitted, depending on the thickness and electron transparency (allowing electrons to pass through with minimal electron scattering) of the sample. Scanning emission microscopy (SEM) has a similar principle but creates an image by detecting reflected electrons, rather than the transmitted ones. An advantage of electron-based microscopy as opposed to light microscopy is that it can achieve higher resolutions by many orders of magnitude[322,323].

Although electron microscopy is considered a gold standard for verifying the quality of isolated exosomes, there are serious limitations when used for quantification. Firstly, this method is very labour-intensive and has a low throughput[324]. The dehydration and embedding of the specimen are likely to cause exosome loss and therefore underestimate exosome numbers[324–326]. Because of these limitations, electron microscopy is no longer a preferred method for quantifying exosomes[324].

Nanoparticle tracking analysis (NTA) involves illumination of sample particles by laser beam. The light that is scattered by the particles is recorded and analysed according to algorithms to identify particle concentration. The size distribution within the sample is

also calculated. It is also possible to analyse vesicles tagged with fluorescent antibodies to count antigen-specific subpopulations[324,327,328].

One advantage of NTA is that it has higher resolving capabilities than other light scattering methods, particularly the dynamic light scattering method (described later), and can analyse particles with a mean diameter <100nm[329]. There is minimal sample preparation (often just dilution) and samples are reusable. Measurements are rapid once machine optimisation has been completed[330]. The ability to generate data about particle size is another benefit of NTA, as this information is useful in estimating the success of exosome isolation and purification techniques[328].

NTA has limitations. Firstly, it measures more than just vesicles, as it counts any particles that exceed the detection limit, including protein aggregates, cell debris and other contaminants[331]. Furthermore, NTA has a limited range of particle concentration measurements, roughly 10^7-10^9 particles per millilitre. There is little work on standardisation of NTA protocols. Differences in the camera and detection threshold settings, as well as other aspects of the protocol, can introduce variability and complicate comparisons of NTA results obtained from different groups[324,329]. NTA technology requires several optimisation steps, which can be time-consuming[329].

Additionally, NTA has reduced sensitivity for particles smaller than 50nm as the intensity of scattered light decreases with particle diameter so very small particles may disappear below background noise[331]. Another problem stemming from this is overestimation of average vesicle size[331]. This may be exacerbated as NTA measures the hydrodynamic size, which includes both the solid phase of the vesicle but also the solvent that adheres to it. As a result, size measurements from NTA tend to be larger than those from TEM, with the difference between the two decreasing as particle size increases (TEM size is

~50% larger than NTA for 15nm diameter, and only 5% for 100 nm diameter)[331–333]. Furthermore, presence of a small number of much larger particles e.g. dust can cause issues by scattering light[329].

A similar method often used for exosome quantification is dynamic light scattering (DLS). DLS is based on the Brownian motion of dispersed particles (in this case exosomes), which causes fluctuations in scattered light. Scattered light is proportional to particle diameter to the sixth power, meaning that this technique is especially sensitive to large particles. This is an advantage when intending to measure large particles, but contaminating dust particles or aggregates can affect measurements when smaller particles such as exosomes are the intended target[329].

Advantages of DLS include rapid speed of measurements, with a more straightforward and user-friendly procedure than NTA, and can adjust to different sample concentrations, so dilution of the sample is not necessary[324,329]. As with NTA, samples are reusable afterwards. It has a relatively high throughput and gives information on size distribution. However, DLS has a poor ability to distinguish between particle populations that are close in size, particularly when compared to NTA[329]. Where NTA will present multiple peaks of size distribution in a polydisperse sample, DLS struggles to resolve these peaks, and will present a merged version[329].

Flow cytometry is another method used for exosome quantification. Flow cytometry detects suspended particles via their interaction with a laser beam in a detection cell. As particles encounter the beam, they scatter the light. Any fluorophores included in the sample will fluoresce. This is an advantage as flow cytometry can be combined with fluorescent labels for surface proteins to give information on vesicle phenotype[334]. Another advantage of flow cytometry is that it is generally accurate for particles above a

certain size threshold[330]. The issue with flow cytometry is that it is not accurate for particles below 200nm diameter, with some reviews giving an even higher threshold for accuracy e.g. 300nm [330,331]. This presents a clear issue for analysis of exosomes, which fall below this size threshold. To somewhat overcome this limitation and produce a semi-quantitative result, nanobeads can be bound to particles to increase their surface area[330].

An additional consequence of the limited sensitivity for low-diameter particles, is that size distributions will be skewed towards larger particles. Swarming effects can also be seen, where multiple vesicles are detected as a single event, also causing a loss of linearity with dilution[334]. Another issue with flow cytometry is that fluorescent signals are easily influenced by cell debris and cytosolic proteins, meaning that high-purity samples are needed. This can be an issue[326,330], as many methods of exosome isolation are unable to provide such high-purity samples as required[335].

This is not an exhaustive list of methods used to quantify exosomes, but gives an overview of the main methodologies. As well as using exosome quantification methods, some studies use proxy measures of exosome number, for example by measuring expression of protein markers by ELISA or quantified western blotting, or enriched nucleic acids by PCR. These methods have the obvious drawback of interference by protein aggregates, non-exosomal particles and cell-debris, and rely heavily on a successful isolation and purification stage. As explained previously, markers are not consistently expressed in exosome populations and this technique is vulnerable to changes in expression. Inconsistent use of methodologies is a widespread issue in exosome research, which poses problems when drawing comparisons or assimilating evidence from different studies. Even commonly used techniques such as NTA are not standardised across groups. More work comparing and standardising quantification techniques would greatly benefit the field[336].

3.3.b The ExoCounter Assay Principle

JVC Kenwood's ExoCounter is a new device for quantifying populations of exosomes. This section will set out the principle of the ExoCounter assay, but a detailed protocol for the assay is given in the General Methods section.

The ExoCounter assay combines immunoassay techniques with size selectivity to target a specific exosome population. The assay begins by immobilising capture antibodies onto a disc with 12 wells. Capture antibody must be specific for a marker with known expression in the target exosome population. Upon incubation with the test sample, the target exosomes bind the capture antibodies and adhere to the disc. The disc has circular grooves which have a diameter of 260nm at the top and taper to 160nm at the bottom. This prevents particles larger than 160nm from adhering to the disc, reducing interference by microvesicles and other contaminants.

Nanobeads with conjugated labelling antibodies will then be used to detect immobilised exosomes. Again, the conjugated antibodies must be specific for a marker with known expression in the target exosome population. The nanobeads bind to the captured exosomes via the conjugated antibodies and become immobilised on the disc. The nanobeads have a diameter of 200nm, which prevents binding of multiple beads to the same exosome, so that exosomes and beads are immobilised at a 1:1 ratio. The disc is then inserted into a disc-reader, which scans the disc with a laser of wavelength 405nm. The beads refract the light from the laser and the refraction is quantified and converted to pulses by a photodetector. The number of pulses corresponds to the number of beads and therefore the number of exosomes on the disc[337,338].

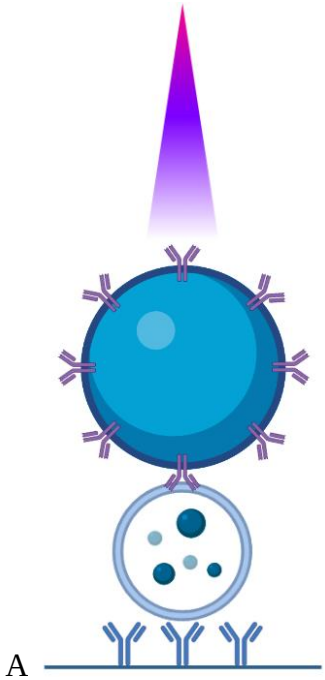

A

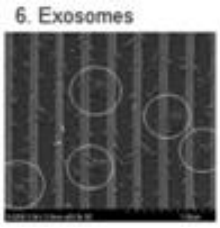

B(a)

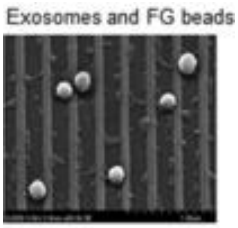

B(b)

Figure 3: Understanding the ExoCounter assay. (A); Diagram illustrating the ExoCounter principle. The horizontal blue line represents the well surface. On the well surface, adhered antibodies (in this project, anti-CD63 antibodies) bind an exosome. This exosome is then bound by an antibody-conjugated bead. This bead is then detected by the ExoCounter device (represented by the purple beam). This diagram is not true to size nor do the relative sizes of the different components reflect real size ratios. (B); Adapted from Kabe et al 2018: scanning electron microscopy images of (a)

immobilised exosomes on the disc and (b) exosomes and conjugated beads immobilised on the disc.

3.3.c Advantages of the ExoCounter Assay

Several samples can be analysed simultaneously by ExoCounter assay. In this project, a maximum of four samples was run per disc, to allow for three repeats and a background measure for each sample. The number of discs that could be run simultaneously was limited to four, because of the number of metal frames we had and the size of our incubator, giving a maximum sample number of 32 per assay. Theoretically, the ExoCounter assay could be scaled up further if not limited by incubator size or metal frames.

The combination of size selectivity and antibody-based detection theoretically reduces interference by contaminants and non-exosomal vesicles, as well as promoting high specificity for the intended target. However, evidence of reduced interference by microvesicles, dust and protein aggregates has not yet been published, so there is a need for experimental evidence of this. This could be achieved by comparing counts of exosomes with and without added contamination.

Kabe et al 2018 performed a characterisation of ExoCounter assay performance compared to other standard techniques. To summarise the findings of the paper, it showed firstly that no primary antibody treatment prevented binding of either exosomes or conjugated beads, suggesting that washing steps are successful in minimising residual unbound particles. Furthermore, discs without antibody coatings did not show pulse signals when measured by the ExoCounter device. When primary antibody and exosomes were added, signal was low without addition of conjugated beads. Additionally, by quantifying

residual unbound exosomes from a disc with bound primary antibody, they found that almost 90% of the exosomes were bound to the disc[338].

Extremely high linearity was shown by the ExoCounter device (R^2 was 0.996 for purified exosomes, 0.955 for serum), and the assay performed better in this respect than ELISA assay and flow cytometry (R^2 was 0.954 for ELISA on purified exosomes, and 0.969 and 0.919 for flow cytometry on purified exosomes and serum respectively). Limit of detection in purified exosomes and serum was determined as the amount of exosomal protein or serum with a signal equal to background. Again, the ExoCounter assay performed better than ELISA and flow cytometry. For purified exosomes, the limits of detection for the ExoCounter assay, ELISA and flow cytometry were 1.16, 926 and 487ng of protein respectively. In serum, the limits of detection for the ExoCounter assay and flow cytometry were 0.39 and 14μl[338].

3.3.d Limitations of the ExoCounter Assay

As with all antibody-based assays, the selectivity and accuracy of the assay is highly dependent on the quality of the antibody. High cross-reactivity or low affinity for intended markers will limit the effectiveness of the ExoCounter technique, and this technique would therefore not be suitable for quantifying exosome populations that do not have well-defined and specific markers, or do not have high-quality antibodies available for those markers. Ideally, antibodies used in the ExoCounter assay should have previously published data supporting their use in identifying this exosome population, and/or data supporting the accuracy of the antibody should be generated by the group before using the antibody in the ExoCounter assay.

Another important aspect to consider is the relatively recent introduction of the ExoCounter assay. Initial findings show significant promise, with high repeatability and sensitivity. Nonetheless, these parameters have been tested in limited contexts: a PubMed search for publications containing the term "ExoCounter" yielded merely four results ("PubMed advanced search, Query box: '(ExoCounter[Title/Abstract]) AND (ExoCounter[Text Word])'"). While all four papers demonstrate the assay's potential, the ExoCounter technology has not been around long enough for thorough experimental analyses of possible limitations, for example understanding how contamination by dust or protein aggregates affects results.

For studies which wish to use the ExoCounter on a sample type that has not been published before or to use a modified version of the protocol should test the performance of the ExoCounter assay. This may include standard tests, such as linearity tests, limit of detection tests and checks of repeatability, but may also include less standard tests, if relevant to the project. In this way, the suitability of the ExoCounter assay for addressing the specific scientific question can be established, and more evidence can be generated on the assay's performance in different biological contexts.

Rationale for the project and hypotheses

As described in earlier sections, healthy and complicated pregnancies are associated with significant and fundamental neurological changes. Preeclamptic pregnancies are associated with neurological dysfunction. Acute neurological symptoms tend to resolve postpartum, but preeclamptic pregnancies increase risk of certain long-term neurological issues. Therefore, it is likely that there are pregnancy-related factors which are biologically active in the CNS.

There is evidence that placenta-derived exosomes can affect various maternal tissues and systems. In preeclampsia the content, number and biological effects of these vesicles are different and may contribute to preeclampsia pathology. There is evidence that BBB permeability is affected in pregnancy, and is increased in preeclamptic pregnancies. Previous research suggests that it is possible for peripheral exosomes of non-placental origin to cross the BBB into the CNS. To date, no human in vivo studies have looked at the possibility that placenta-derived exosomes may reach the CNS.

The ExoCounter assay offers a suitable method for quantifying exosome populations in CSF for the following reasons: it shows high sensitivity and linearity in small volumes of sample, size-exclusion may reduce contamination by non-exosomal particles, antibody-based detection distinguishes between different exosome populations (depending on existence of a suitable marker).

Based on the evidence outlined above, the following hypotheses were drawn up

1. Syncytiotrophoblast-derived vesicles can cross the BBB and be detected in CSF.
2. The ExoCounter assay has high sensitivity with small volumes of sample[338], and will be suitable for detecting placenta-derived vesicles in CSF.
3. Increased BBB permeability in (pre)eclamptic pregnancy, possibly combined with increased numbers of placenta-derived vesicles, leads to increased numbers of these vesicles in (pre)eclamptic CSF.
4. Syncytiotrophoblast-derived vesicles may be biologically active in the neurological system and contribute to complications and changes.

This project focused on hypotheses 1, 2 and 3. To investigate these hypotheses, the project had the following aims.

1. To demonstrate robustness of the ExoCounter assay and assess suitability of the assay for use in CSF. This will include:
    a. Optimisation of the ExoCounter assay protocol.
    b. Demonstration that the ExoCounter assay is reproducible and that background measures can sufficiently correct for inter-assay variation.
    c. Demonstration that the NDOG2 antibody is a suitable marker for placenta-derived vesicles in cerebrospinal fluid, and has minimal cross-reactivity in neurological tissues.
    d. Demonstration that high linearity is retained when used on CSF.
2. Provided that the above aims show suitability of the ExoCounter for use in CSF, to obtain ExoCounter measurements for matched plasma and CSF samples from pregnant women.
3. Analyse obtained data. This will include:
    a. Analysis for associations between ExoCounter data and clinical grouping and other relevant factors.
    b. Determining whether ExoCounter values from pregnant CSF are significantly different to those obtained from non-pregnant CSF.
    c. Analysis for associations between plasma and CSF values.

Chapter 2 focuses on Aim 1 and Hypothesis 2, while Chapter 3 focuses on Aims 2 and 3 and Hypotheses 1 and 3.

Chapter 2 - General Methods

Plasma Samples from the John Radcliffe Hospital, Oxford

Plasma samples were collected from consented patients at the Women's Centre, John Radcliffe Hospital, Oxford. Blood was collected from patients by research midwives and then centrifuged at 1500g, 21°C for 15 minutes, in a swing bucket centrifuge (Beckman Coulter Avanti J-20XP, Beckman Coulter JS-5.3 swing-out rotor). Any visibly haemolysed samples were discarded at this stage; for non-haemolysed samples, supernatant was removed and placed into 15ml falcon tube. Supernatant was spun at 13000g, 21°C for 2 minutes. The supernatant from this centrifugation was then stored in aliquots at -80°C. Where used for ExoCounter, samples were thawed on the day of the assay and centrifuged at 13000g for 2 minutes before being assayed.

Non-Pregnant CSF

Non-pregnant CSF was obtained from the Autoimmune Neurology Group, Nuffield Department of Clinical Neurosciences, University of Oxford.

Non-pregnant CSF was also obtained from BioIVT, product 'Human Cerebrospinal Fluid (Remnant) No Diagnosis', HUMANCSFR-0101364.

Plasma and CSF Samples from South Africa

For CSF samples: lumbar puncture was performed at the time of caesarean section. CSF then drips directly into the collection tube, and was transferred into a Sarstedt polypropylene tube. CSF that was visibly contaminated by blood was discarded and CSF

was tapped into a new tube once the bleeding had stopped. CSF was then centrifuged at 2200 x g for 10 minutes at 20°C. Sample was then aliquoted into cryotubes (Sarstedt, no. 72.377 or 72.377.007) and frozen at -80°C.

For plasma samples: blood was collected into EDTA-K2 tubes. Plasma was centrifuged at 2200 x g for 10 minutes at 20°C. Sample was then aliquoted into cryotubes (Sarstedt, no. 72.377.005) and frozen at -80°C.

Samples were transferred to Oxford under HTA Licence 12217.

Placental Perfusion and Ultracentrifugation

Placentas were obtained from pregnant women undergoing elective Caesarean sections before labour onset at the Women's Centre, John Radcliffe Hospital, Oxford. Written informed consent was obtained before placenta collection. Placentas were perfused within 20 minutes of delivery, having been transported to the laboratory in warm Hank's solution. The umbilical cord was clamped, and excess was cut off and discarded. The membrane covering the foetal side was pulled away. An intact peripheral lobe with no identifiable villus breakage was chosen, and the umbilical artery and vein associated with that lobe identified. Sutures are applied to prevent flow of blood from the umbilical cord to the cannulation area. The artery and vein were cannulated and secured.

The lobe was perfused with 0.1 μm filtered medium (Medium 199 with Earle's salts, L-glutamine and sodium bicarbonate, liquid, sterile-filtered (Sigma Life Science) containing 0.8% dextran 20, 0.5% bovine serum albumin, and 5000U/L sodium heparin), at a rate of 5ml/min and exudate collected in a cylinder and measured to calibrate the system. The whole placenta was then inverted, with the maternal surface facing up and

laid in a Perspex water jacket warmed to 37°C. The maternal surface was then perfused with filtered medium (as above, but without dextran, and continually oxygenated), through six 1.7mm foetal feeding tubes pushed into the lobe. Both the foetal and maternal circuit are initially run 'open' to remove excess red blood cells. Following this, the circuits were closed by recycling measured foetal medium from the cylinder back into the foetal reservoir. The volume of foetal effluent was measured throughout the perfusion to ensure that the circuit was intact. Perfusion was continued for three hours at a 4 to 5 ml/min flow rate to obtain perfusate.

After three hours, perfusate was centrifuged twice at 1500g for 10 minutes at 4°C in a Beckman Coulter Avanti J-20XP centrifuge with a Beckman Coulter JS-5.3 swing-out rotor to remove cell debris. The supernatant was then pooled and spun at 10,000g in a Beckman Ultracentrifuge SW32 Ti Swinging-Bucket Rotor at 4°C for 30 minutes. The resulting supernatant was then centrifuged at 150,000g at 4°C for 30 minutes. The exosome-enriched pellet was washed and resuspended in filtered (through a 0.1um membrane) PBS to a concentration of 2 to 5 μg/μl (BCA measurement) and stored at -80°C.

Bicinchoninic Acid (BCA) Assay

Protein standards at concentrations 1, 0.5, 0.25, 0.125, and 0.0625 mg/ml were prepared in advance of the BCA assay from bovine serum albumin stock of known protein concentration. Samples were diluted with distilled water to a concentration estimated to be within those of the protein standards (plasma samples were diluted 1 in 200). All samples, standards and blanks were run in duplicates.

12.5µl of sample, standard or blank (distilled water) was pipetted into each well on a 96 well plate (Nunclon Delta Surface, ThermoFisher). BCA Reagent B was mixed into Reagent A (both Pierce) in a 1 in 50 concentration (B being the lesser component). The plate was covered with aluminium foil, mixed for 30 seconds on a plate shaker, and incubated for 30 minutes at 37°C. The plate was then allowed to cool to room temperature before absorbance at 562nm was read using a FLUOStar OPTIMA (BMG) plate reader. Absorbance readings were converted to protein concentrations using the standard curve produced from the absorbance readings of the known concentration standards. Concentration of diluted samples was then scaled up to the undiluted value.

Western Blotting

A known concentration (as determined by BCA) of sample was mixed with 4x Laemmli buffer with 5% 2-mercaptoethanol, and diluted with double distilled water. Sample mixes were then warmed at 95°C in a heating box for 10 minutes, before being centrifuged for 1 minute at 9000rpm. Samples were loaded onto NuPAGE TM 4-12% Bis-Tris Gel 1.0 mm x 10 well gels (Invitrogen by ThermoFisher Scientific), along with Precision Plus Protein Dual Colour Standards (Bio-Rad), within a Novex minicell tank (Invitrogen, UK) filled with NuPAGETM MOPS SDS running buffer (Novex by Life Technologies). Electrophoresis was then run at 150V until the proteins were near the bottom of the gel. Following electrophoresis, proteins were transferred onto a polyvinylidene fluoride membrane (Immuno-Blot PVDF Membrane, Bio-Rad). The membrane and gel were sandwiched between four filter papers soaked in anode 1, two soaked in anode 2, and, on the other side of the gel and membrane, three soaked in cathode buffer solution. Protein transfer was completed by running at 25V for 45 minutes.

Buffer solution	Composition	pH
Anode 1	300mM Tris, 10% methanol	10.4
Anode 2	25mM Tris, 20% methanol	10.4
Cathode	25mM Tris, 40mM e-aminohexanoic acid, 20% methanol	n/a

Table 3: Composition of buffer solutions used in Western blotting protocol

Successful protein transfer was checked by soaking the membrane in Ponceau S Staining Solution (ThermoFisher), according to manufacturer instructions. Ponceau stain was then washed by soaking in TBST (10xTBS stock diluted 1 in 10 in double distilled water, 0.1% Tween20). The membrane was then blocked with 5% skim milk powder (Sigma Aldrich) diluted in TBST for 45 minutes. The membrane was then placed in a falcon tube containing 5% milk powder with primary antibody at 1 in 1000 concentration. This was incubated in a roller overnight at 4°C.

The next day, the membrane was washed thrice in TBST for 5 minutes, and then incubated with the corresponding secondary antibody (HRP-conjugated anti-mouse or anti-rabbit antibody, Cell Signalling Technology) at 1 in 1000 concentration in 5% milk solution for 1 hour. After 1 hour, the membrane(s) was washed thrice in TBST for 5 minutes. The membranes were then treated with EZ-ECL chemiluminescence detection kit for horseradish peroxidase (HRP) (Pierce ECL Western Blotting Substrate) for one minute, before transfer to a cassette.

The membrane was then incubated with Cl-Xposure Film (Thermo Scientific) for 1 minute (time can be altered according to signal intensity) in the dark. Film was developed

by soaking in developer solution (Champion Devalex XD2 Developer) rinsing in double distilled water and soaking in fixer solution (Champion Fixaplus X-ray Fixer). Developer and fixer solution were prepared as such: for developer, 125ml Devalex A, 10ml Devalex B, 12.5 Devalex C, and 352.5ml distilled water; for fixer: 120ml Fixaplus A, 22.5ml Fixaplus B, 357.5ml distilled water. Following development and fixing, film was left to dry then scanned.

Total protein from Ponceau S staining and band intensity in the final blot were quantified using ImageJ. Briefly, the image was inverted, background subtracted, and intensity was measured.

Nanoparticle Tracking Analysis (NTA)

NTA was performed using NanoSight NS500 system (Malvern Instruments, Malvern, United Kingdom). Fluidics were primed with PBS (Dulbecco's phosphate buffered saline, Sigma Aldrich), and quality control performed using 100nm silica beads (Polysciences Inc.) diluted in fPBS. Samples were injected into the sample chamber via a 1ml syringe. Laser beams are directed at the samples in the sample chamber, where they illuminate the particles. The illuminated particles are then visualised using a standard optical microscope. Captured images were analysed by NTA software to calculate particle size and concentration.

ExoCounter Assay

The ExoCounter (JVCKENWOOD corp.) assay in performed on a plastic disc provided by JVCKENWOOD with 16 'wells'. Samples were analysed in triplicates, with a fourth

well being used for background measurement for each sample. Firstly, 90µl of primary antibody was incubated in each well at a concentration of 5ug/ml for 1 hour at 37°C with a plate cover. The wells were washed with 3x300µl of fPBST (filtered phosphate-buffered saline with 0.05% Tween20). Each well was filled with 200µl of blocking buffer (1% casein, diluted in PBST) and incubated at room temperature for 1 hour with a plate cover. After this hour, the disc was again washed with 3x300µl PBST. 50µl of sample was applied to each well, with plasma being diluted 1 in 4 in PBST. The disc was incubated for 2 hours at 37°C with a plate seal on a plate shaker, then washed as before. 50µl of antibody-bead solution (JVCKENWOOD) at a concentration of 20µg/ml, diluted in 1% casein in PBST, was added to each well and the disc was incubated for 90 minutes at 37°C on a plate shaker, with a plate seal. Finally, the disc was washed with 3000µl PBST, followed by 3000µl double-distilled water to prevent salt crystal formation, then set to dry for 15 minutes at 37°C.

At this point the disc could be read by the optical system. In brief, this uses a Blu-ray laser device to convert diffraction of light caused by the beads attached to the disc into an exosome count. Corrected counts were calculated by subtracting the background count from the mean raw count of the triplicate. Where two of the three raw counts within a triplicate were very close in number and the third was not, the third was considered an outlier. To avoid subjectivity when removing outliers, outliers were only removed if these conditions were satisfied:

- The largest of the two ‘non-outliers’ was no more than 130% of the smaller ‘non-outlier’.
- The difference between the average of the ‘non-outliers’ and the ‘outlier’ was at least three times larger than the difference between the two ‘non-outliers’.

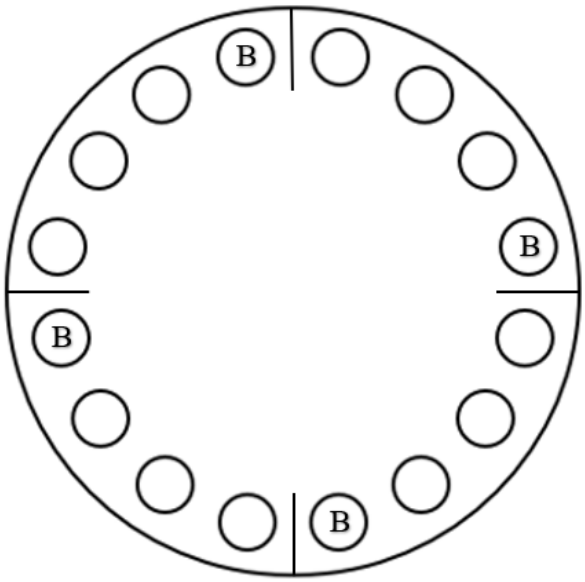

Figure 4: Example of ExoCounter disc layout. Each smaller circle represents a well. B = background.

Human Anti-Mouse Antibody Enzyme-Linked Immunosorbent Assay (HAMA ELISA)

ELISA was performed using the LEGEND MAX^{TM} Human Anti-Mouse Ig (HAMA) ELISA Kit according to supplier instructions. Briefly, the Wash Buffer was diluted 20X in deionised water. The lyophilised HAMA Standard was reconstituted to 1000ng/mL in Assay Buffer A, incubated at room temperature for ten minutes, then vortexed. Lyophilised Matrix A was reconstituted by adding 3mL of deionised water into the vial, incubated at room temperature for 15 minutes. The lyophilised Quality Controls were reconstituted by adding 400 and 650µl Assay Buffer A to each vial respectively, as directed by the specific labels. These were incubated for 10 minutes at room temperature, then vortexed. All standards and samples were run in duplicates, and samples were not diluted. Serial dilution of standards was performed to produce standards of the

concentrations 250, 125, 62.5, 31.3, 15.6, 7.8, 3.9 ng/mL. Neat Assay Buffer A was used as a zero standard.

The ELISA plate was washed 4 times with 300µl of 1x Wash Buffer per well, and residual buffer was blotted onto absorbent paper. 50µl of Mouse Ig Conjugate was added to each well. 25µl of reconstituted Matrix A was added to the standard and quality control wells, and 25µl of Assay Buffer A was added to the sample wells. Then, 25µl of standard, quality control or sample was added to the standard, quality control and sample wells respectively. The plate was sealed with the provided plate sealer and incubated at room temperature for 2 hours, while shaking at 200rpm. The plate contents were then discarded and the plate washed 5 times with 1x Wash Buffer, as done earlier. In the final wash, the wells were soaked for 1 minute.

100µl of Substrate Solution C was added to each well and incubated for 15 minutes in the dark. The reaction was then stopped by adding 100µl of Stop Solution to each well. The absorbance was read at 450nm using CLARIOstar (BMG LabTech). Readings were converted to antibody concentrations based on the standard curve using BMG LabTech's data analysis software MARS.

Statistical Analysis

Statistical testing was performed using IBM SPSS and GraphPad Prism software.

Antibodies Used in This Project

Target antigen	Application	Supplier
CD63	ExoCounter	BioLegend Inc
PLAP	ExoCounter, western blotting	In-house antibody (NDOG2)
Beta-actin	Western blotting	Life Technologies Limited
Vinculin	Western blotting	Sigma-Aldrich

Table 4: Antibodies used in this project.

Chapter 3 - Optimising and Characterising the ExoCounter Assay

1. Optimising the ExoCounter Protocol and Determining Dependence on Intact Exosomes

Initial runs of ExoCounter showed very high variation within the three wells of the same sample ('intra-triplicate' variation) on the first disc, while this issue was not seen where a second disc was run. High intra-triplicate variation suggests suboptimal function of the ExoCounter assay, as the readings from the same sample should be relatively similar. It was found that double priming of the JVCKENWOOD ExoCounter washing device significantly reduced intra-triplicate variation on the second disc ($p<0.02$), with no difference seen in the mean deviation on the second disc ($p>0.95$) (Fig. 5A).

Secondly, different concentrations of casein blocking solution were tested to reduce background without reducing signal (Fig. 5B). It was found in two samples that a blocking solution with 0.1% casein in PBST performed better than 0.01% casein in PBST, effectively increasing the corrected signal (the mean raw signal after subtraction of the background signal) by reducing the background signal. This difference was not significant ($p=0.09$), but 0.1% casein blocking solution was used from now onwards.

In addition, it was important to make sure that the ExoCounter assay was really detecting intact lipid-bound exosomes. Possible mechanisms of exosome-independent PLAP-bead retention could potentially include cross-linking of CD63 antibody and PLAP-beads by protein aggregates, insufficient washing to remove excess bead from the wells or direct binding between CD63 and PLAP-beads. Diagrams of possible mechanisms of exosome-independent bead retention can be seen in Fig. 5C.

To test the possibility of exosome-independent signal, the following experiment was carried out. Placenta-derived exosomes extracted by placental perfusion and ultracentrifugation were spiked-in to a non-pregnant plasma sample. One aliquot of this sample was treated with 1% NP-40 (ThermoFisher) diluted in filtered PBST. A second aliquot was treated with an equal volume of PBST, without NP-40. Both aliquots were then incubated at 37°C for 30 minutes before being tested by ExoCounter assay in the usual way. NP-40 is a surfactant used to disrupt lipid membranes such as those of exosomes[339,340]. If the ExoCounter detects intact exosomes, the count observed in the membrane-disrupted NP-40 sample should be significantly reduced compared to the other sample.

This was exactly what was observed (Fig. 5D), with the NP-40^{+} sample having only 2.15% of the NP-40^{-} sample count. This experiment showed that ExoCounter signal is significantly reduced following membrane disruption ($p<0.0001$). The small signal observed in the NP-40-treated sample is likely due to a combination of incomplete exosome disruption and exosome-independent signal e.g. incomplete removal of the beads through washing and cross-linking by protein aggregates.

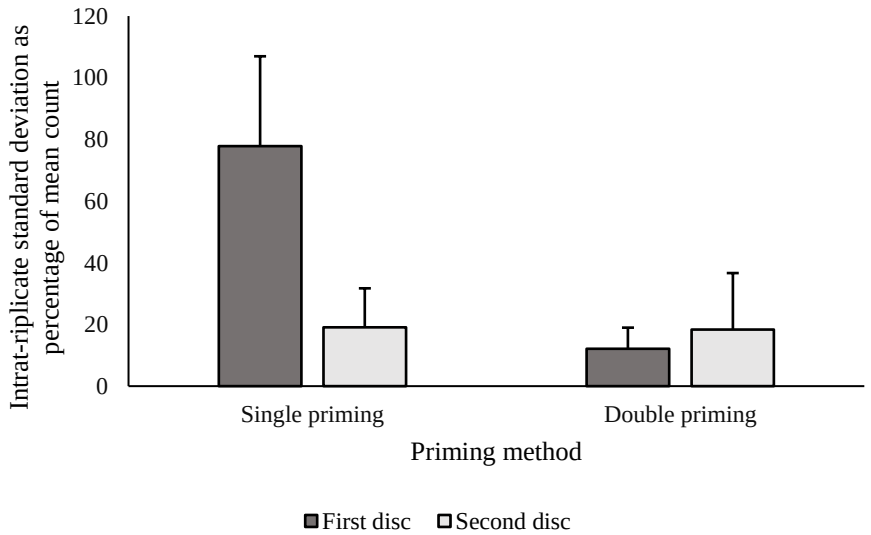

A

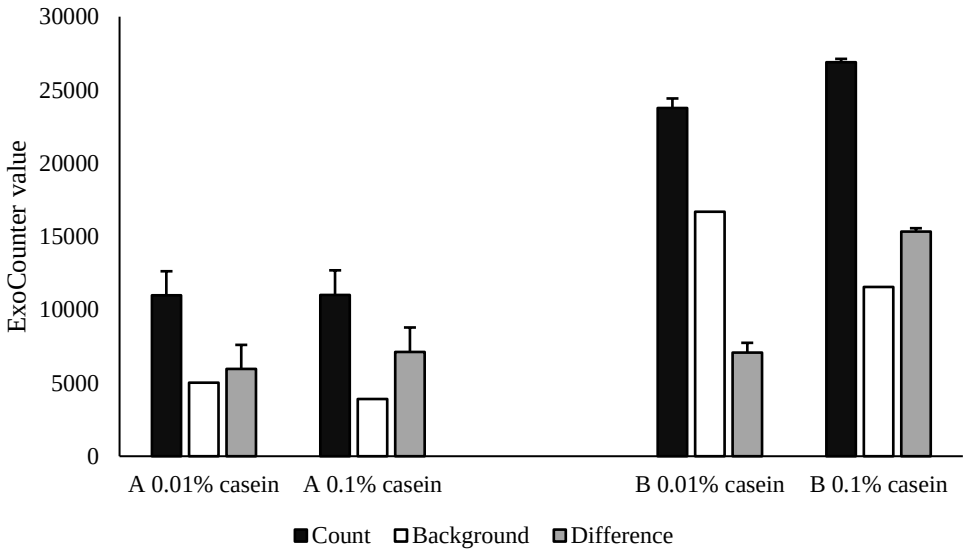
30000
25000
20000
15000
10000
5000
0
ExoCounter value
A 0.01% casein
A 0.1% casein
B 0.01% casein
B 0.1% casein
Count
Background
Difference

B

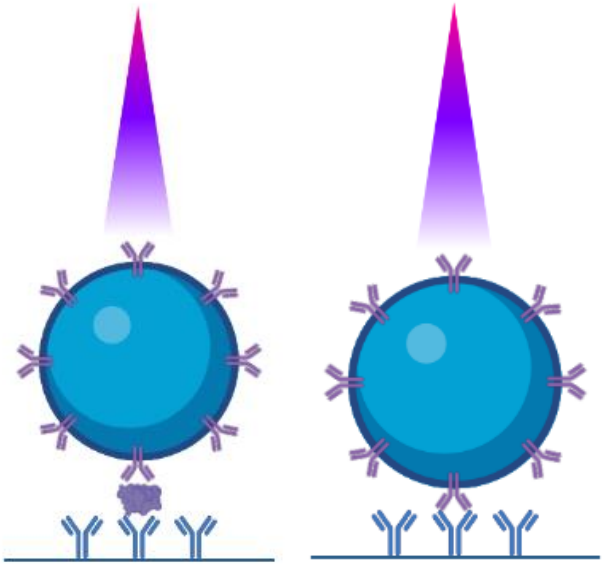

C

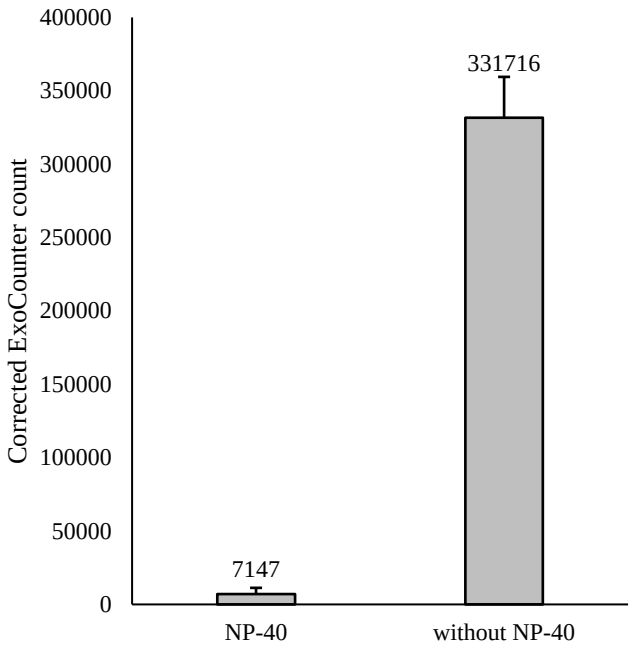

D

Figure 5: Optimisation of ExoCounter assay protocol and effects of NP-40. Error bars represent standard deviation. (A); graph showing the effects of double priming of the ExoCounter washing device on intra-triplicate standard deviation, as a percentage of overall count. For each bar (e.g. first disc, double priming), n=3 discs/12 triplicates. (B); graph showing the effects of 0.01 and 0.1% casein blocking solution on raw count, background count and the corrected count in two samples (A and B). (C); diagrams showing possible exosome-independent mechanisms of signal. The first diagram shows the secondary bead bound by protein aggregates, and the second shows direct binding between the coating antibody and the secondary bead. (D); graph showing the corrected counts of exosome samples with and without NP-40.

2. Testing for Cross-Reactivity of the NDOG2 Enzyme

The anti-PLAP antibody used to detect placental exosomes was NDOG2, an in-house antibody. This has previously been tested for cross-reactivity against multiple tissues (unpublished data from the Vatish group and Sunderland et al 1984[341]), with minimal

cross-reactivity found. Of note, Sunderland et al did find reactivity of the NDOG2 antibody against the cervix, lung, fallopian tube, and thymus, as well as the placenta. RNA analysis confirms that PLAP is expressed in the cervix, lung, and fallopian tube, although not in the thymus. There was low but non-zero expression found in neurological tissues[342]. No reactivity of the antibody was found for testes, duodenum, colon, adrenal and pituitary glands, liver, myometrium, heart, kidney, and tonsils. Therefore, while PLAP is enriched in the placenta and placenta-derived vesicles, it is not an entirely placenta-specific marker, and low levels of signal in non-pregnant samples may be expected but should be significantly lower than those in pregnant samples.

As this project would focus heavily on CSF, it was important to understand how NDOG2 reacts with neurological tissues. Reactivity of the NDOG2 antibody with neurological tissues had not been previously tested. Quantified western blotting was performed to determine reactivity of the NDOG2 antibody to neurological tissues. Beta-actin and vinculin were added as loading controls, but PLAP signal was normalised to total protein rather than beta-actin or vinculin signal, based on the recommendations of several papers[343–348].

Neat non-pregnant CSF was tested against PLAP. This posed problems as the protein concentration of cerebrospinal fluid is typically very low[349], and there was insufficient sample available for protein concentration or BCA testing. Maximum sample volume was added in the cerebrospinal fluid lane, and a minimum possible total protein was calculated based on reported ranges of CSF protein levels. Placental lysate was loaded alongside CSF as a positive control. Protein concentration of placental lysate was calculated by BCA, and the protein loaded matched the minimum possible protein calculated for the CSF.

In addition, PLAP was tested against tissues that contribute to CSF formation. Three non-pregnant plasma samples were tested, to represent the contribution of the peripheral circulation to CSF formation, and brain lysate was tested, representing the neurological contribution to CSF. Placental lysates and exosomes extracted by perfusion were used as positive controls.

As expected, the placental exosomes showed the highest normalised signal, followed by placental lysates. All non-pregnant samples showed significantly lower signals compared to placental lysate ($p<0.01$). The brain lysate showed a marginally higher signal than the CSF and plasma, possibly due to the very low but non-zero expression of PLAP in brain tissues described above. If this was the reason, it did not appear to affect PLAP signal within CSF, which had a very similar signal to non-pregnant plasma. This is consistent with previous findings that plasma is the main contributor to CSF protein content.

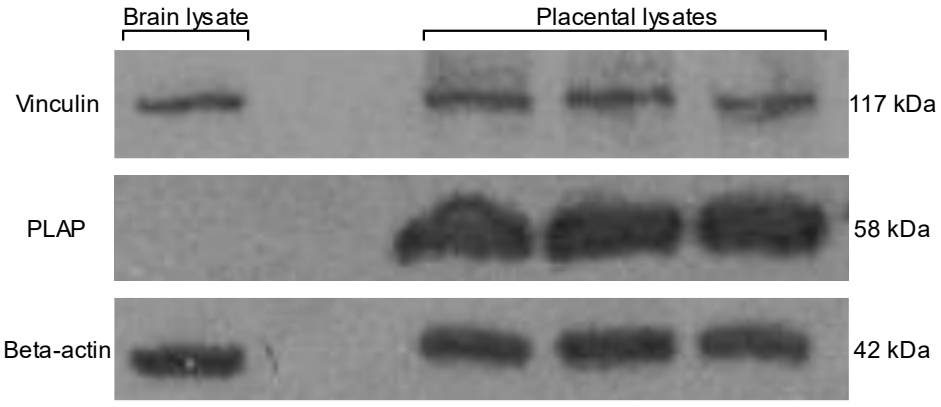

A

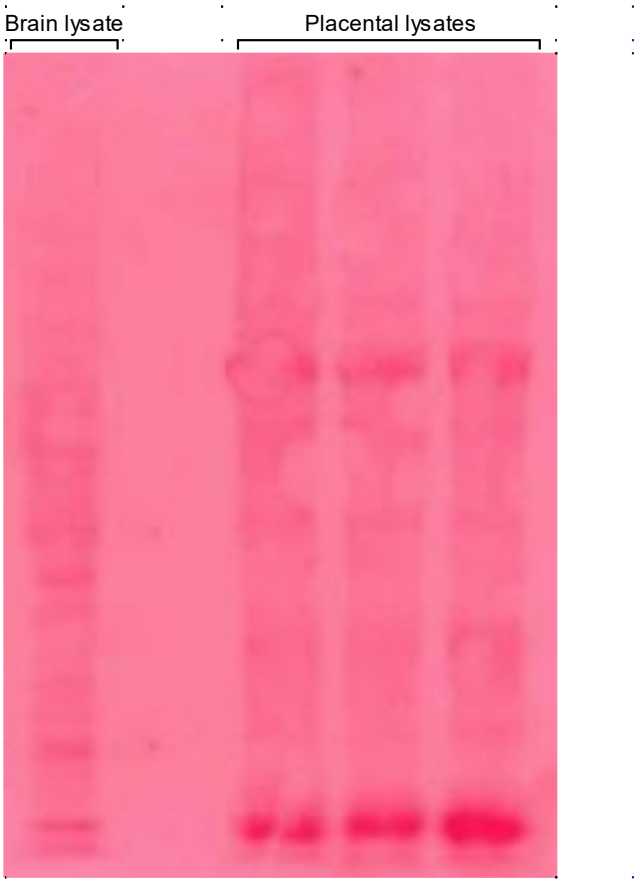
Brain lysate
Placental lysates

B

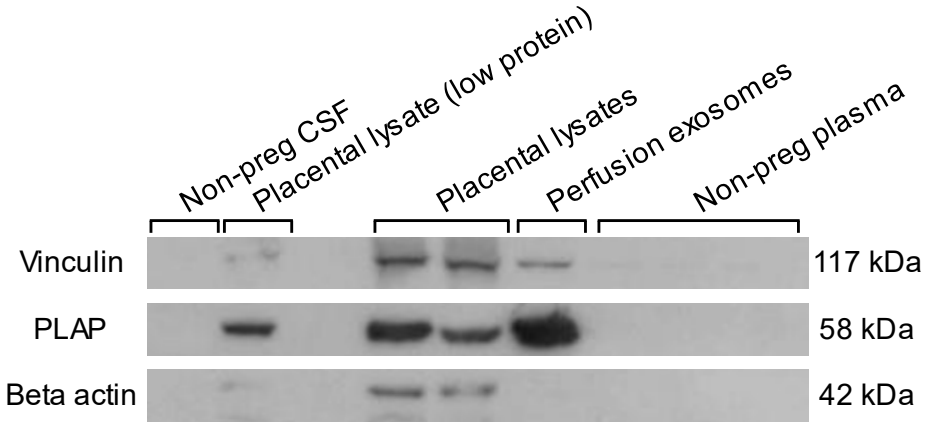
Non-preg CSF
Placental lysate (low protein)
Placental lysates
Perfusion exosomes
Non-preg plasma
Vinculin
PLAP
Beta actin
117 kDa
58 kDa
42 kDa

C

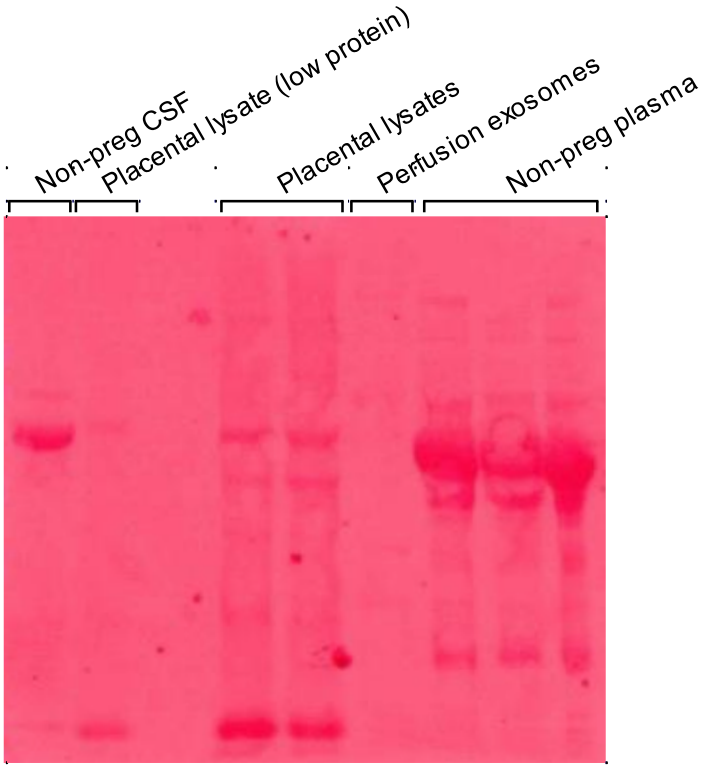
Non-preg CSF
Placental lysate (low protein)
Placental lysates
Perfusion exosomes
Non-preg plasma

D

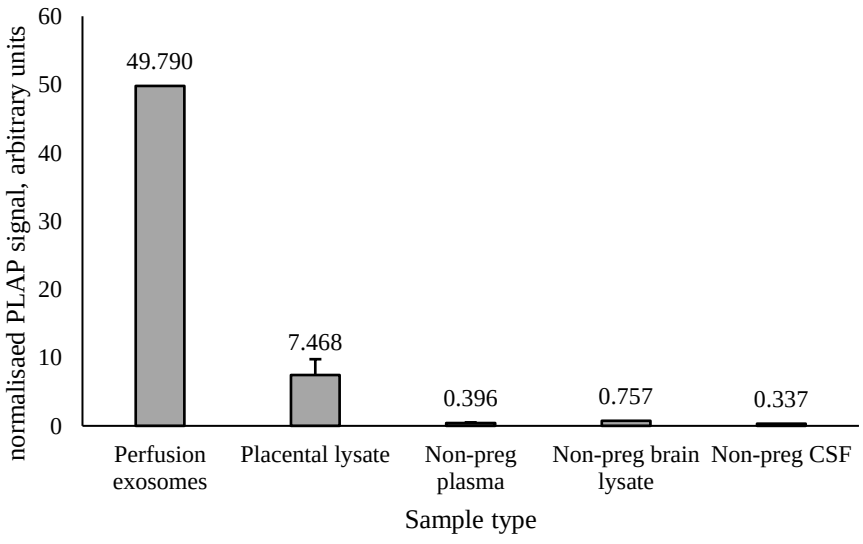
normalisaed PLAP signal, arbitrary units
60
50
40
30
20
10
0
49.790
7.468
0.396
0.757
0.337
Perfusion exosomes
Placental lysate
Non-preg plasma
Non-preg brain lysate
Non-preg CSF
Sample type

E

Figure 6: Western blots and Ponceau S stains of different sample types. Error bars represent standard deviation (A); western blot of three placental lysates and brain lysate against PLAP, (B) shows the corresponding Ponceau S stain for total protein, as used for normalisation. (C); western blot of multiple sample types against PLAP and (D) the corresponding Ponceau S stain. (E); the quantified PLAP signals of different samples, normalised to total protein (Ponceau S).

3. Reproducibility of the ExoCounter Assay and Impact of Freeze-Thaw Cycles

Reproducibility of the ExoCounter assay was tested by running the same sample multiple times on different days (Fig. 7A). To reduce the impact of freeze-thaw samples, following the first run, the sample was split into aliquots that could then be run on three different days with no added freeze-thaw cycles. Following the first freeze-thaw cycle, the ExoCounter result remains very consistent for the sample (coefficient of variation <6). Breaking down the corrected signal into raw count and background count shows the importance of the background count in correcting for inter-assay variability (Fig. 7B). The raw count is much less consistent between runs, but the shape of the background count mirrors that of the raw count, resulting in a very consistent corrected count.

The initial decrease in count between runs 1 and 2 of 20.7% is fairly consistent with data from four other samples that were run twice with a freeze-thaw cycle in between (Fig. 7C). These samples had an average decrease of 37.05% (SD: 15.1%, p=0.032) between runs. This is also consistent with literature on the impact of freeze-thaw cycles on small EV yield[221], with Gelibter et al 2022 finding a 44% reduction in small EV yield after a freeze-thaw cycle[222]. Given the impact of freeze-thaw cycles on exosome yield, care was taken to limit freeze-thaw samples in the South African samples used later on.

To test the reliability of the ExoCounter disc-reading technology, two discs were run three times consecutively (Fig. 7D). Variation between the reads was very small, although a small decrease was seen with each read. This may be due to minor damage from the laser used or a result of increased drying. Furthermore, repeated reading of the same disc over almost 7 weeks showed that a large proportion of the signal is retained on the disc long-term (Fig.7E). Again, a small but consistent decrease is seen over time, at an average rate of 0.4% of the original signal per day. Notably, the standard deviation (of the proportion of original) increases with time ($p<0.001$), as some wells retained signal much better than others (Fig.7F). It is not clear what causes this disparity, with no correlation between signal retention and original signal, and no difference between background and non-background wells.

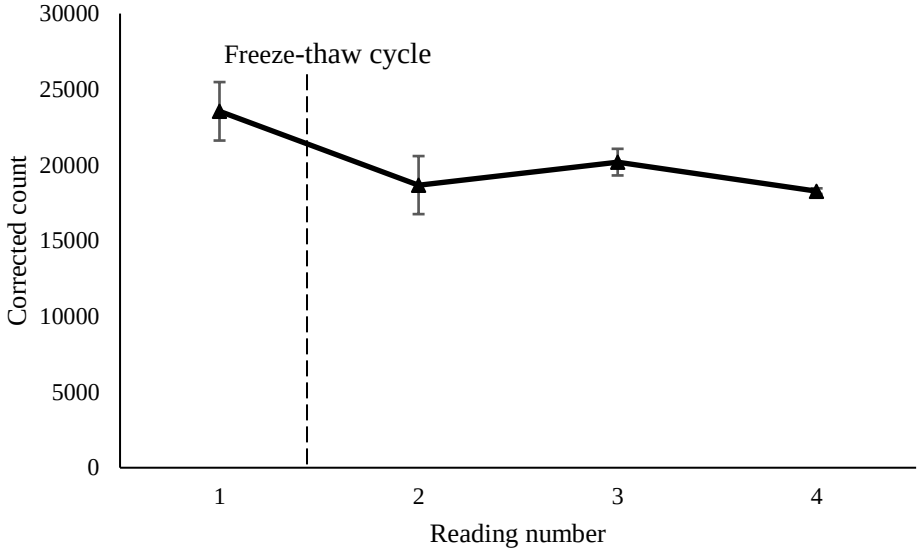

A

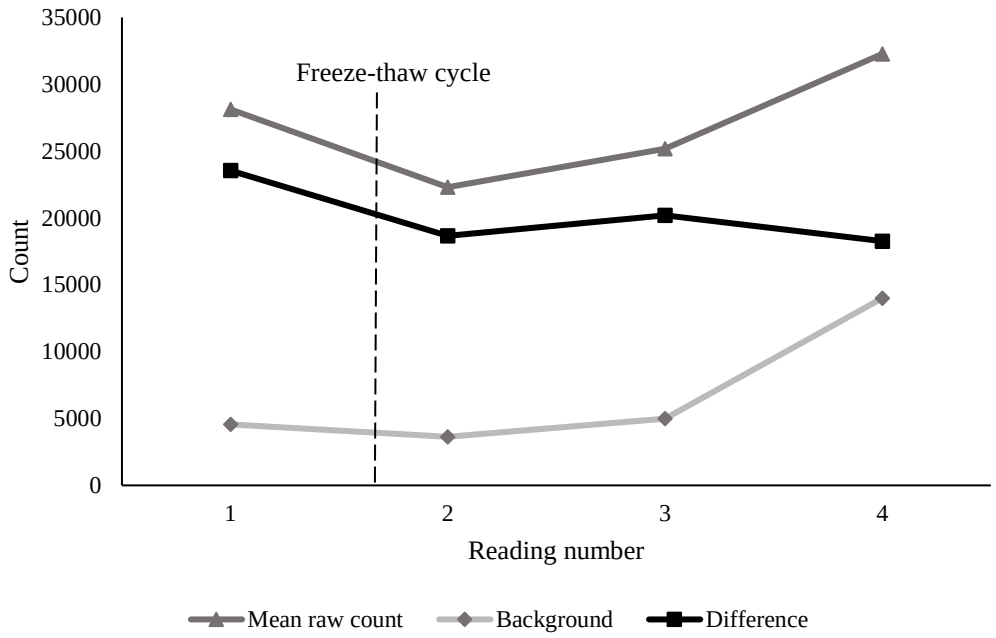
35000
30000
25000
20000
15000
10000
5000
0
Count
Freeze-thaw cycle
1
2
3
4
Reading number
Mean raw count
Background
Difference

B

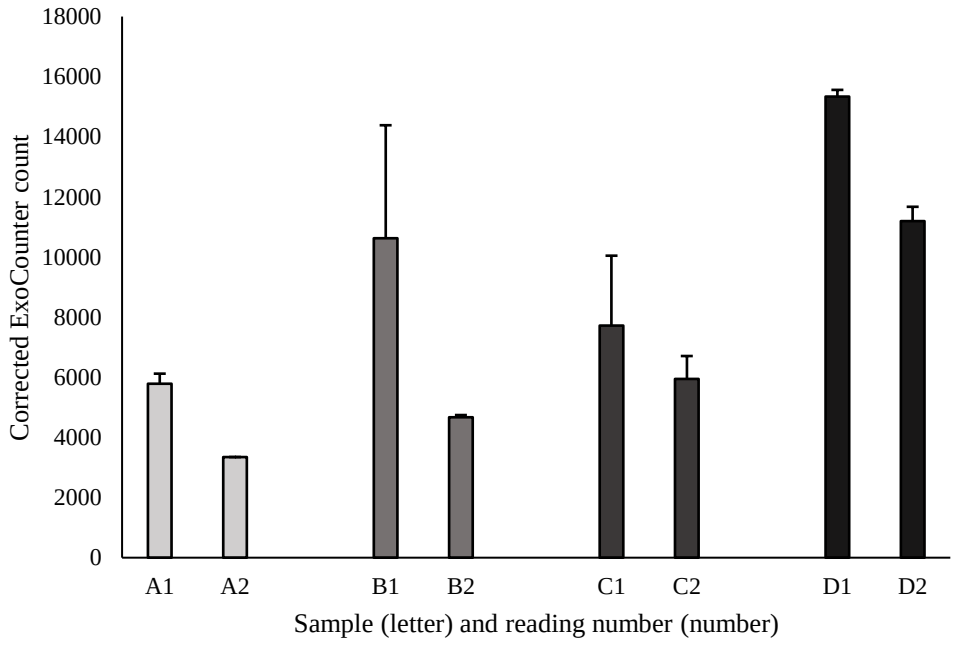
18000
16000
14000
12000
10000
8000
6000
4000
2000
0
Corrected ExoCounter count
A1
A2
B1
B2
C1
C2
D1
D2
Sample (letter) and reading number (number)

C

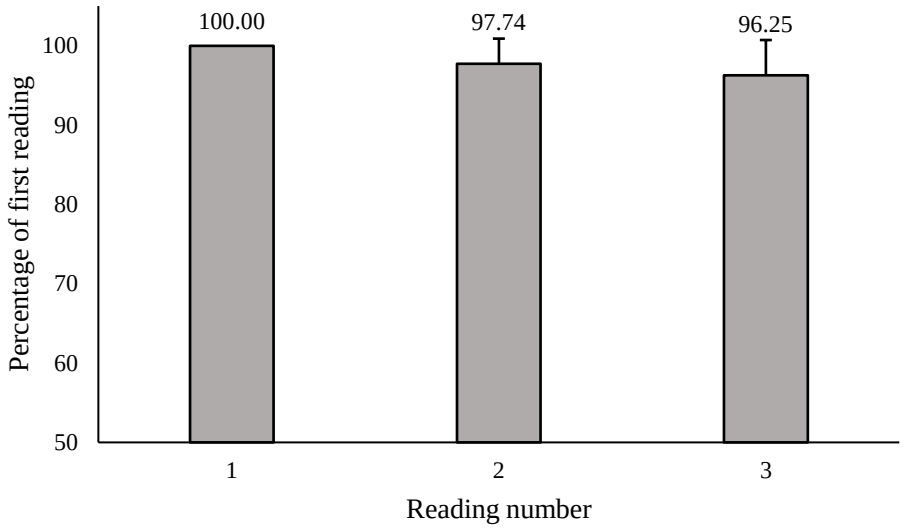
100.00
97.74
96.25
100
90
80
70
60
50
Percentage of first reading
1
2
3
Reading number

D

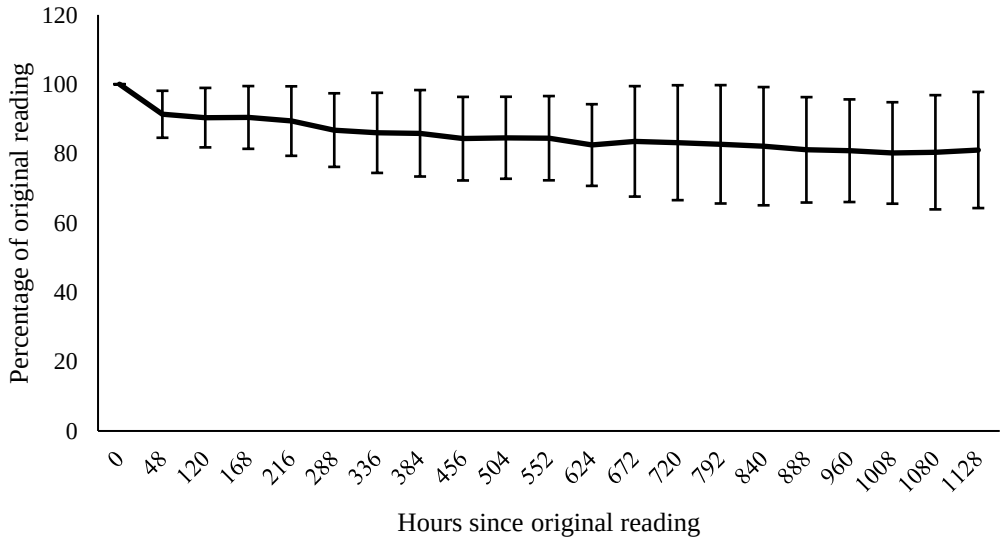
120
100
80
60
40
20
0
Percentage of original reading
0
48
120
168
216
288
336
384
456
504
552
624
672
720
792
840
888
960
1008
1080
1128
Hours since original reading

E

F

Figure 7: Testing reproducibility and the effects of freeze-thaw cycles. Error bars represent standard deviation. (A); graph showing the corrected counts of the same sample run four times, with one freeze-thaw cycle shown by the dotted line. (B); the same sample, with background and raw counts shown. (C); graph showing the corrected counts of four samples before and after a freeze-thaw cycle. For all samples, the first sample was run in October, and the second in January, with the sample stored at -80°C in between. (D); graph showing the counts of two discs read three times consecutively. Counts are shown as a percentage of the original count. (E); graph showing changes in counts obtained from the same disc read repeatedly over several weeks. (F); graph showing the change in standard deviation of the same disc as in (E), demonstrating increasing variation in the retention of signal by different wells.

4. Linearity testing

One of the most important parameters for assessing assay performance is linearity[350], which is defined by the ICH Q2A guideline as the 'ability (within a given range) to obtain

the test results, which are directly proportional to the concentration (amount) of the analyte in the test sample'[351]. JVCKENWOOD already demonstrated that the ExoCounter displayed a high linearity of >0.99 in their 2018 paper[338]. However, there were slight changes in the assay protocol used by JVCKENWOOD compared to the protocol used in this project (see table below). Furthermore, it was important to show linearity in samples relevant to those used in this project and using the CD63-PLAP antibody combination.

	JVCKENWOOD 2018[338]	*This project*
Diluent for coating antibody	Carbonate-bicarbonate buffer (pH 9.6)	Filtered PBS
Incubation of coating antibody	Overnight at 4°C	1 hour at 37°C
Blocking solution	1% skim milk in PBST	0.1% casein in filtered PBST
Incubation of antibody-beads	2 minutes under a magnetic field	90 minutes at 37°C, shaking

Table 5: Key differences between the ExoCounter protocols used in JVCKENWOOD's 2018 paper and this project.

Firstly, linearity was tested on different dilutions of plasma in fPBST, between 1 in 4 to neat, to ensure that dilution of plasma would not obscure obtained values. Linearity was found to be high for the full range of dilutions (Fig. 8A), with an R^2 coefficient >0.98. Both background and raw signals also showed high linearity (Fig. 8B).

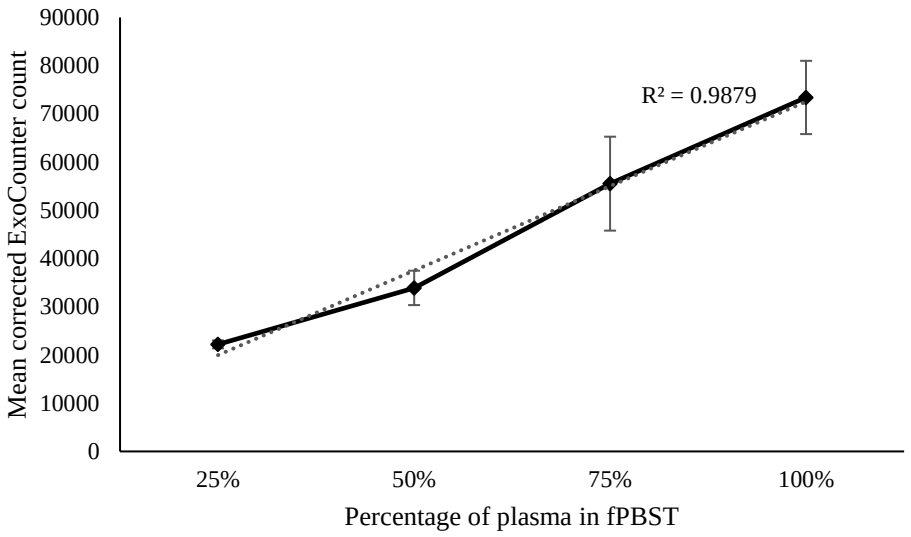

A

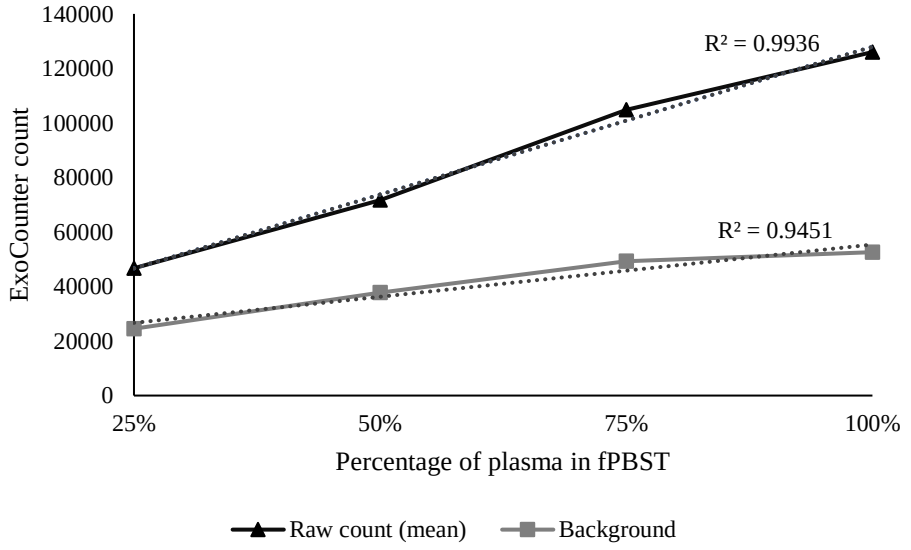

B

Figure 8: Initial linearity tests with diluted plasma. Error bars represent standard deviation. (A); graph showing corrected ExoCounter values for different dilutions of plasma. (B); graph showing the raw and background counts of the same dilutions of plasma.

Linearity was then tested using a series of 'exosome spike-in' experiments. These experiments used exosomes isolated by placental perfusion and ultracentrifugation, as described in the Methods chapter. Isolated exosomes were aliquoted and tested by nanoparticle tracking analysis for an estimate of particle size and concentration. The modal diameter of particles was 152.8nm, which is consistent with exosomes. Secondly, the protein concentration of isolated exosomes was tested by BCA, which gave a concentration of 2.689 mg/ml. A known concentration of isolated exosome can then be spiked into either non-pregnant CSF or 25% non-pregnant plasma (diluted in fPBST), and the sample was then tested by ExoCounter assay.

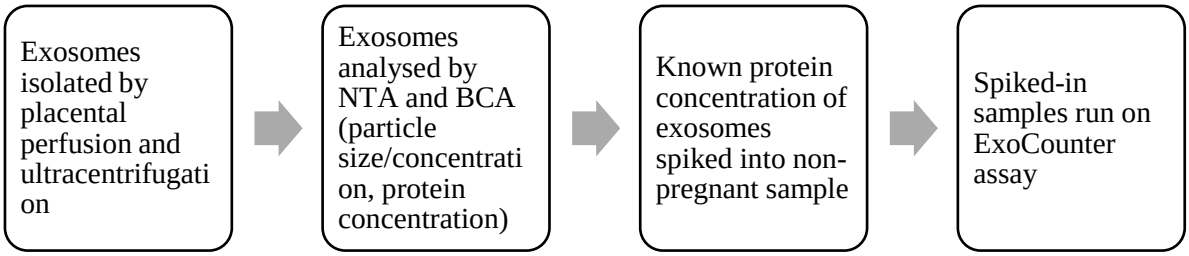

Figure 9: Workflow of spike-in linearity tests.

A previous paper by Jiang et al 2023[337] suggested that linearity plateaus at an upper boundary between 1 and 3μg protein per well, and a lower boundary between 0.04 and 0.001μg. Considering variation in exosome samples, and the use of different diluents (PBST in Jiang et al versus plasma and CSF in this project), it was decided to repeat the spike-in experiment over a wide range of protein concentrations, to get an estimate of the upper linearity range for subsequent spike-in experiments.

The results of this experiment (Fig. 10B) were consistent with those from Jiang et al, suggesting that linearity reached an upper plateau above 2 μg protein per well, potentially due to oversaturation of the disc or inability to sufficiently wash away such high numbers

of exosomes. Below this upper plateau, linearity was high, with an R^2 coefficient >0.98. From here onwards, all linearity experiments were tested below the 2µg range.

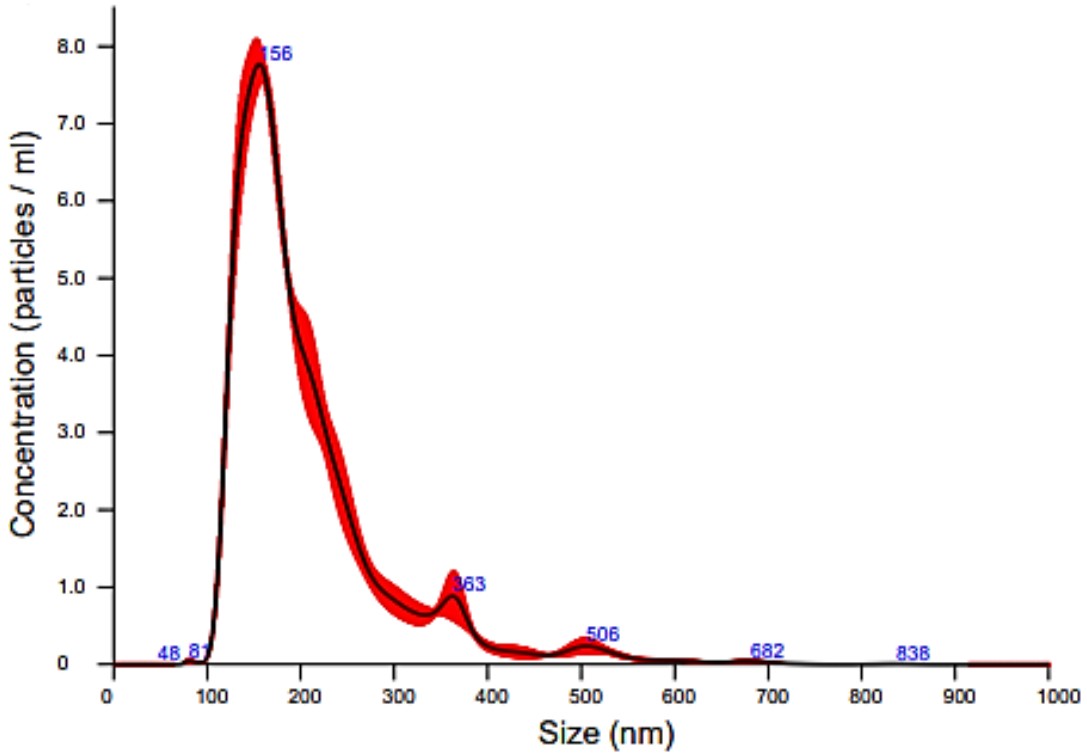

Parameter	*Value +/- standard deviation*
Mean diameter	206.1 +/- 1.7 nm
Mode diameter	152.8 +/- 5.3 nm
10th Percentile	132.2 +/- 1.2 nm
50th Percentile	178.8 +/- 0.8 nm
90th Percentile	322.0 +/- 5.9 nm
Particles per ml	8.37e+11 +/- 1.92e+10
Particles per frame	77.5 +/- 1.1 particles/frame

A

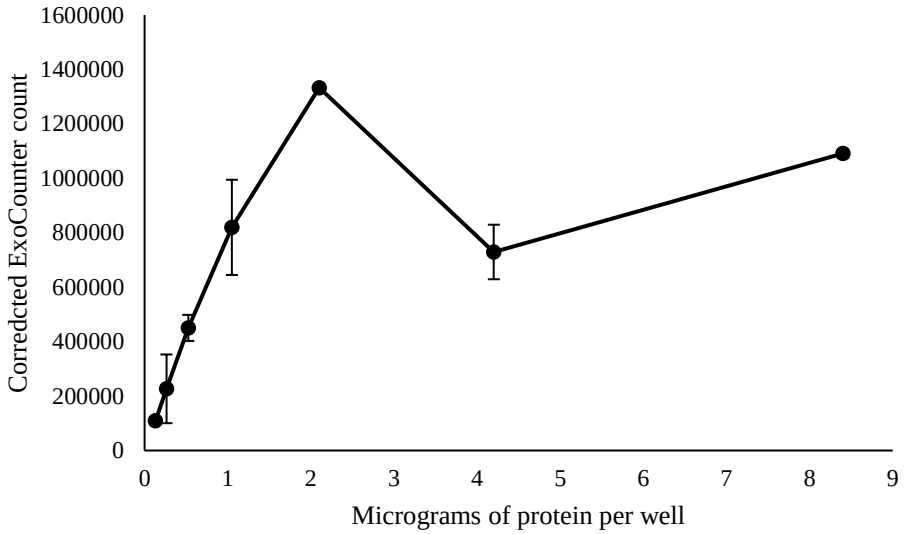

B

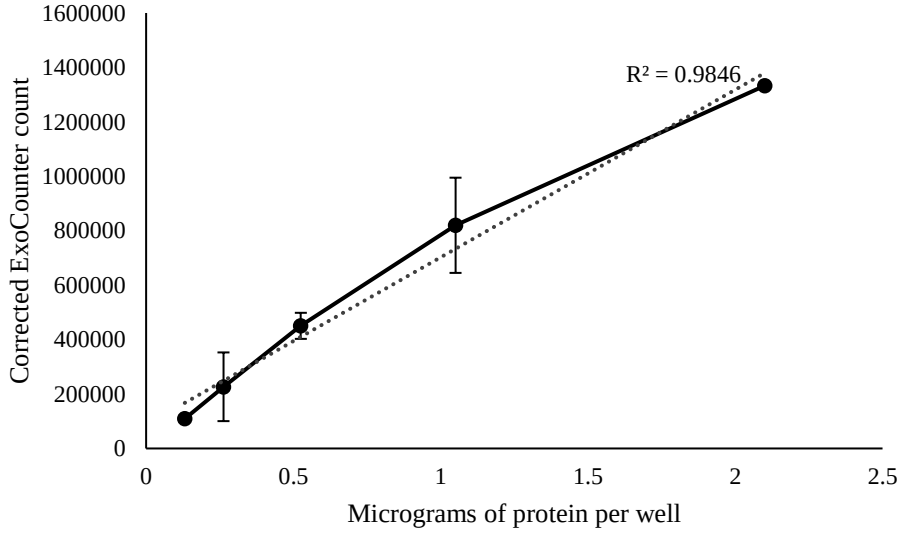

C

Figure 10: NTA results and initial spike-in linearity tests. Error bars represent standard deviation. (A); graph showing the distribution of particle diameters observed in the isolated exosome sample during nanoparticle tracking analysis. The sample was diluted 1 in 1000 for analysis. Table 6: NTA results. (B); linearity test of different

protein concentrations of isolated exosomes 'spiked-in' to non-pregnant plasma. This identified the upper limit of linearity as between located between 2 and 4μg of exosome protein per well. (C); graph showing the linearity of the same sample as in (B), with higher values excluded.

Following the initial test of linearity, which had a primary aim of determining a good protein concentration range for further linearity tests, exosome 'spike-in' tests were carried out on non-pregnant CSF and plasma. The CSF spike-in test showed high linearity, even at very low protein concentrations per well (Figs. 11A and B) with raw and background counts also being highly linear (Fig. 11C). Calculated numbers of exosomes per unit of protein were relatively consistent (some variation is to be expected from pipetting error) until the lowest value (0.004μg of protein per well), which suggest that the lower limit of linearity in CSF is between 0.012μg and 0.004μg (Fig. 11D).

In the plasma spike-in experiment, the linearity was high for the first four protein concentrations (1, 0.333, 0.111, 0.037μg protein per well), but dropped off after that (Figs. 11E and F). The calculated particles per protein unit were less consistent than in the CSF experiment, particularly at smaller concentrations (Fig. 11G).

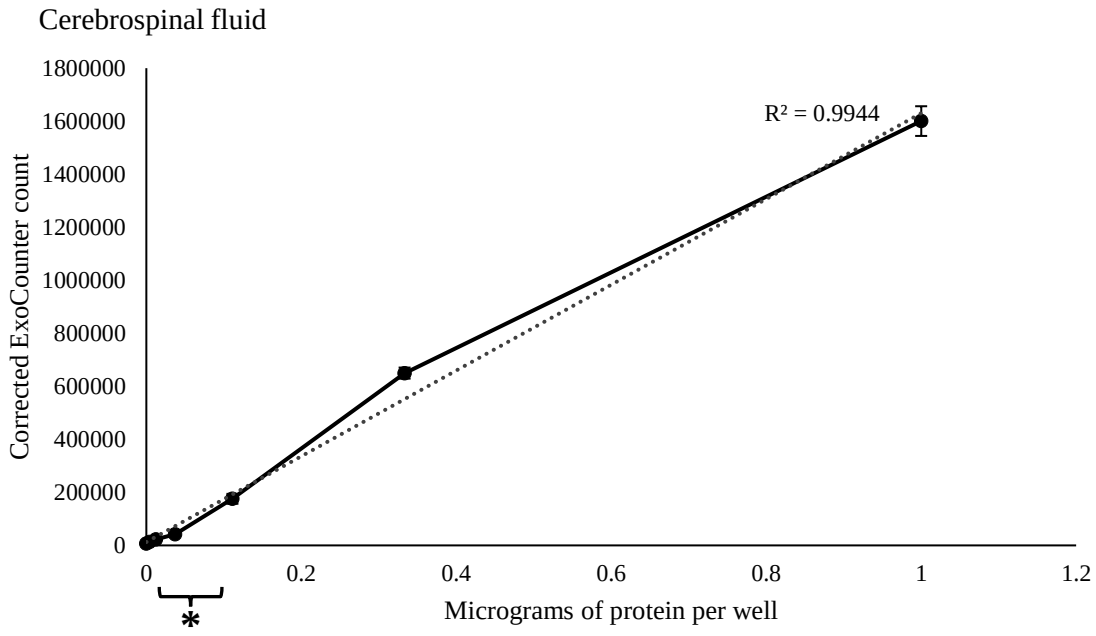

A

*Lower range shown in Fig. 11B

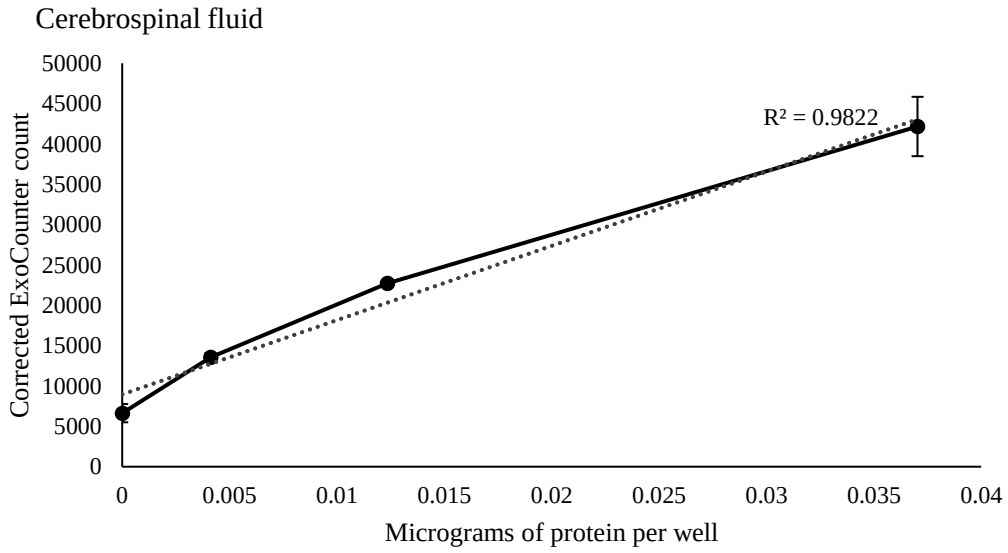

B

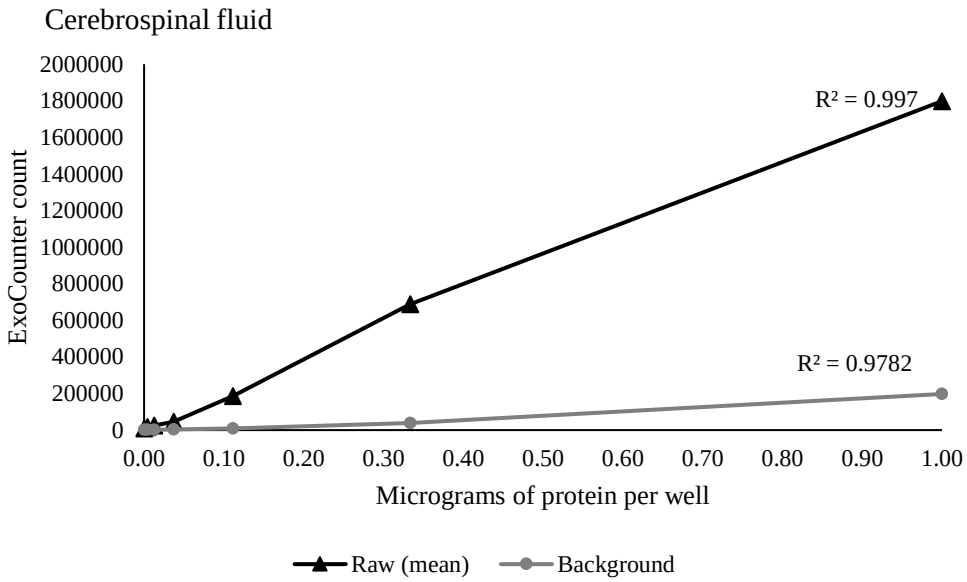
Cerebrospinal fluid
2000000
1800000
1600000
1400000
1200000
1000000
800000
600000
400000
200000
0
ExoCounter count
R² = 0.997
R² = 0.9782
0.00
0.10
0.20
0.30
0.40
0.50
0.60
0.70
0.80
0.90
1.00
Micrograms of protein per well
Raw (mean)
Background

C

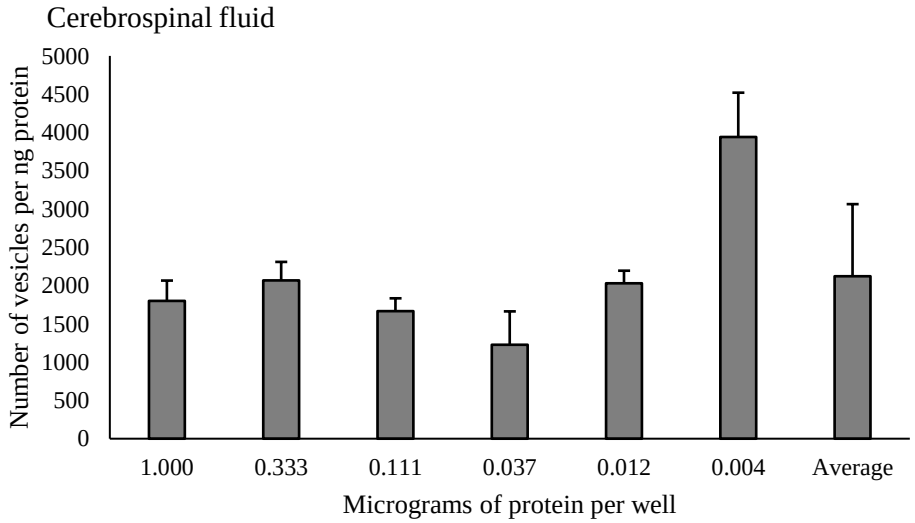
Cerebrospinal fluid
5000
4500
4000
3500
3000
2500
2000
1500
1000
500
0
Number of vesicles per ng protein
1.000
0.333
0.111
0.037
0.012
0.004
Average
Micrograms of protein per well

D

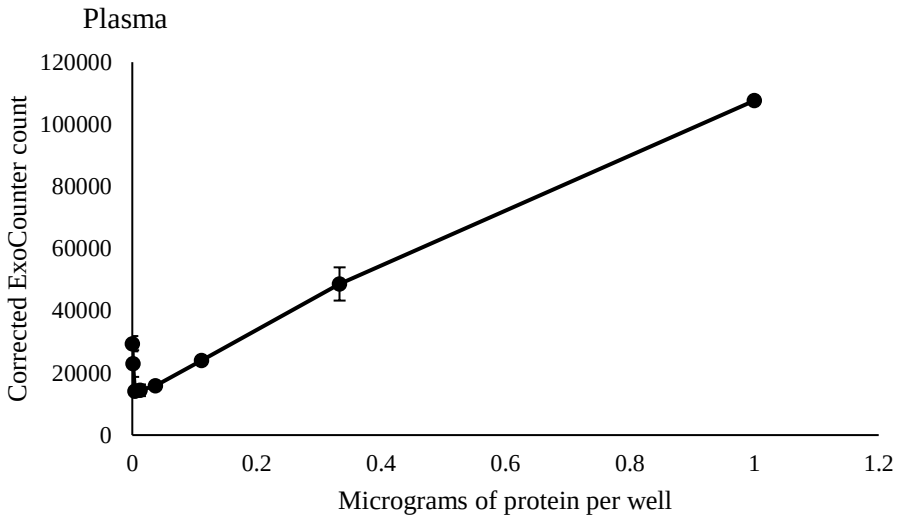
Plasma
120000
100000
80000
60000
40000
20000
0
Corrected ExoCounter count
0
0.2
0.4
0.6
0.8
1
1.2
Micrograms of protein per well

E

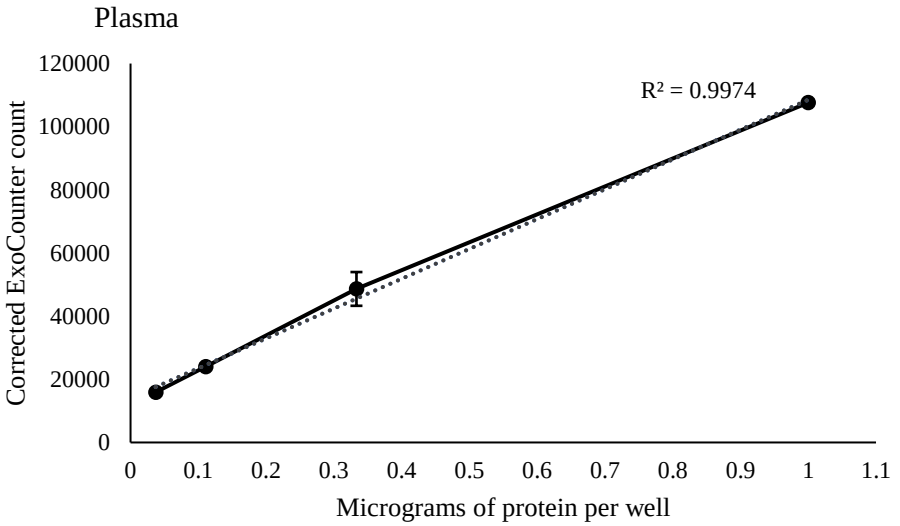
Plasma
120000
100000
80000
60000
40000
20000
0
Corrected ExoCounter count
R² = 0.9974
0
0.1
0.2
0.3
0.4
0.5
0.6
0.7
0.8
0.9
1
1.1
Micrograms of protein per well

F

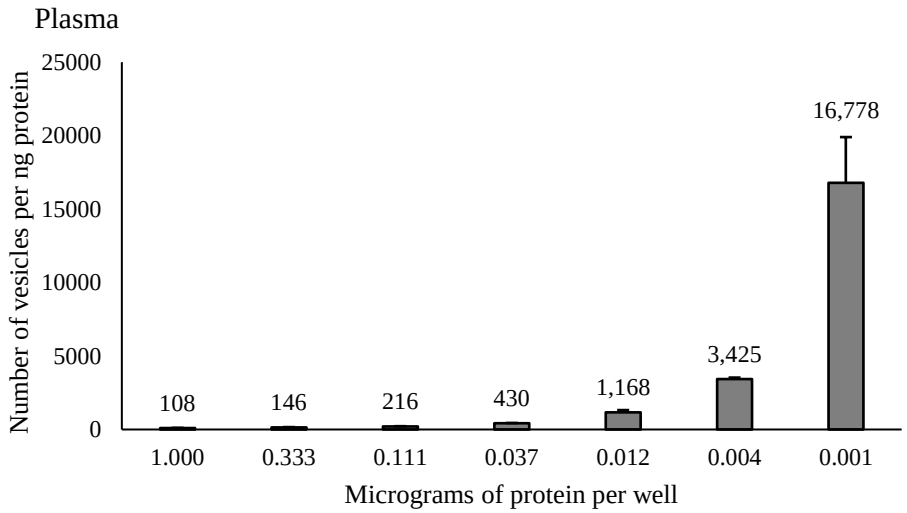

G

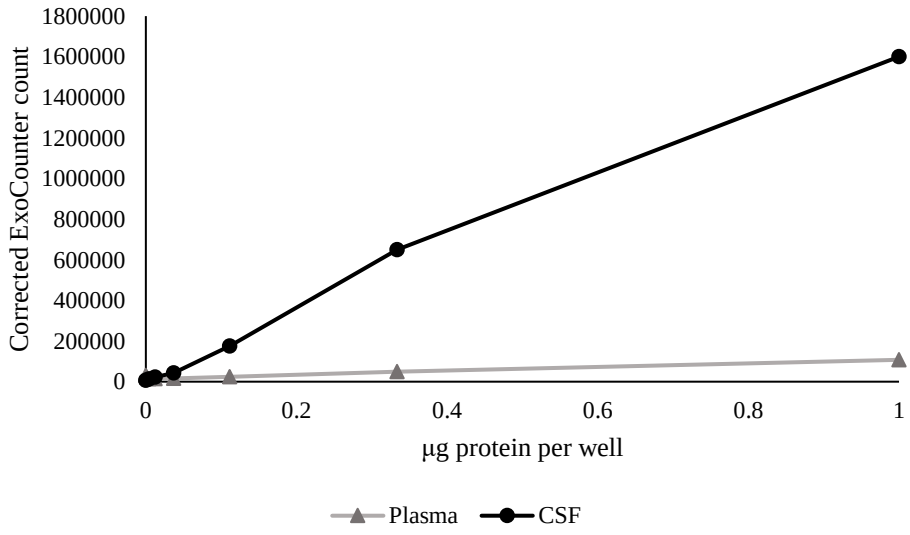

H

Figure 11: Linearity spike-in experiments. Error bars represent the standard deviation. (A); graph showing corrected values obtained from different protein concentrations of isolated exosome spiked-in to neat non-pregnant CSF. (B); graph showing the lower

values of (A). (C); graph showing the raw and background counts observed in (A). (D); graph showing the calculated vesicles per nanogram of protein (calculated from corrected ExoCounter values and BCA) in the different concentrations of protein per well. These were relatively consistent, until 0.004μg of protein per well, suggesting a potential lower limit of linearity. (E); graph showing corrected values obtained from different protein concentrations of isolated exosome spiked-in to non-pregnant plasma, diluted 1 in 4 in fPBST. (F); graph showing the higher values of (E). (G); graph showing the calculated vesicles per nanogram of protein (calculated from corrected ExoCounter values and BCA) in the different concentrations of protein per well. These showed lower consistency, particularly as protein concentration per well decreased. (H); graph comparing the corrected ExoCounter values obtained when the same calculated protein concentration of isolated exosome protein was spiked-in to non-pregnant CSF or plasma. Of note, different aliquots of isolated exosomes were used to avoid a freeze-thaw cycle.

Notably, the values obtained in the plasma spike-in experiment were lower than those obtained for the same protein concentration in CSF (Fig. 11H). This could potentially be due to the different biological properties of the two fluids, for example blocking of antibody binding due to the higher concentration of protein in plasma. However, different aliquots of isolated exosome were used for the two experiments, to avoid a freeze-thaw cycle, and the plasma experiment was repeated later than the CSF experiment. It was not clear whether the large difference was due to biological fluid properties, or due to differences in the aliquot, as some studies suggest that exosome yield decreases with long-term freezing[222]. To examine these possibilities, a test was performed in which the same protein concentrations from the same aliquot of isolated exosomes were spiked into

plasma and CSF, and analysed on the same test run. Protein concentrations were chosen that were within the linear range for both CSF and plasma in the earlier experiments.

In this experiment (Figs. 12A and B), the values obtained in CSF and plasma showed a much smaller difference in size, with CSF having the lower values this time. This suggests that the large difference in values seen earlier may be due to unequal aliquots or damage to the exosomes used in the plasma experiment due to longer freezer storage. It is not clear what drives the increased values seen in the plasma samples. Possible mechanisms may include improved antibody function at the higher pH, small contribution of PLAP+ exosomes from non-placental tissues, e.g. lungs, in plasma and better exosome stability or reduced aggregation in plasma. Additionally, this is only one experiment, and further repeats would be beneficial to see if this is a consistent pattern.

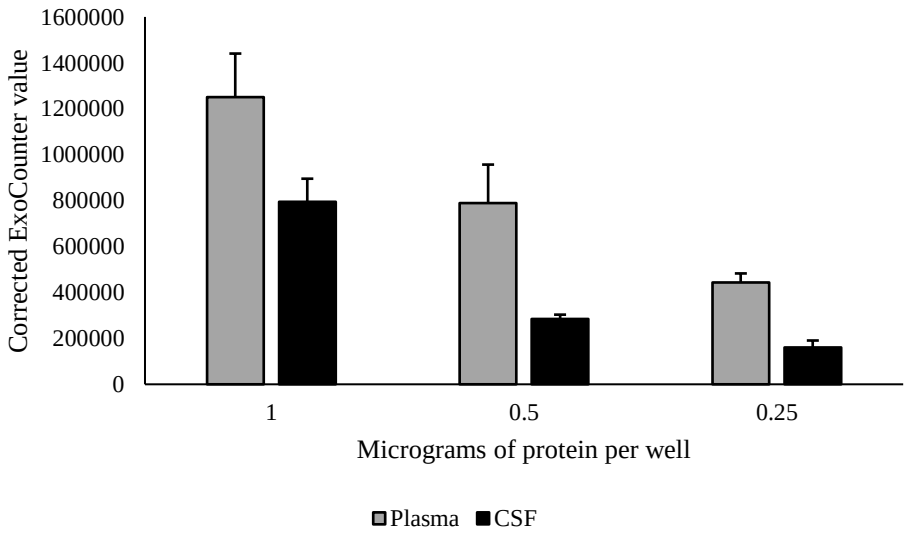

A

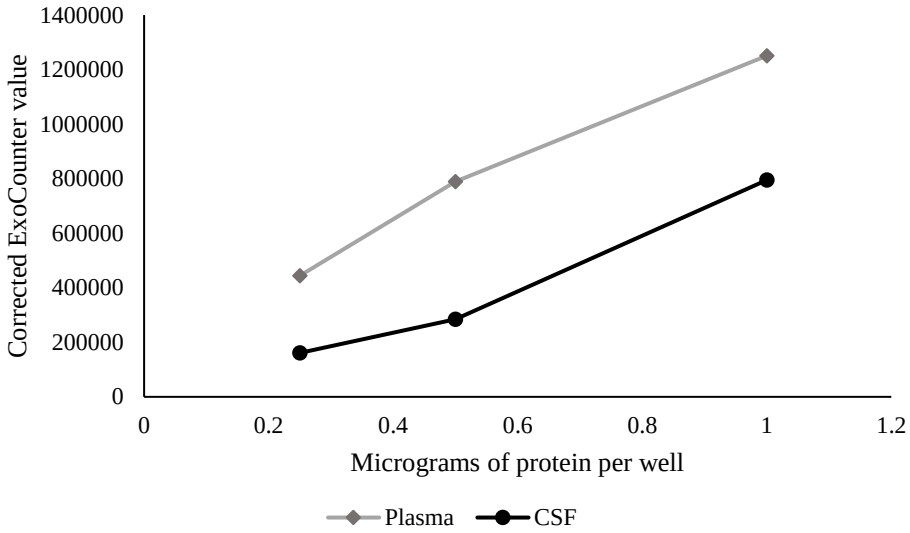

B

Figure 12: Comparing spike-in tests of CSF and plasma. (A); graph showing the values obtained from the same protein concentration of exosome being spiked-in to non-pregnant plasma and CSF on the same assay run. (B); graph showing the same as (A).

Additionally, a comparison was drawn between the values obtained from NTA and those obtained from ExoCounter (see table below). Using the BCA value of protein concentration in the isolated exosome sample, ExoCounter and NTA values were converted to particles per microgram of protein, to allow for comparison. Only particles with a diameter of 150nm or below were included in the NTA values, to exclude larger contaminating non-exosomal particles and exosome aggregates[223]. The ExoCounter values were significantly lower than those obtained in NTA ($p<0.0001$). This is to be expected for several reasons:

- NTA does not distinguish between exosomes of different populations and origins, while ExoCounter assay only detects exosomes with specific markers of origin (in this case, PLAP). Many of the exosomes in the isolated exosome sample will be

of non-syncytiotrophoblast origin e.g. exosomes derived from various blood cells[352].

- Not all exosomes of placental origin will express CD63 and PLAP simultaneously. Although CD63 was previously shown by MACSPlex to be the most abundant tetraspanin expressed by placenta-derived exosomes, expression is not 100%[337].
- NTA has been suggested to overestimate particle number due to lipoprotein and protein aggregate contamination[353].
- The ExoCounter assays were performed after NTA, so longer freezer time may have reduced exosome content[222].

In addition, this is roughly consistent with unpublished data from the Vatish group, which found in another sample that the CD63+ PLAP+ count per microgram protein from ExoCounter were 0.64% of total particle count per microgram protein obtained with NTA. Notably, the unpublished data includes particles with a diameter above 150nm. If the NTA data from this project included particles above 150nm, the ExoCounter value (plasma) as a percentage of NTA would be 0.48%, which is very similar to the value obtained previously.

	Particles per microgram protein	*As a percentage of NTA*
NTA	$8.1x10^7$ +/- $4.9x10^6$	n/a
In plasma	$1.5x10^6$ +/- $2.7x10^5$	1.85%
In CSF	$6.7x10^5$ +/- $1.2x10^5$	0.83%

Table 6: Comparing the number of particles observed per microgram of protein (BCA) using different techniques. The plasma and CSF values were calculated from all three protein concentrations used in the experiment directly above this table.

5. Summary of Chapter 3

Firstly, the ExoCounter assay was optimised to reduce intra-triplicate variation and increase signal, by double priming the washing device and using a higher concentration of casein in the blocking solution respectively. The assay was found to be dependent on intact exosomes, as addition of a lipid-membrane-disrupting agent drastically reduces signal. Reproducibility testing suggested high reproducibility of the ExoCounter assay provided that freeze-thaw cycles are avoided.

The cross-reactivity of the NDOG2 (anti-PLAP) antibody against neurological tissues compared to placenta-derived samples was tested. It was found that there was very low reactivity of the antibody to non-pregnant CSF, brain lysate and plasma, and high reactivity with exosomes isolated from the placenta and placental lysate.

Linearity testing found high linearity of the ExoCounter except at very low concentrations of exosomes. ExoCounter values were lower than those obtained by NTA, but that was to be expected for multiple reasons.

Chapter 4 – Analysing the South African samples

1. Demographic and clinical information on South African samples

36 samples were included in the South African dataset. Clinical and demographic data was collected alongside the samples. Information was given on the date of sample collection, maternal outcome, maternal age, race, gravidity, HIV status and viral load at last assessment if positive, tobacco use, diabetes, chronic hypertension, pre-pregnancy weight, height, data and time of delivery, gestational age at delivery, indication for delivery, mode of delivery, liveborn or stillborn, sex of offspring, magnesium sulphate treatment, stroke incidence, cortical blindness, creatinine greater than 120μmol/l, liver rupture, HELLP syndrome, admission to ICU, maternal death, post-partum haemorrhage (PPH), Glasgow coma score <13, sepsis, intubation, intrauterine foetal death, neonatal or infant death and abruption. No cases of stroke, cortical blindness, high creatinine, liver rupture, ICU admission, maternal death, postpartum haemorrhage, coma, sepsis, intubation, neonatal or infant death, or abruption were seen.

The average age of mothers was 28.6, with a range from 14 to 43, with an average gestational age at delivery of 35+6 (weeks, days), and a range of 27 to 41+2. As calculated from height and weight measurements given, mean pre-pregnancy maternal body mass index was 30.157 (obese), and ranged from 17.54 (underweight) to 54.62 (severely obese)[354]. One sample was missing information needed for BMI calculations, so is not included. 66% of the sample set was overweight or obese (20% overweight, 46% obese), 29% were normal, and 6% were underweight (percentages rounded to whole numbers). This is consistent with BMI patterns in the general South African population[355].

All participants identified as black or ‘coloured’ (South African term for people of multiracial ancestry, potentially including African, European, and Asian heritage[356]). All pregnancies were singleton pregnancies delivered by Caesarean section. There was variation in parity, with some mothers being primiparous and others having up to 8 previous children. The mean gravidity was 2.75. Mean gestational age at delivery was 35+6, with a range of 27 to 41+2.

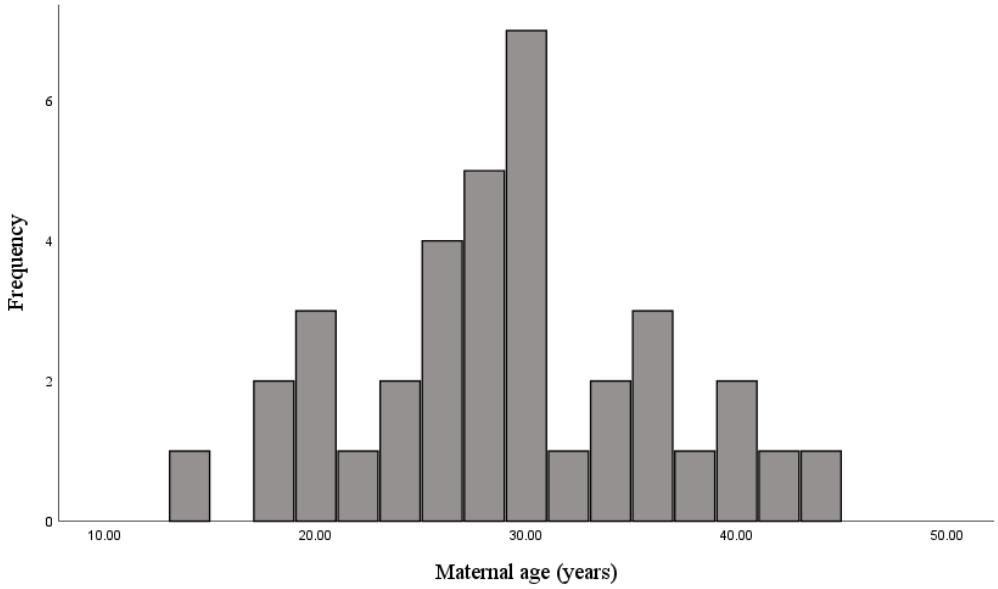

A

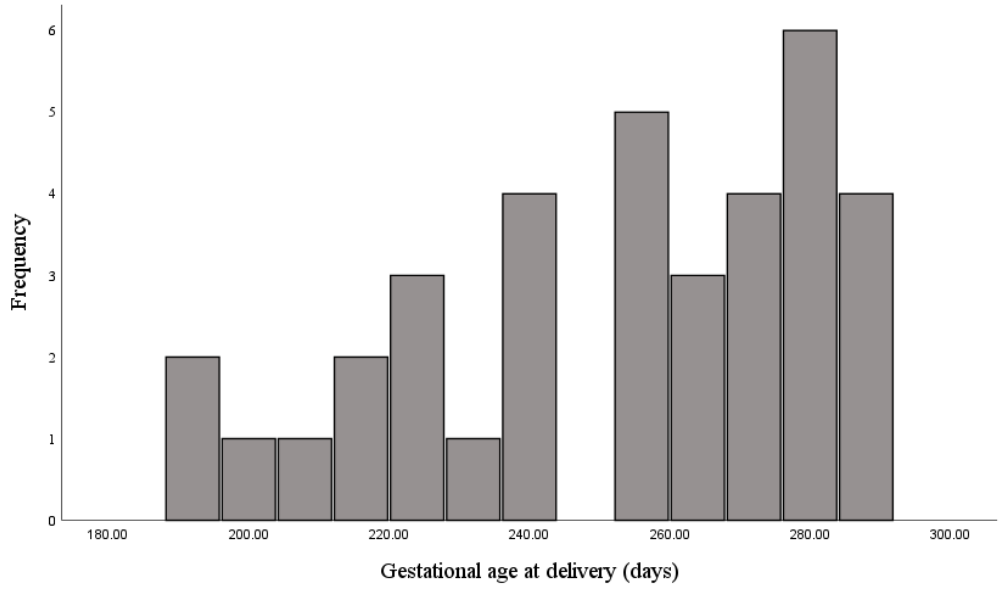
Frequency
0
1
2
3
4
5
6
180.00
200.00
220.00
240.00
260.00
280.00
300.00
Gestational age at delivery (days)

B

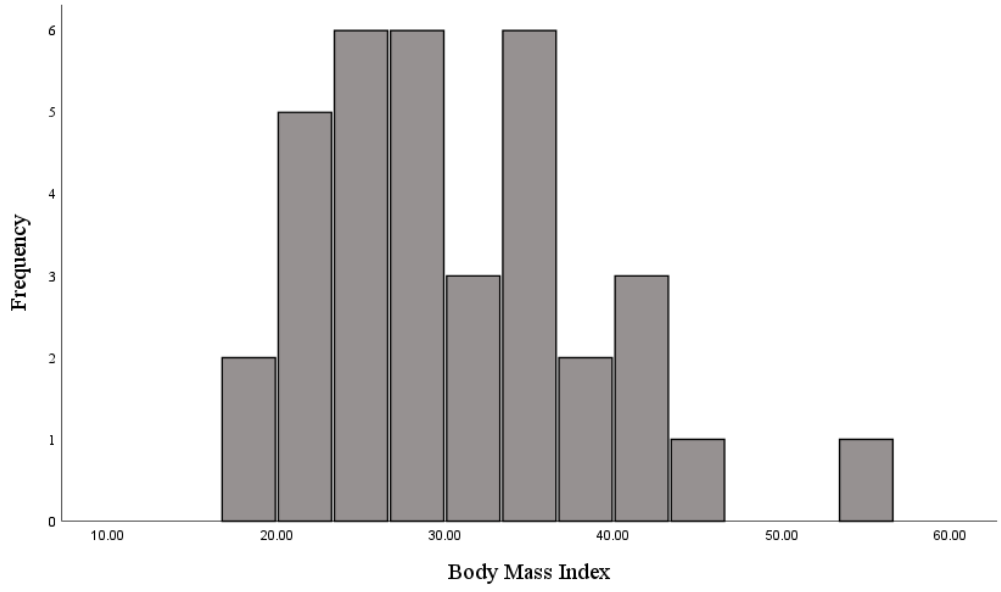
Frequency
0
1
2
3
4
5
6
10.00
20.00
30.00
40.00
50.00
60.00
Body Mass Index

C

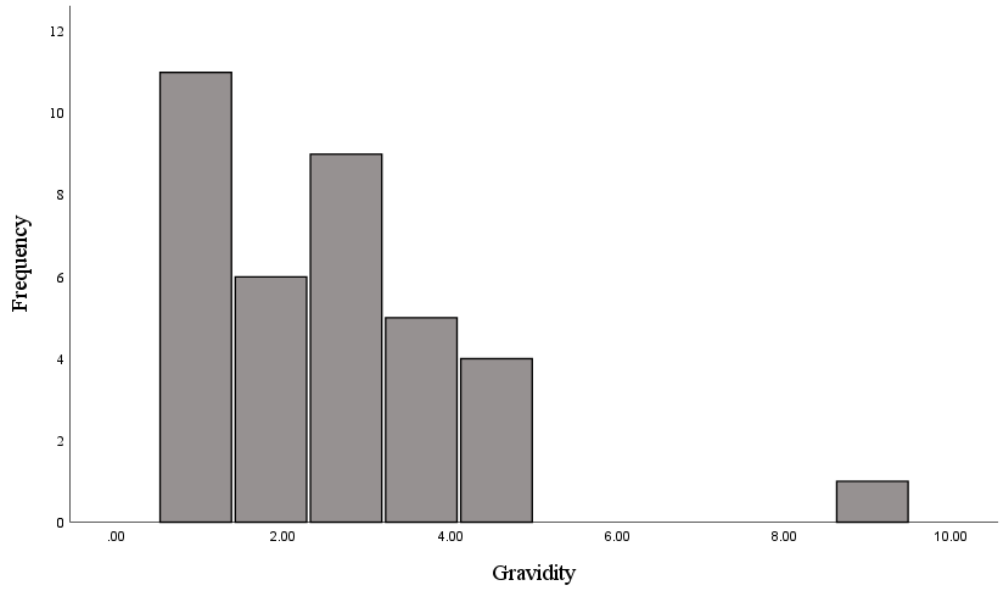

D

Figure 13: Histograms showing the distribution of variables within the South African sample set. (A); maternal age in years, (B); gestational age at delivery in days, (C); pre-pregnancy body mass index, calculated from height and pre-pregnancy weight, in kg/m^2, (D); gravidity.

Samples were divided into three groups based on clinical outcome: no diagnosis of preeclampsia or eclampsia (group 1), preeclampsia without progression to eclampsia (group 2), and pregnancies with progression to eclampsia (group 3). Within the normal group, there were no instances of severe hypertension (defined as systolic blood pressure higher than 160 mmHg or diastolic blood pressure higher than 110 mmHg), no intrauterine or postnatal foetal death. There were two cases of intrauterine death, both in the eclamptic group. A summary of the relevant clinical and demographic data in the different groups can be seen below.

Clinical group	*Gestational age at birth (days)**	*Pre-pregnancy BMI*	*Maternal age*	*Percentage of black participants*	*Percentage primiparous participants**
1, n=12	276	33.1	29.2	58%	0%
2, n=12	246	27.8	29.1	42%	58%
3, n=12	231	29.8	27.4	75%	50%
Total, n=36	251	30.2	28.6	58%	31%

Clinical group	*Gravidity*	*Percentage of male offspring*	*Percentage HIV positive*	*Instances of intrauterine death*	*Percentage with severe hypertension**	*Percentage needing emergency C-section**
1, n=12	3.5	50%	17%	0	0%	8%
2, n=12	2.3	50%	9%	0	50%	58%
3, n=12	2.5	42%	9%	2	58%	92%
Total, n=36	2.8	47%	11%	2	36%	53%

Table 7: Demographic and clinical data between clinical groups. An asterisk denotes non-random distribution between clinical groups. All non-black participants were coloured, all non-male offspring were female. Severe hypertension is defined in the previous paragraph.

Statistical tests were used to identify associations between the clinical groupings and other clinical and demographic data. Chi-squared tests found no significant association between clinical grouping and ethnicity, sex of the child, smoking during pregnancy and HIV status. Primiparity was non-randomly distributed between the clinical groups, with

primiparous pregnancies preferentially falling in the preeclamptic or eclamptic groups. This is consistent with previous studies that have shown increased risk of preeclampsia in the first pregnancy[357]. Eclampsia was associated with increased risk of a stay in the Obstetric Critical Care Unit ($p=0.002$). Similarly, both preeclampsia and eclampsia were associated with severe hypertension ($p<0.001$). One-way ANOVA analysis found no association between clinical grouping and maternal pre-pregnancy BMI or maternal age. Due to insufficient homogeneity of variance in the gestational age at delivery, Welch's test was used and found non-random distribution of gestational age between the clinical groups, with the mean gestational age being lower in the preeclamptic and eclamptic groups. It is likely that this is attributable to clinical guidelines, which promote early delivery of the baby to relieve symptoms of preeclampsia and reduce risk of adverse outcomes[358]. Similarly, a chi-squared test also found non-random distribution of emergency Caesarean section, with a strong association between emergency Caesarean section and eclampsia or preeclampsia (Cramer's $V = 0.686$).

Overall, the demographic and clinical characteristics reflect demographics within the South African population and patterns observed in previous literature on eclampsia and pre-eclampsia.

2. Introduction to Analysis of Samples by ExoCounter

Plasma samples from 35 of the 36 participants and CSF samples from 33 of the 36 participants were analysed by ExoCounter. One participant's CSF and plasma samples were not analysed due to safety concerns regarding HIV positivity, and the other two CSF samples were not analysed due to insufficient sample volume. This reduced the sample size for normal plasma and CSF samples from 12 to 11, and reduced the sample size for

eclamptic CSF to 10. All plasma samples were diluted 1 in 4 in fPBST, and CSF was assayed neat. All values were then corrected for background and extrapolated to 1ml (for CSF, multiplied by 20, for plasma multiplied by 80), and ExoCounter values given in graphs below are per ml of sample. The table below shows the spread of data.

	Plasma (per ml)	CSF (per ml)
10^{th} (percentile)	853,856	4,932
20^{th}	1,091,061	40,097
30^{th}	1,170,128	65,179
40^{th}	1,478,533	69,845
50^{th}	1,668,853	74,860
60^{th}	2,022,235	89,364
70^{th}	3,604,651	102,573
80^{th}	16,835,795	137,536
90^{th}	280,141,440	179,933
Minimum	0	0
Maximum	518,612,053	228,380
Mean	52,943,713	86,993
Median	1,668,853	74,860

Table 8: Descriptive statistics on ExoCounter values obtained from CSF and plasma samples.

3. Plasma samples

This section focuses on analysis of the South African plasma samples by ExoCounter and other techniques. The figure below displays the spread of the data (Fig. 14).

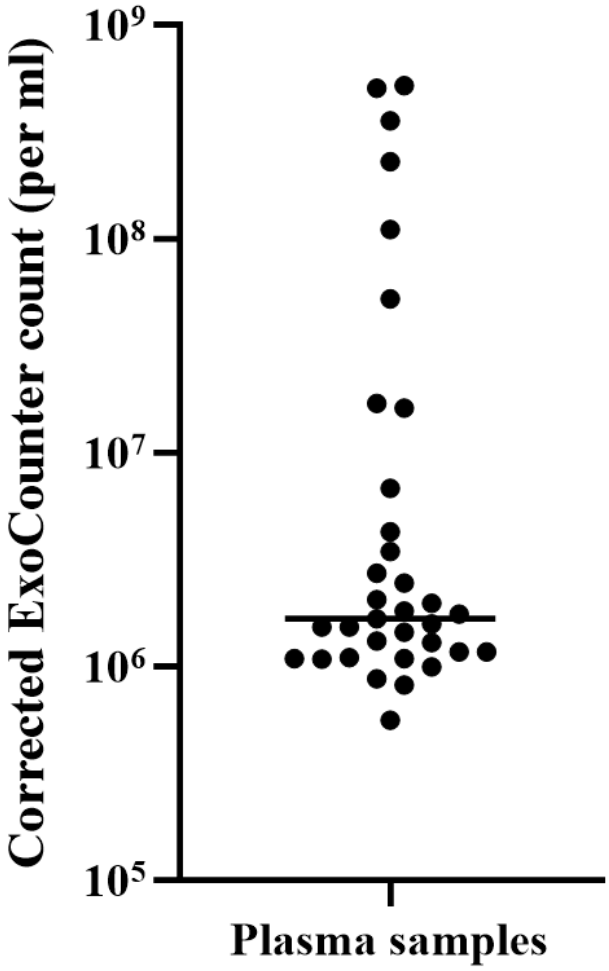

A

Figure 14: Scatter plot of ExoCounter values obtained from South African samples

3.1 Investigating Human Anti-Mouse Antibodies and Protein Concentration of Plasma

The most striking aspect of the plasma data is the huge upper range seen. While the largest value is ~$5.2x10^8$, 83% of the values were less than 5% of this upper value. There was a large cluster of values between $1x10^6$ and $5x10^6$, with 21 out of 35 (60%) samples falling within these values. The large upper spread of the data can be seen in Fig. 14A.

As the highest values were so much larger than the majority, it was considered that it may not be due to true signal. The highest values were obtained on several different runs of the ExoCounter assay, so it seemed unlikely that the issue was related to an issue in the ExoCounter performance or protocol, particularly as nothing similar had been observed while characterising the assay (Chapter 3). Instead it seemed more likely that some property of these samples influenced the observed count.

One hypothesis was that the observed counts were influenced by human anti-mouse antibodies (HAMAs). HAMAs are immunoglobulins with specificity for epitopes found on mouse antibodies. As mouse antibodies are frequently used in in vitro immunoassays, these antibodies can potentially interfere with assay results. Both the anti-PLAP antibody, NDOG2, and the anti-CD63 antibody were produced in mice. Although there are limited studies on the prevalence of HAMAs, it seems that prevalence in different populations varies between ~10 to 40%[359]. Increased prevalence of HAMAs is associated with contact with mice e.g. laboratory or veterinary workers, owners of mice as pets, dietary animal products or administration of therapeutic mouse-related therapies, for example monoclonal antibodies produced in mice[360].

It is difficult to predict the direction and magnitude of interference by HAMAs. Falsely positive results can be caused by cross-linking of the signal antibody to the capture antibody, and falsely negative results can be caused by caused by HAMAs blocking

binding sites for the signal antibody. In this case, HAMAs were suspected of causing the strikingly high values, particularly as these occurred at a frequency that was roughly like that of HAMAs. Fig. 15A shows two potential mechanisms for signal elevation by HAMAs: direct exosome-independent crosslinking of the disc-bound CD63 antibody and the PLAP-covered beads or adherence of the HAMA to the disc followed by binding of the PLAP-covered bead.

Another possibility that was considered was that the results of these plasma signals may be influenced by plasma protein concentration. This, however, seemed less likely as literature reports on plasma protein concentration show relatively low variation between samples, certainly in a significantly lower magnitude than the variation seen in ExoCounter values. A correlation between ExoCounter values and protein concentration may suggest that plasma proteins are interfering with measurements, either reducing signal by blocking binding or increasing signal through cross-linking. To investigate this possibility, the protein concentration of the plasma samples was analysed by BCA assay. Four plasma samples were not included in the BCA analysis due to HIV-related safety concerns.

A 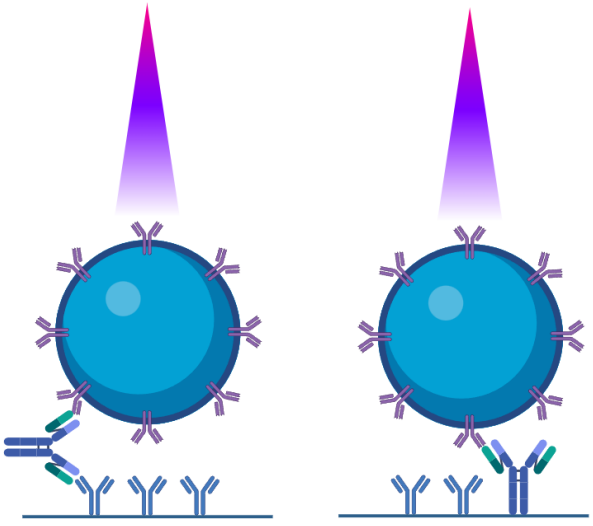

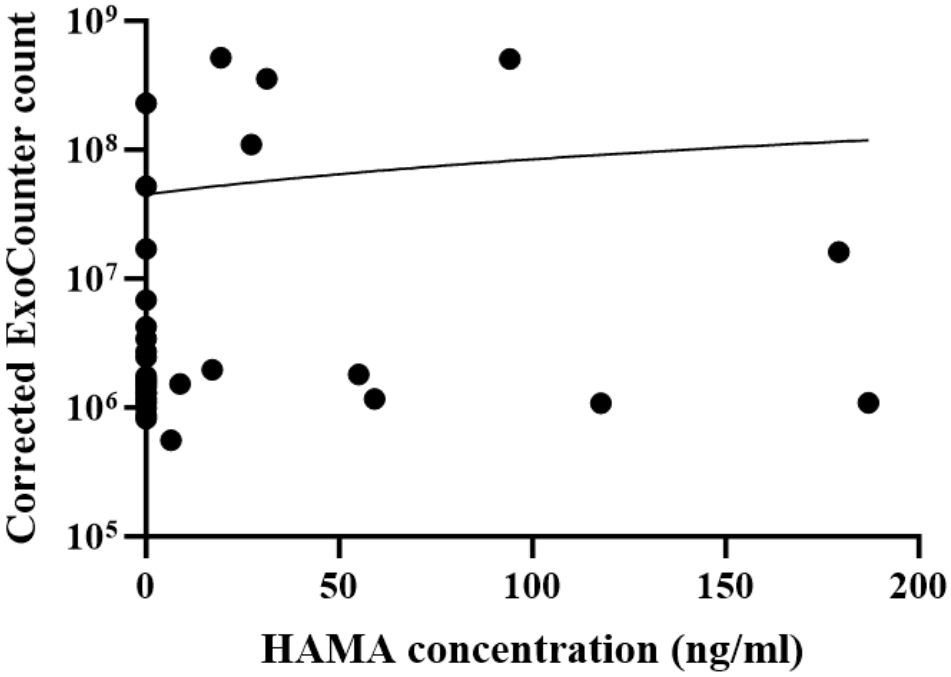
Corrected ExoCounter count
10^9
10^8
10^7
10^6
10^5
0
50
100
150
200
HAMA concentration (ng/ml)

B

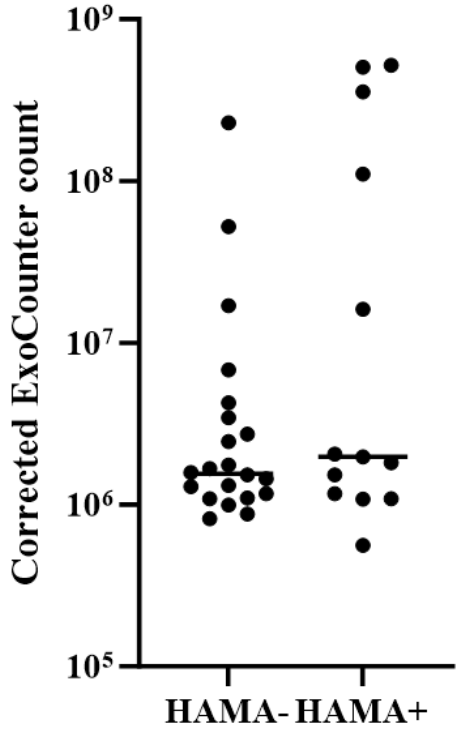
Corrected ExoCounter count
10^9
10^8
10^7
10^6
10^5
HAMA-
HAMA+

C

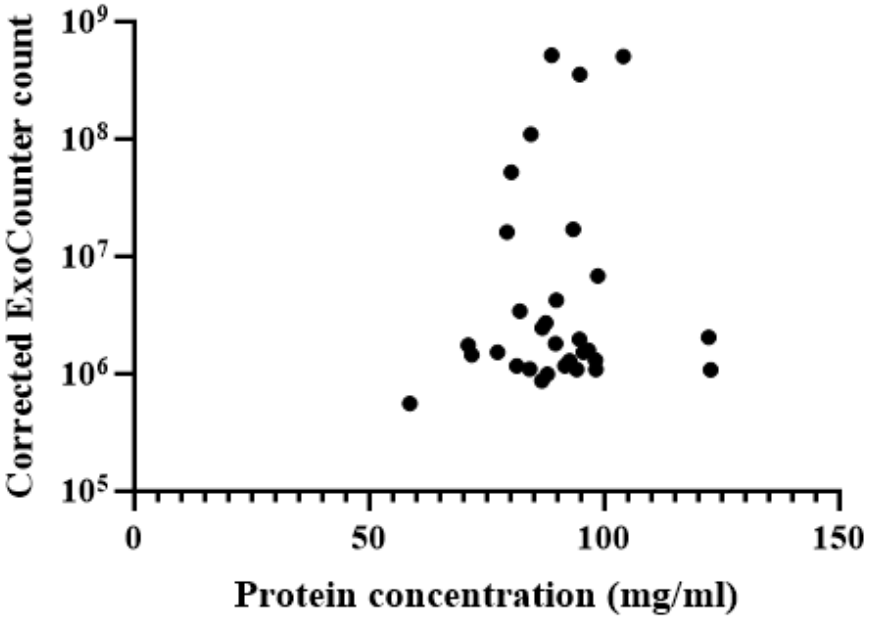
Corrected ExoCounter count
10^9
10^8
10^7
10^6
10^5
0
50
100
150
Protein concentration (mg/ml)

D

Figure 15: HAMAs and protein concentration. (A); illustrations showing potential mechanisms of HAMA interference: cross-linking and direct binding after adherence to the disc. (B); graph showing ExoCounter values and corresponding HAMA concentration. (C); graph showing the ExoCounter values in samples with and without HAMA. The horizontal line represents the median value. (D) graph showing ExoCounter values and corresponding protein concentration.

25% of the normal samples, 50% of the preeclampsia samples and 33.3% of the eclampsia samples were positive for HAMA. This was found by Chi-square to be a non-significant distribution (p=0.569), suggesting no association between grouping and HAMA incidence. For those that were positive for HAMAs, a qualitative comparison could be made between the concentration of HAMA (as compared to the standard curve) and the plasma count. One HAMA+ sample was excluded because the value for HAMA concentration was above the highest concentration used in the standard curve. There was no correlation between the measured value of HAMAs and corrected ExoCounter count (R^2=0.02, p=0.424).

If samples were divided qualitatively into HAMA-positive and HAMA-negative samples, the HAMA-positive samples had a higher mean (117,000,000 vs 15,200,000 (3 s.f.)), but this was mainly due to the three highest HAMA-positive values. The median values were more similar between the two groups (1,560,000 for HAMA-negative, 1,970,000 for HAMA-positive). As expected from the large overlap in HAMA-positive and HAMA-negative ExoCounter values, no significant difference was seen between the two groups (Mann-Whitney-U test, p=0.302).

It does seem notable that of the five highest values, four lay in the HAMA-positive group. Not all HAMAs are alike, as they can target different immunoglobulin types e.g. IgM or

IgG, and can target different isotopes on mouse antibodies[359]. It may be possible that HAMAs have an effect only in some samples, causing the most extreme results. However, for the rest of the analysis, it was assumed that HAMAs did not have any effect on count. This will be further discussed in the Future Directions section of the Discussion.

No correlation was seen between BCA protein concentrations and corrected ExoCounter counts (R^2=0.019, p=0.4467). This is a positive sign, suggesting that the ExoCounter assay is reflecting true differences in exosome presence, rather than differences in overall plasma concentration. The median concentration was lower in both the PE and eclampsia groups, with the mean decreasing across the three groups (97.45, 89.13, 83.13 mg/ml for normal, PE and eclampsia respectively, Fig. 16A). This was found to be statistically significant by Kruskal-Wallis test (p=0.0145).

The decreased protein concentration may relate to levels of albumin, which is the most abundant protein in the blood, accounting for approximately half of all plasma proteins[361]. A 2004 study found that serum albumin is reduced in severe preeclampsia, and showed a trend between disease severity and lower albumin levels, although this did not reach significance[362]. A later study confirmed that lower albumin levels were associated with worse outcomes in preeclamptic patients, but did not draw a comparison between normal and preeclamptic measurements[363]. No significant association was seen between subgroups of severity within preeclampsia and eclampsia: mild/moderate PE, severe PE, eclampsia without admission to the Obstetric Critical Care Unit (OCCU), eclampsia with admission to the OCCU (Kruskal-Wallis test, p=0.477, Fig.16B).

The association between clinical grouping and plasma protein concentration may also account for the correlation seen between gestational age and total protein concentration (Spearman r = 0.319, p=0.0375, Fig. 16C). As gestational age is lower in both the preeclampsia and eclampsia groups, and lower protein concentration is also associated

with these groups, it is no surprise that there is an association between gestational age and protein concentration. This correlation is also consistent with a 2016 paper that found gestational age at delivery was lower in preeclampsia patients with severe hypoproteinaemia compared to mild hypoproteinaemia[363]. A slightly lower mean protein concentration was seen in the early onset (<34 weeks) preeclamptic patients than late onset (81.1 vs 89.6 mg/ml, Fig. 16D), but this was not significant (Mann-Whitney-U test, p=0.324).

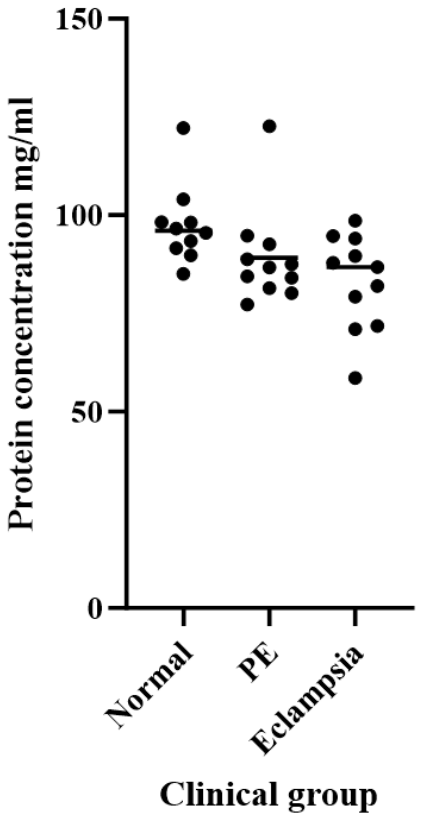

A

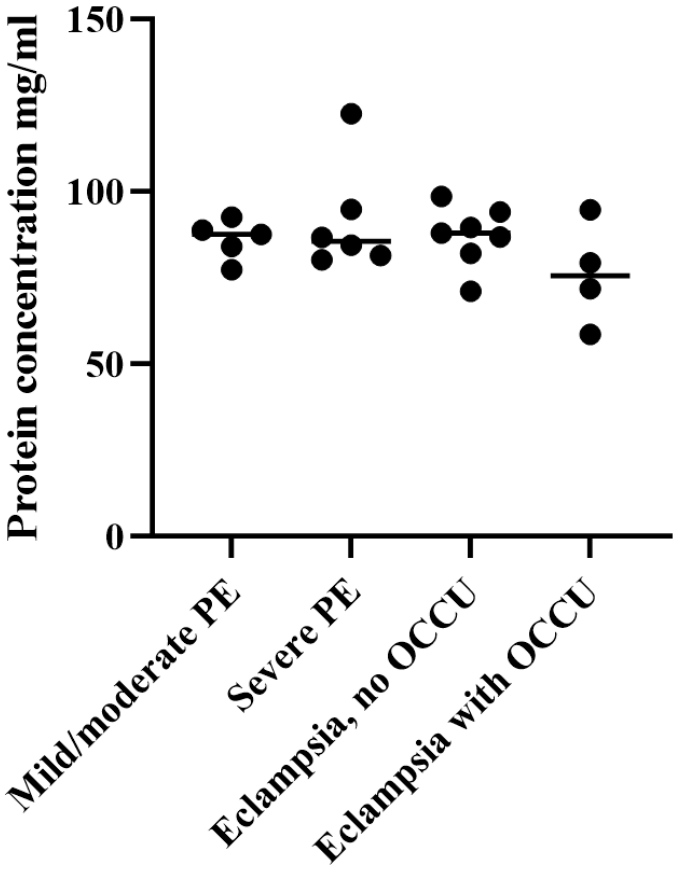
Protein concentration mg/ml
150
100
50
0
Mild/moderate PE
Severe PE
Eclampsia, no OCCU
Eclampsia with OCCU

B

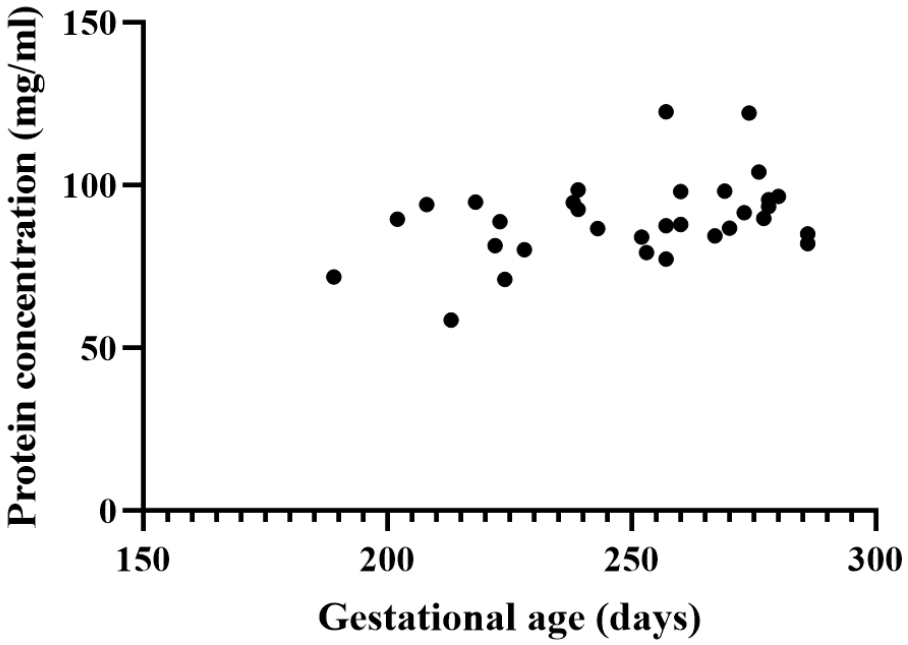
Protein concentration (mg/ml)
150
100
50
0
150
200
250
300
Gestational age (days)

C

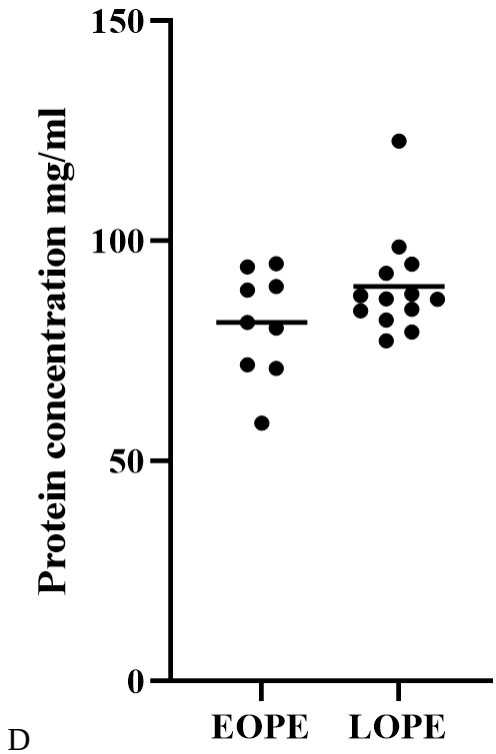

D

Figure 16: Investigating associations with plasma protein concentration. (A); scatter plot showing the distribution of protein concentrations within each clinical group. The horizontal line represents the mean. (B); scatter plot showing the distribution of protein concentrations within more detailed clinical groupings. The horizontal line represents the median. (C); graph showing the relationship between gestational age in days and protein concentration. (D); scatter plot showing the distribution of protein concentrations within early onset and late onset preeclampsia and eclampsia (34-week cutoff). The horizontal line represents the mean.

3.2 Testing for Outliers in ExoCounter Data

Before analysing ExoCounter data in the context of clinical information, outliers were first addressed. Identification of outliers was performed using the 'robust regression followed by outlier identification' (ROUT) method in GraphPad Prism[364]. This was chosen over Grubbs' method as ROUT has previously been shown to perform better where there is more than one outlier present[365]. Therefore, to allow for the possibility of more than one outlier, the ROUT method was used. The ROUT method can be used with as few as three values in a dataset[366].

The Q value refers to the False Discovery Rate. For example, a Q of 5% means that fewer than 5% of the statistically significant outliers will be false positives, while 95% will be real[364]. It is often recommended that Q be set to 1%, but given the relatively low sample sizes, Q was conservatively set to 0.1% to greatly reduce likelihood of removing true data points[366].

The ROUT method identified four outliers: two in the normal group, one in the preeclampsia group and one in the eclampsia group. Figs 17A and 17B below show the data with and without identified outliers.

As mentioned previously, one normal sample was not tested due to concerns about HIV-positivity. Including the loss of this sample and the removal of outliers, the final sample sizes were n=9, n=11, n=11 for normal, preeclampsia and eclampsia respectively.

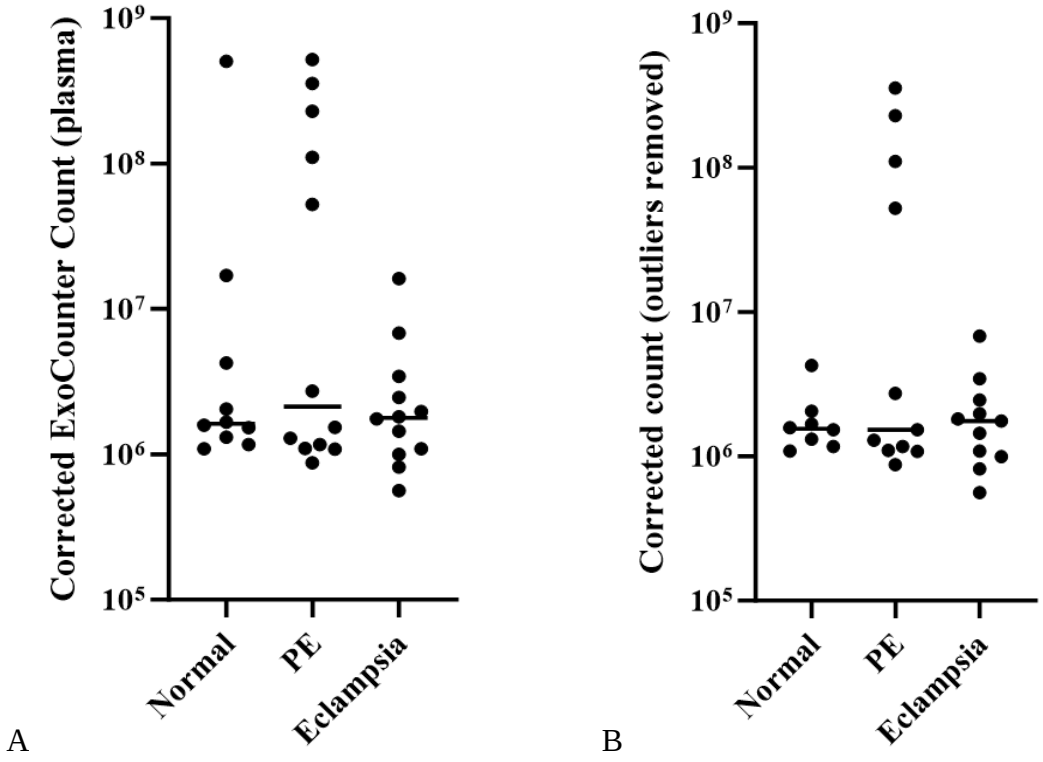

Figure 17: Outliers in the plasma dataset. (A); scatter plot showing the distribution of ExoCounter values for plasma in clinical groups, before removal of outliers. Horizontal lines represent the median (B); (A) after removal of outliers.

3.3 Testing for Correlations with Clinical Data

No significant difference was found between the different clinical groupings (Kruskal-Wallis test, p=0.627). The means varied a lot between groups (1,630,000, 68,900,000, 2,110,000 per ml for normal, preeclampsia and eclampsia respectively, 3 s.f.), but the medians were more consistent (1,530,000, 1,530,000, 1,760,000 per ml for normal, preeclampsia and eclampsia respectively, 3 s.f.). It is not surprising that no significant difference is reached as previous studies show large overlap between preeclampsia and normal controls, where the majority of preeclamptic values are within the range seen in non-hypertensive controls[265].

A notable feature of the ExoCounter data was the spread of the preeclampsia data, which seemed to fall into two groups. Seven of the eleven data points were tightly clustered and smaller than the remaining four points (Fig. 17B). It was considered that this may reflect differences in underlying pathology or physiology in these women.

The preeclampsia and eclampsia groups were further divided into early onset (<34 weeks) and late onset (≥34 weeks) disease. In the early onset preeclampsia group the median was higher than the late onset group (52,400,000 vs 1,414,000, 3.s.f.) but the reverse was true in the eclampsia group (1,270,000 vs 2,460,000 in early vs late onset, 3 s.f.). Neither difference was statistically significant (Mann-Whitney U Test, $p=0.376$ and $p=0.052$ for preeclampsia and eclampsia respectively), nor was there a statistically significant difference when eclampsia and preeclampsia were combined (Mann-Whitney U Test, $p=0.752$).

Preeclamptic and eclamptic groups were then divided further into various measures of disease severity. Firstly, preeclampsia was divided into cases with severe hypertension and those without. Severe hypertension was defined as systolic blood pressure higher than 160mmHg or diastolic blood pressure higher than 110 mmHg. Within both the preeclampsia and eclampsia groups there was no significant difference (Mann-Whitney U test, $p>0.999$ and $p=0.315$ for preeclampsia and eclampsia respectively).

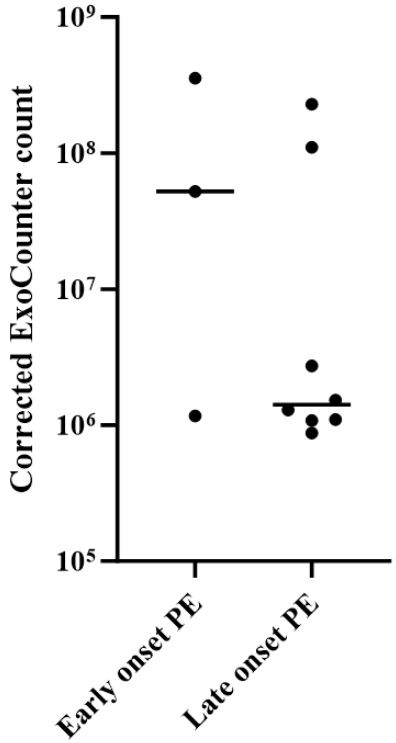
Corrected ExoCounter count
10⁹
10⁸
10⁷
10⁶
10⁵
Early onset PE
Late onset PE

A

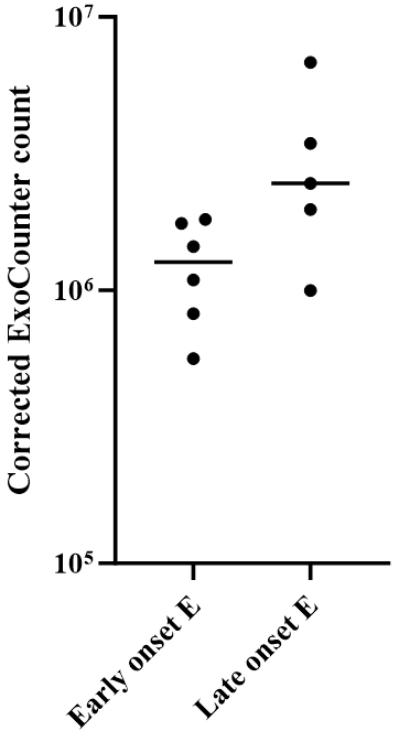
Corrected ExoCounter count
10⁷
10⁶
10⁵
Early onset E
Late onset E

B

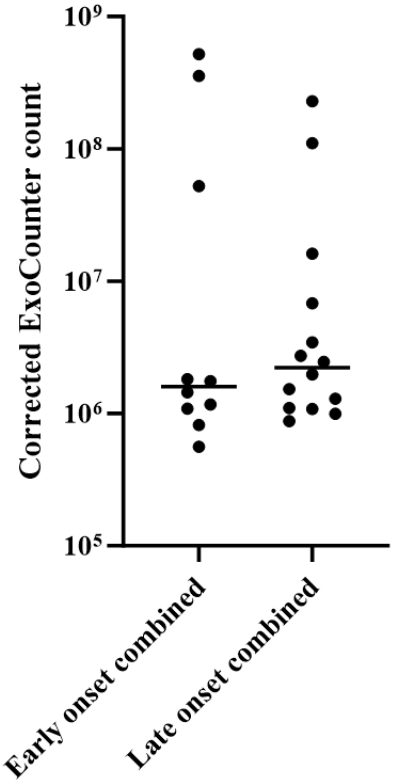
Corrected ExoCounter count
10⁹
10⁸
10⁷
10⁶
10⁵
Early onset combined
Late onset combined

C

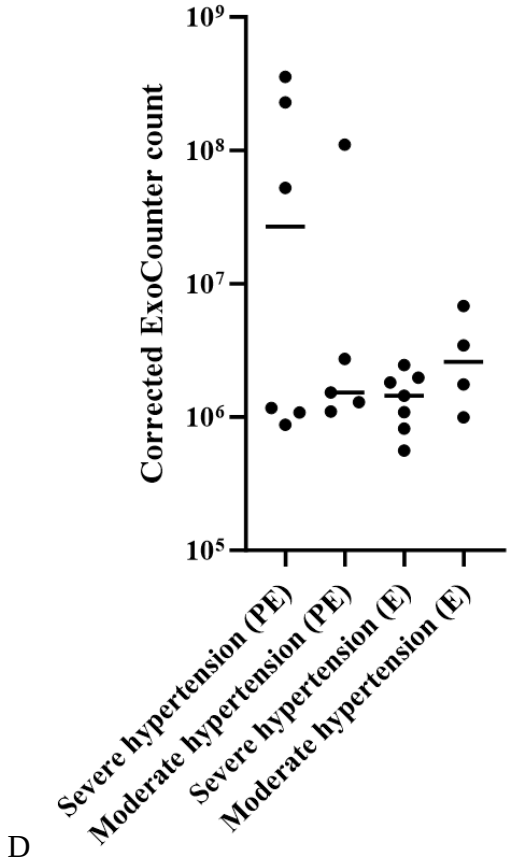

D

Figure 18: Testing for correlations with clinical data. (A); scatter plot showing ExoCounter values in early and late onset preeclampsia samples. Horizontal lines represent the median. (B); scatter plot showing ExoCounter values in early and late onset eclampsia samples. Horizontal lines represent the median. (C); scatter plot showing ExoCounter values in early and late onset preeclampsia and eclampsia combined. Horizontal lines represent the median. (D); scatter plot showing ExoCounter values in severe and moderate hypertension in the eclampsia and preeclampsia clinical groupings. Severe hypertension was defined as systolic pressure >160mmHg or diastolic pressure >110mmHg. Horizontal lines represent the median.

It was interesting that both severe hypertension and early onset in the eclampsia group showed lower median values than the moderate hypertension and late onset groups, as

severe hypertension and early onset are associated with more severe disease. In addition, cases with HELLP and OCCU admission showed slightly lower median values than those without (Fig. 19A), but neither reached significance.

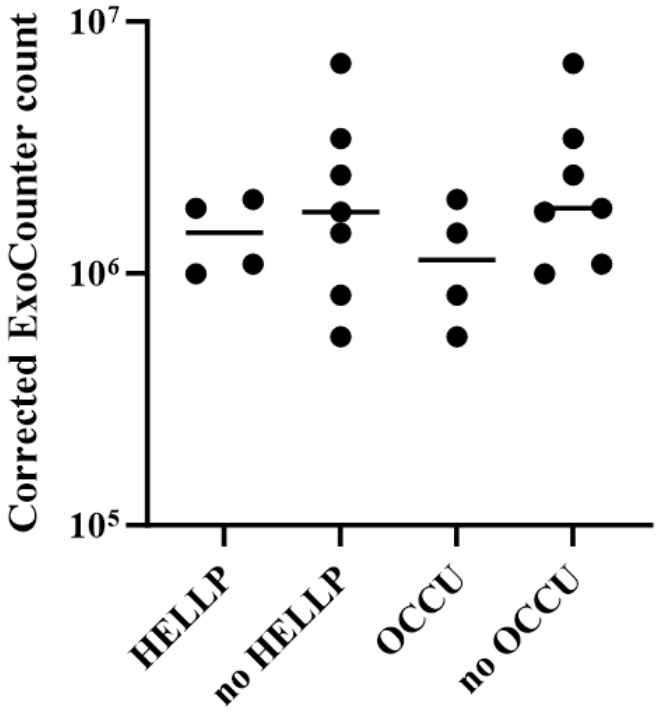

A

Figure 19: ExoCounter values and eclampsia severity. (A); scatter plot showing ExoCounter values in eclampsia with and without HELLP and OCCU admission. Horizontal lines represent the median.

3.4 The role of Gestational Age

Several studies have reported increasing numbers of placental extracellular vesicles with increasing gestational age[232,265,367–369]. In this project, there was no significant association between gestational age and plasma count in any of the three clinical groups, although

eclampsia was the closest to reaching significance (correlation matrix, p=0.613, p=0.795, p=0.076 for normal, preeclampsia, and eclampsia respectively). Eclampsia was the only clinical group where the linear regression showed a positive slope value (22100, 3.s.f.). Both normal and preeclampsia had negative slope values (-7250 and -62600 for normal and preeclampsia respectively), and very low R^2 values (R^2=0.003, R^2=0.0001 for normal and preeclampsia, compared to R^2=0.1655 for eclampsia).

In other studies of vesicle count and gestational age, a large degree of overlap is seen between different gestational ages in the studies, despite the trend towards increasing count. Secondly, many of the studies showing an association between gestational age and vesicle count have larger sample numbers, use multiple samples from the same individuals over certain timeframe (limiting the impact of interindividual variation), and use a wider range of gestational age, with many beginning in the first or early second trimester. Therefore, it is not necessarily surprising that no effect was seen in this project, as the small sample sizes and range of gestational ages may obscure any correlation.

Furthermore, there is evidence that the increase in placental extracellular vesicles seen in later gestational age is associated with an even greater increase in total extracellular vesicle numbers, meaning that the proportion of placental extracellular vesicles within total extracellular vesicles is decreased[367]. It is not clear how the ExoCounter assay is affected by the ratio of target vesicles to overall vesicles, particularly as the capture antibody does not distinguish between vesicle subpopulations. It is possible, that the ExoCounter results are affected by the existence of high levels of non-placental vesicles, and would be useful to test this experimentally.

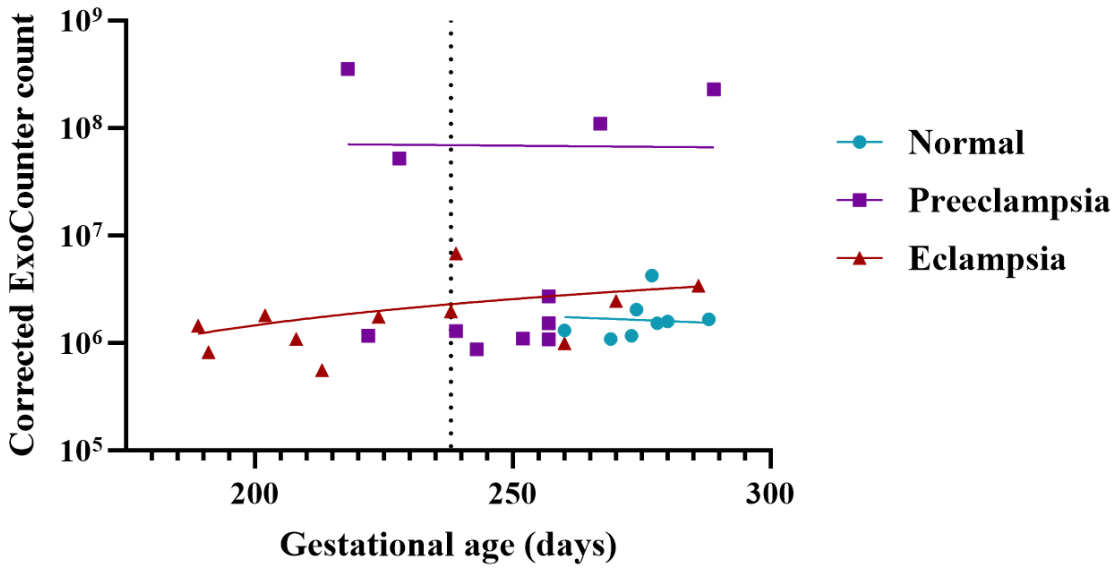

Figure 20: Graph showing the relationship between gestational age in days and ExoCounter values within the three clinical groups. The lines represent the line of best fit found by linear regression (GraphPad). Lines appear curved due the log scale on the y axis. The vertical dotted line denotes 34 weeks.

3.5 Testing for Remaining Possible Associations

The plasma ExoCounter data was also tested against various other clinical and demographic parameters. In order of the graphs below, the plasma data was tested against maternal age (Spearman nonparametric correlation, Spearman r=-0.230, p=0.214, not significant), maternal BMI (linear regression, p=0.0682, not significant), ethnicity (Mann-Whitney U test, p=0.637, not significant), sex of child (Mann-Whitney U test, p=0.654, not significant), parity (Mann-Whitney U test, p=0.814, not significant), and HIV status (Mann-Whitney U test, p=0.875, not significant). To check that extra time in the freezer did not affect sample count, plasma counts were tested against month taken by Kruskal-Wallis test, and no significant difference was found (p=0.628).

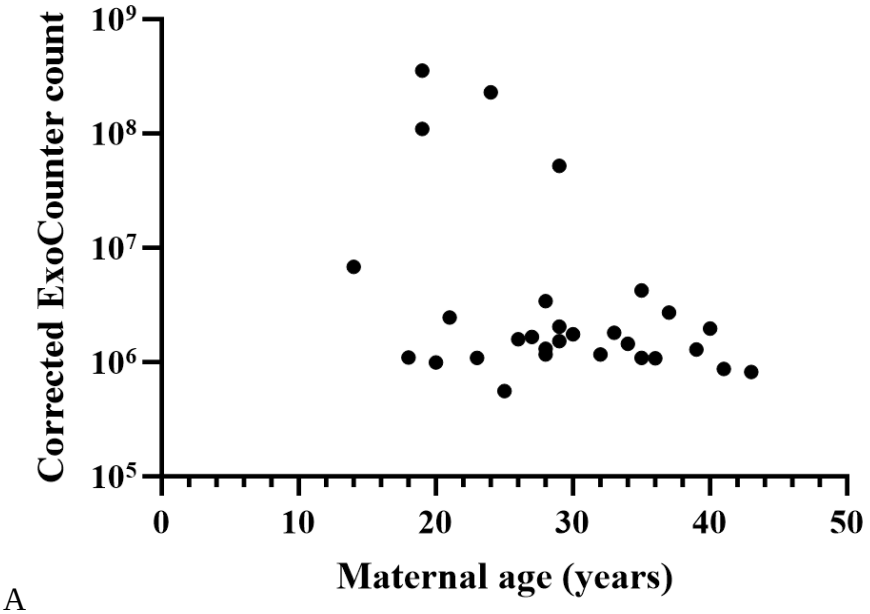
Corrected ExoCounter count
10^9
10^8
10^7
10^6
10^5
0
10
20
30
40
50
Maternal age (years)

A

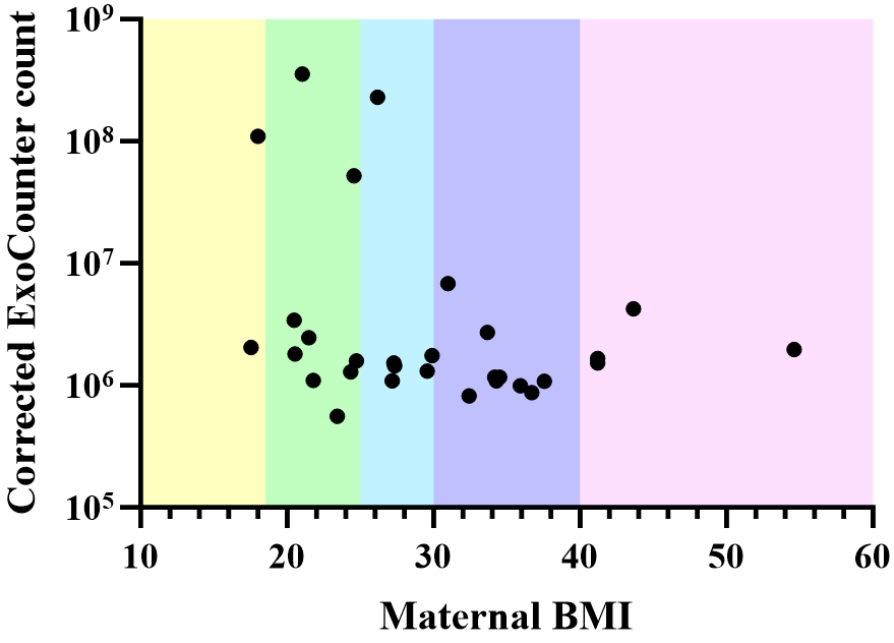
Corrected ExoCounter count
10^9
10^8
10^7
10^6
10^5
10
20
30
40
50
60
Maternal BMI

B

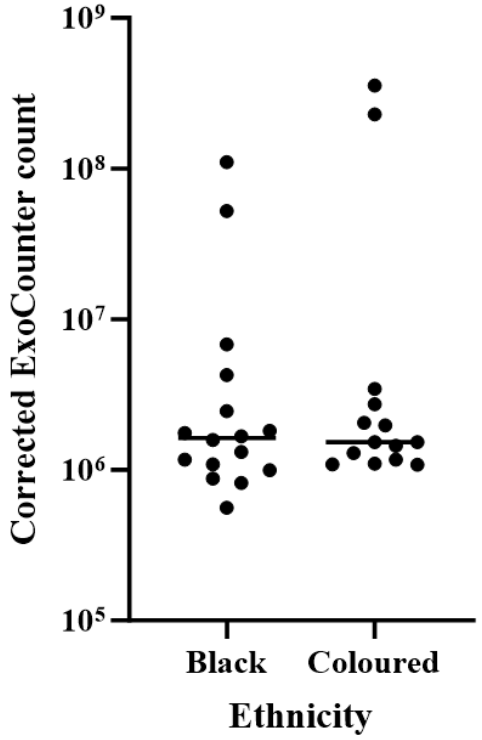
Corrected ExoCounter count
10^9
10^8
10^7
10^6
10^5
Black
Coloured
Ethnicity

C

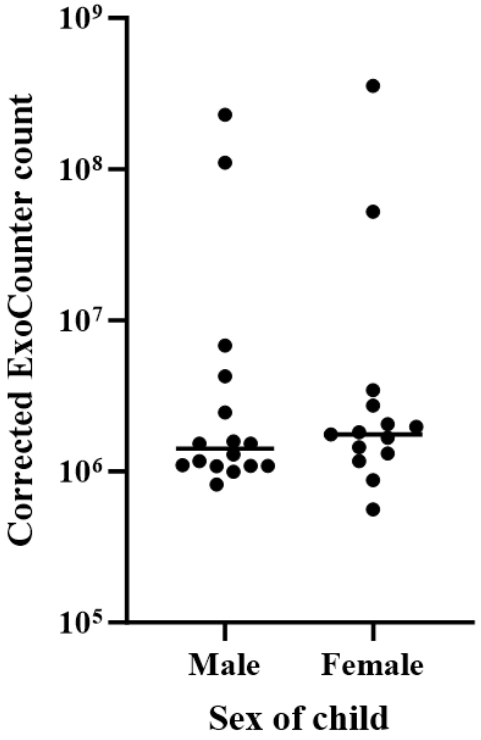
Corrected ExoCounter count
10^9
10^8
10^7
10^6
10^5
Male
Female
Sex of child

D

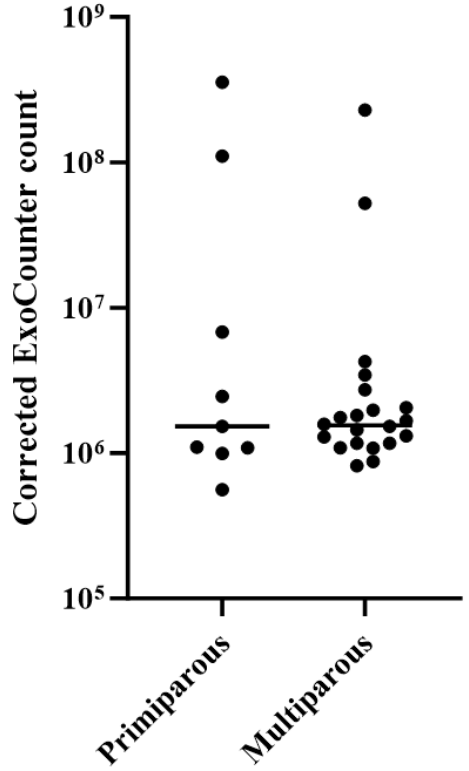
Corrected ExoCounter count
10^9
10^8
10^7
10^6
10^5
Primiparous
Multiparous

E

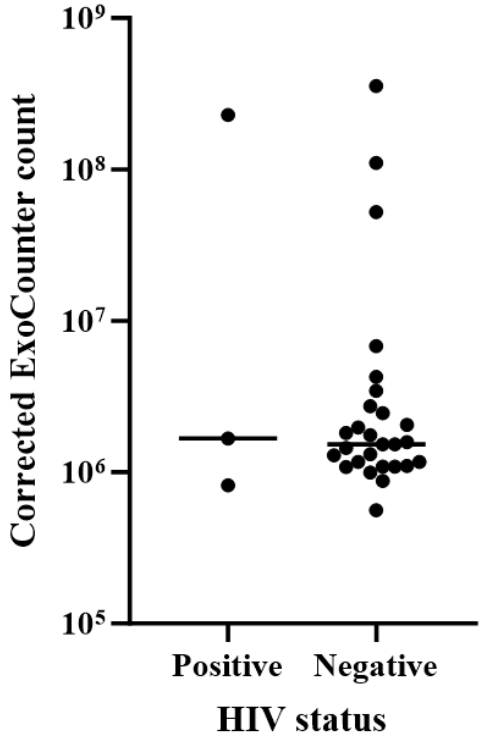
Corrected ExoCounter count
10^9
10^8
10^7
10^6
10^5
Positive
Negative
HIV status

F

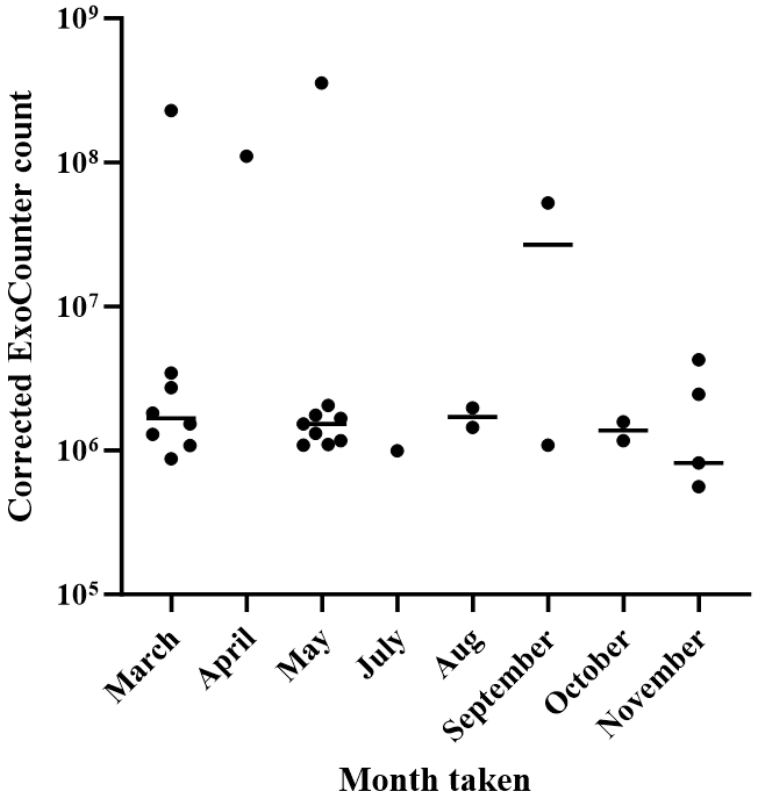

G

Figure 21: Plasma ExoCounter values and other parameters. (A); graph showing the relationship between maternal age and ExoCounter values. (B); graph showing the relationship between maternal pre-pregnancy BMI and ExoCounter values. The graph is colour-coded according to corresponding BMI categories[354]*.In order, yellow is underweight, green is healthy weight, blue is overweight, purple is obese, and pink is severely obese. One value was not included because there was no data on the height of the woman. (C); scatter plot showing ExoCounter values in black and coloured individuals. Horizontal lines represent the median. (D); scatter plot showing ExoCounter values in pregnancies with male and female offspring. Horizontal lines represent the median. (E); scatter plot showing ExoCounter values in primiparous and*

multiparous samples. Horizontal lines represent the median. (F); scatter plot showing ExoCounter values in HIV-positive and negative samples. Horizontal lines represent the median. (G); scatter plot showing ExoCounter values sorted according to the month of 2021 in which the sample was taken. Horizontal lines represent the median.

4. Cerebrospinal Fluid Samples

CSF samples were analysed by ExoCounter assay. Unlike plasma samples, they were run neat (as opposed to 1 in 4 dilutions in fPBST). One sample was not analysed due to HIV-related concerns, and another two CSF samples could not be run due to insufficient volume. ExoCounter values were extrapolated to one millilitre of sample. No patients were treated with magnesium sulfate, except for one eclampsia sample which was already excluded due to low sample volume. The CSF data was tested for outliers using the same methodology described for plasma samples (ROUT method, Q=0.1%), and no outliers were identified, regardless of whether all CSF samples were tested together or as separate clinical groups.

The spread of the CSF data is described earlier in Chapter 4, Section 2 'Introduction to Analysis of Samples by ExoCounter'. Briefly, the median was 74,860, mean was 86,993 and range was 228,380. CSF samples showed a much lower standard deviation than plasma samples (58300 vs 52,900,000 for CSF and plasma respectively). A scatter plot showing the values obtained for CSF values can be seen below (Fig. 22A).

4.1 Testing for Correlations with Clinical Data

After separation into clinical groups, the mean ExoCounter values were 108,000, 64,400, and 91,300 for normal, preeclampsia and eclampsia groups respectively, while the

medians were 98,300, 63,600, and 85,600 in the same order. As compared to the plasma samples, the medians and means were closer in value in the CSF samples, showing that extremely large values skewing the mean was less of an issue in these samples. No significant difference was seen between the clinical groupings in the CSF samples (Kruskal-Wallis test, p=0.1955, Fig. 22B).

The CSF data was also tested for an effect of HAMA by quantitatively grouping CSF samples into those with and without positive HAMA values in corresponding plasma. The median CSF values between the HAMA+ and HAMA- groups were very similar (88600 and 68400 for HAMA- and HAMA+ respectively, Fig. 22C). Furthermore, Mann-Whitney U test did not find a significant difference between the two groups (p=0.291). Therefore, there is no evidence that presence of HAMA in plasma affects CSF values.

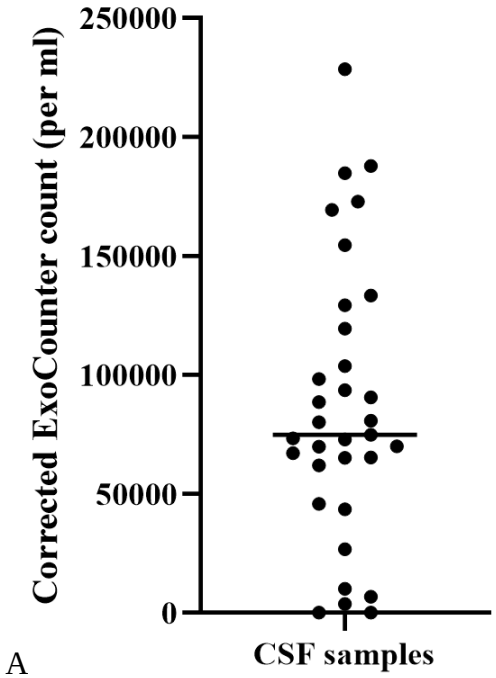

A

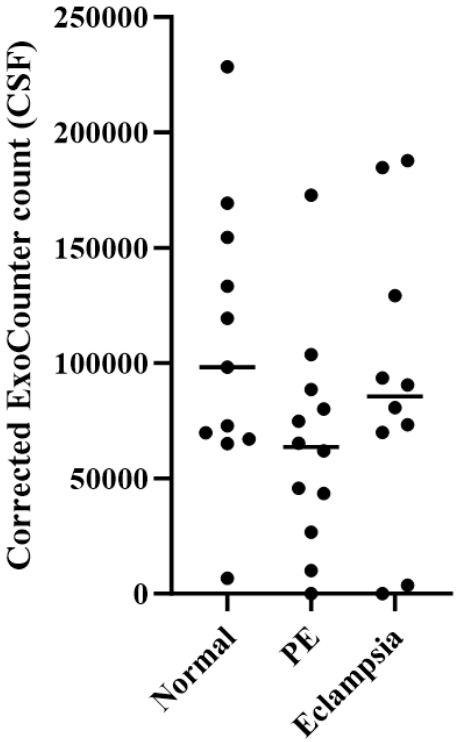
Corrected ExoCounter count (CSF)
250000
200000
150000
100000
50000
0
Normal
PE
Eclampsia

B

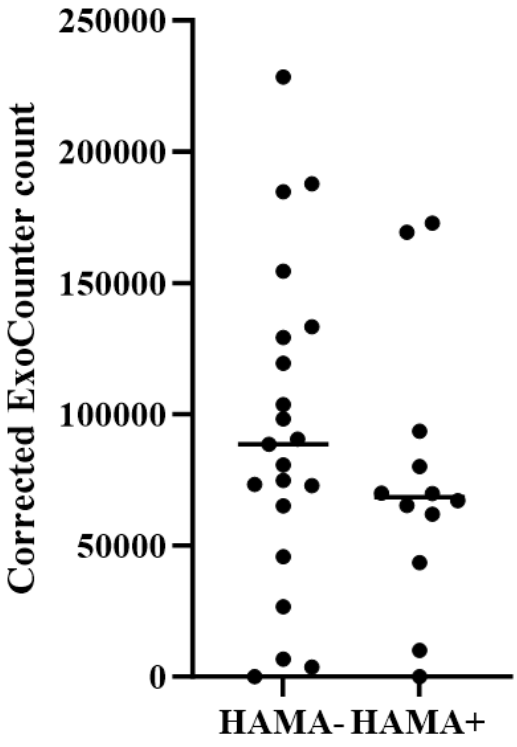
Corrected ExoCounter count
250000
200000
150000
100000
50000
0
HAMA-
HAMA+

C

Figure 22: CSF ExoCounter values. In all graphs the horizontal line represents the median. (A); scatter plot showing the distribution of ExoCounter values from the South African CSF samples. (B); scatter plot showing the distribution of ExoCounter values from CSF of different clinical groups. (C); scatter plot showing the distribution of ExoCounter values from CSF where the corresponding plasma was HAMA-positive or HAMA-negative.

The CSF sample counts showed no correlation with the corresponding plasma counts. In fact, the linear regression line was almost flat, with a slope of 2.437×10^{-6}. Spearman's nonparametric correlation test gave a result of $p=0.290$. Furthermore, the South African CSF results were compared with the values from four non-pregnant CSF samples. The means and medians were similar for each group but higher in non-pregnant samples (means: 99,700 and 87,000; medians: 105,000 and 74,900 for non-pregnant and pregnant samples respectively, 3 s.f.). No significant difference was seen between the two groups (Mann-Whitney U test, $p=0.239$).

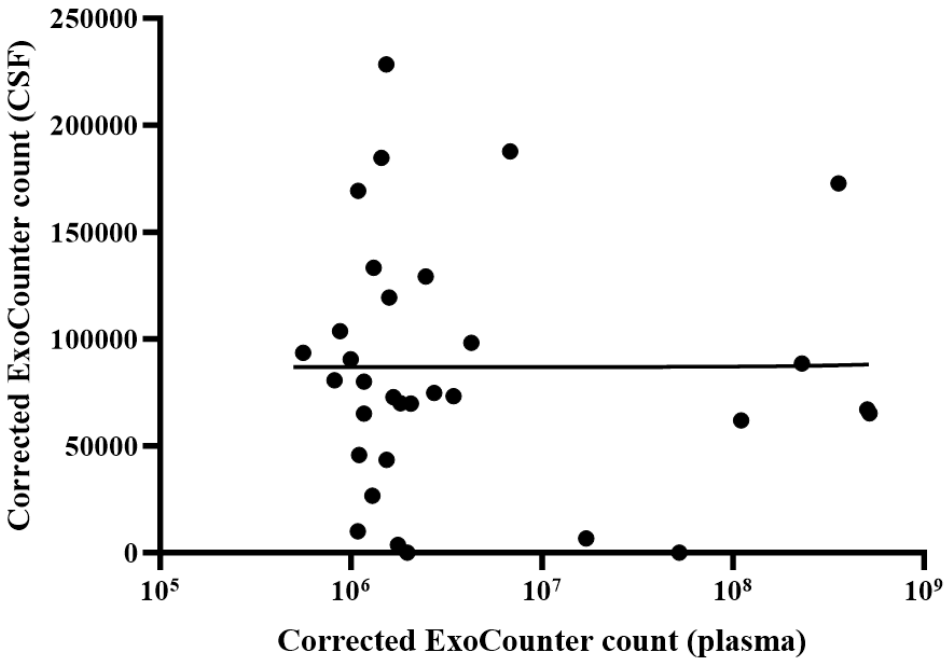
250000
200000
150000
100000
50000
0
Corrected ExoCounter count (CSF)
10^5
10^6
10^7
10^8
10^9
Corrected ExoCounter count (plasma)

A

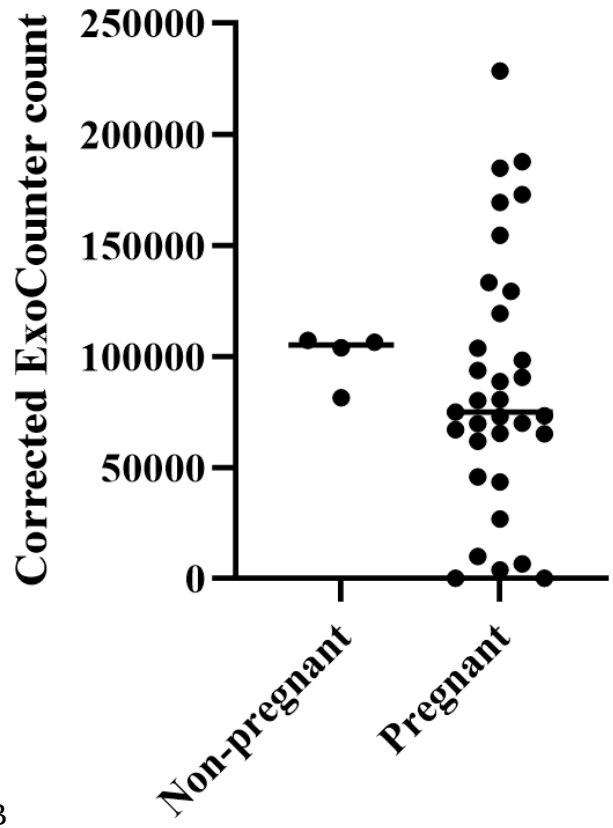
250000
200000
150000
100000
50000
0
Corrected ExoCounter count
Non-pregnant
Pregnant

B

Figure 23: Relationship with matched plasma; comparing pregnant and non-pregnant CSF. (A); graph showing the relationship between the ExoCounter values in corresponding plasma and CSF samples. (B); scatter plot showing distribution of ExoCounter values in pregnant and non-pregnant CSF samples. The horizontal line represents the median.

4.2 Testing for Remaining Associations

Based on data above, it seemed unlikely that the pregnant CSF values related to anything more than background signal, for example from the low levels of PLAP expression observed in neurological tissue[342]. However, as there was still a range of values seen in the CSF, the values were tested against various clinical and demographic parameters. No correlations were seen between CSF count and gestational age, neither separated into clinical groups (nonparametric Spearman's correlation, $p=0.940$, $p=0.601$, $p>0.999$ for normal, preeclampsia and eclampsia respectively) nor combined (nonparametric Spearman's correlation, $p=0.594$), maternal age (nonparametric Spearman's correlation, $p=0.229$), sex of the child (Mann-Whitney U test, $p=0.523$), ethnicity (Mann-Whitney U test, $p=0.562$), HIV status (Mann-Whitney U test, $p=0.887$) or parity (Mann-Whitney U test, $p=0.614$). CSF samples did not seem affected by extra time in the freezer (Kruskal-Wallis, $p=0.523$).

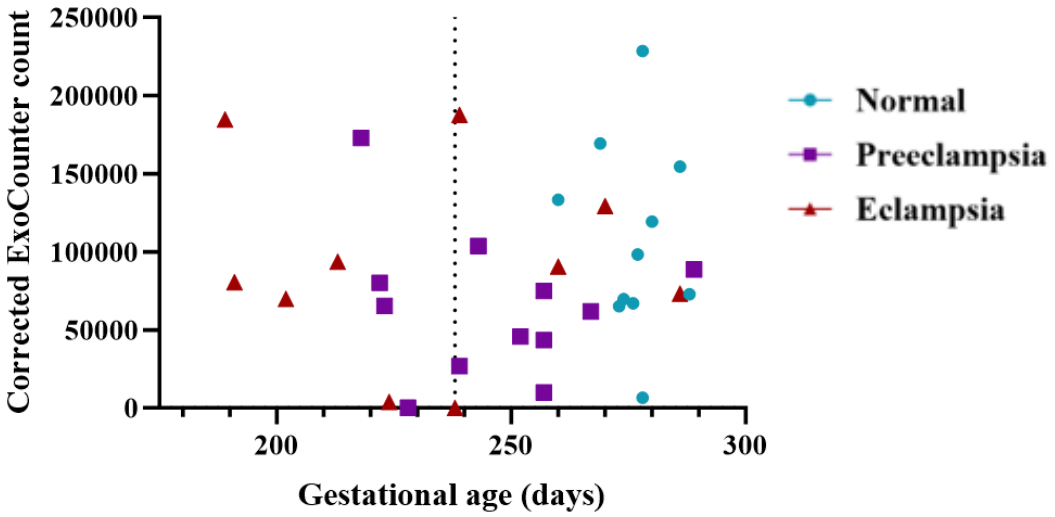
Corrected ExoCounter count
250000
200000
150000
100000
50000
0
200
250
300
Gestational age (days)
Normal
Preeclampsia
Eclampsia

A

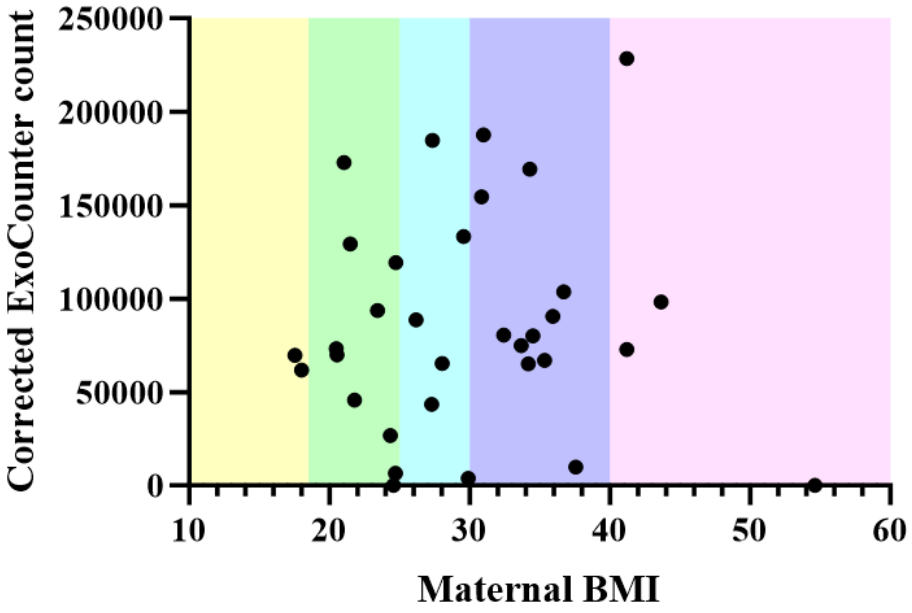
Corrected ExoCounter count
250000
200000
150000
100000
50000
0
10
20
30
40
50
60
Maternal BMI

B

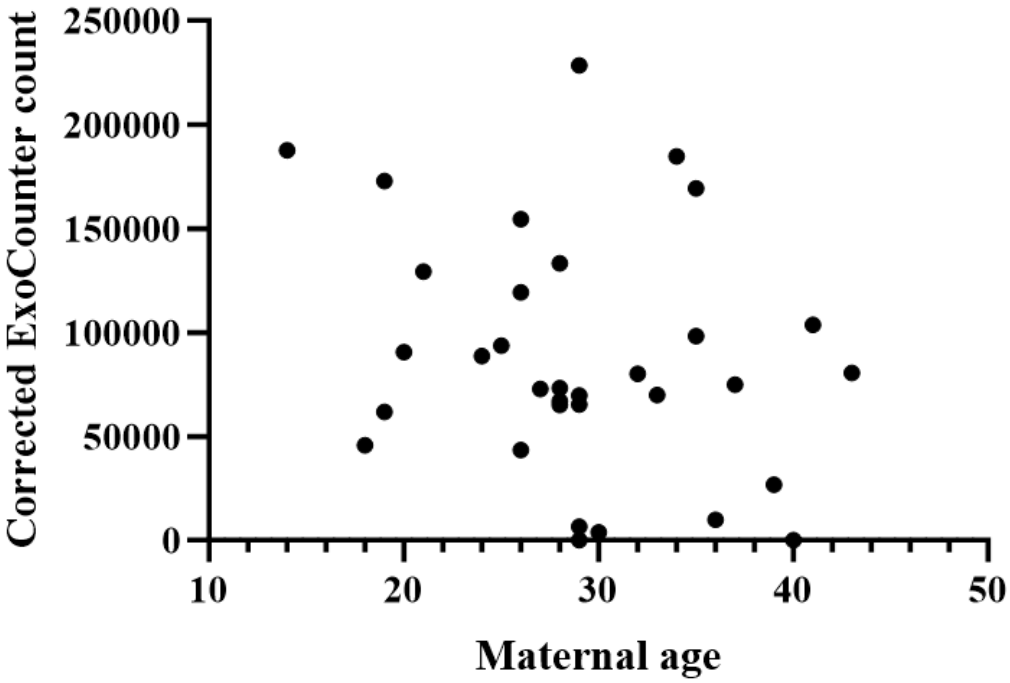
Corrected ExoCounter count
250000
200000
150000
100000
50000
0
10
20
30
40
50
Maternal age

C

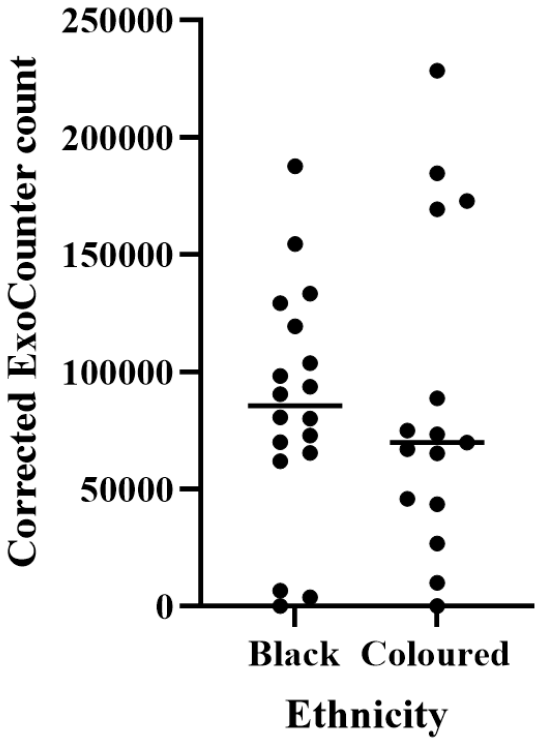
Corrected ExoCounter count
250000
200000
150000
100000
50000
0
Black
Coloured
Ethnicity

D

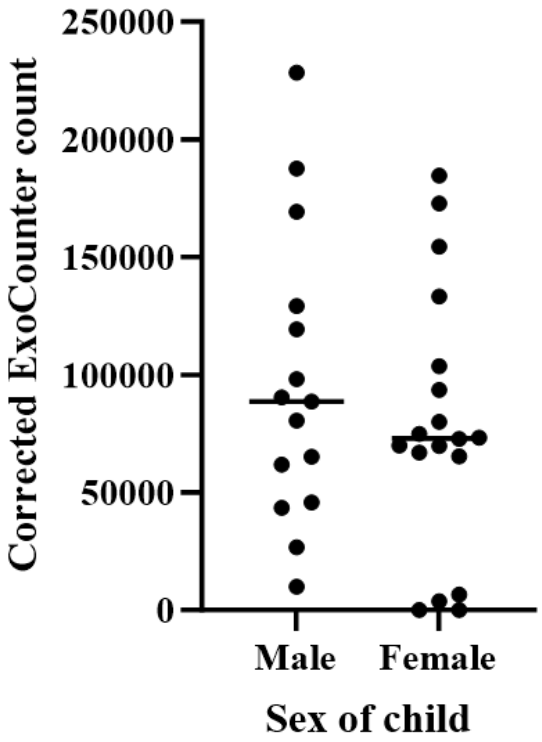
250000
200000
150000
100000
50000
0
Corrected ExoCounter count
Male
Female
Sex of child

E

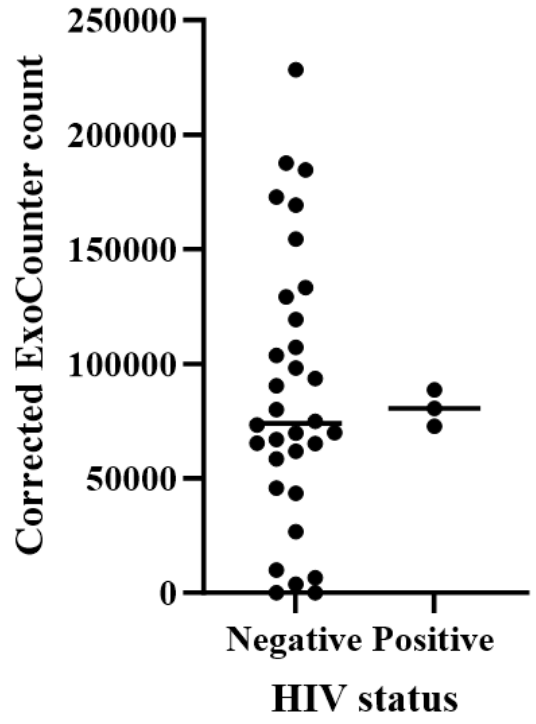
250000
200000
150000
100000
50000
0
Corrected ExoCounter count
Negative
Positive
HIV status

F

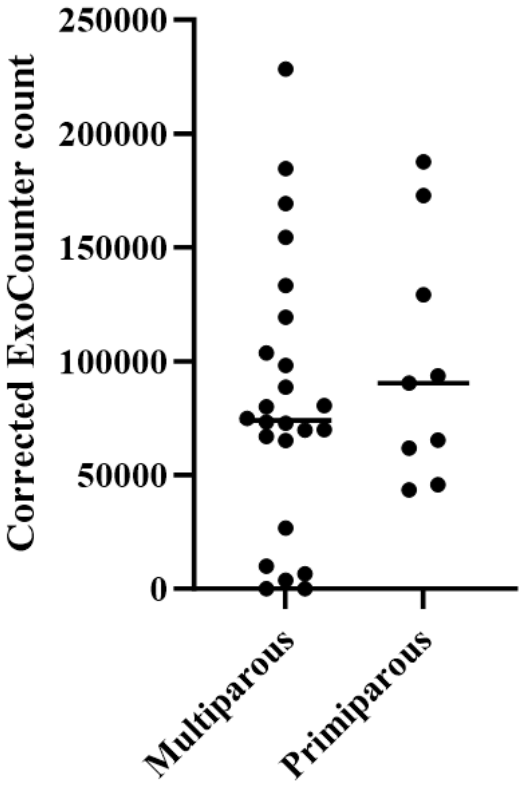
Corrected ExoCounter count
250000
200000
150000
100000
50000
0
Multiparous
Priniparous

G

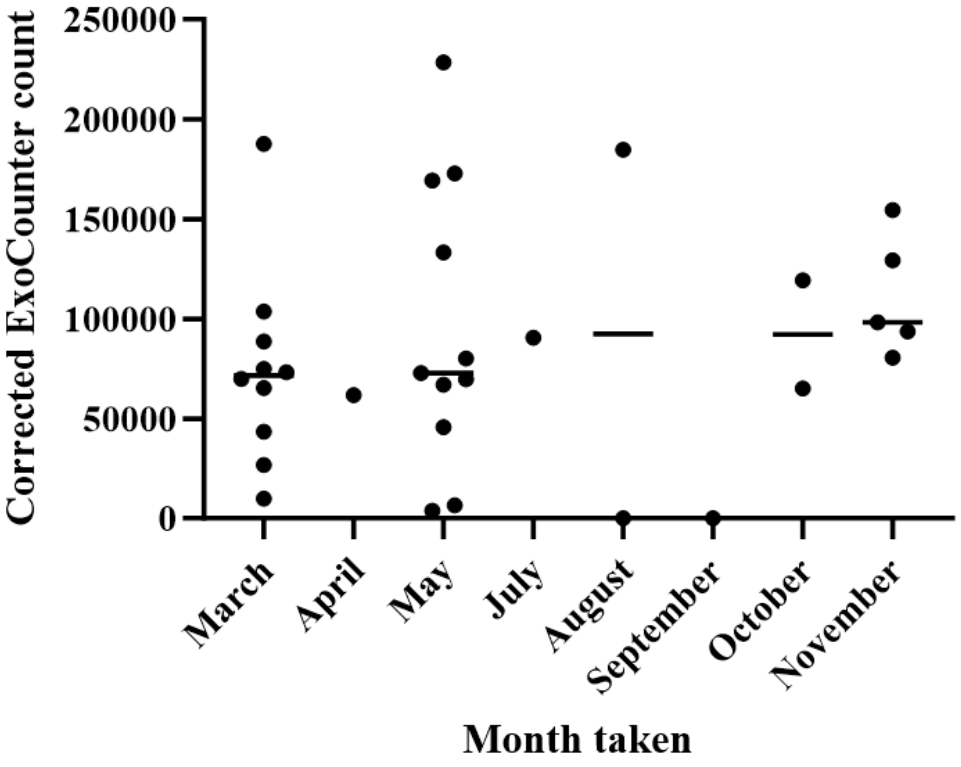
Corrected ExoCounter count
250000
200000
150000
100000
50000
0
March
April
May
July
August
September
October
November
Month taken

H

Figure 24: CSF ExoCounter values and other parameters. (A); graph showing the relationship between gestational age and ExoCounter values in different clinical groups. The vertical dotted line denotes 34 weeks. (B); graph showing the relationship between maternal BMI and ExoCounter values. The different background colours represent the BMI categories[354]*: yellow for underweight, green for normal weight, blue for overweight, purple for obese, and pink for severely obese. (C); graph showing the relationship between maternal age and ExoCounter values. (D); scatter plot showing the distribution of ExoCounter values by ethnicity. The horizontal bars represent the median. (E); scatter plot showing the distribution of ExoCounter values by sex of child. The horizontal bars represent the median. (F); scatter plot showing the distribution of ExoCounter values by HIV status. The horizontal bars represent the median. (G); scatter plot showing the distribution of ExoCounter values by parity. The horizontal bars represent the median. (H); scatter plot showing the distribution of ExoCounter values according to the month of 2021 in which the samples were taken. The horizontal bars represent the median.*

5. The Influence of Human and Pipetting Error on the ExoCounter Assay

The ExoCounter assay involves multiple rounds of precise pipetting in small volumes. Due to its disc shape, a multichannel pipette cannot be used for this task. This repetitive pipetting of small volumes into wells can introduce human errors. However, there is no available published nor, to the best of my knowledge, unpublished data addressing the susceptibility of the ExoCounter assay to such errors.

Since a consistent pipetting pattern was used (in order: well 1, 2, 3), it is possible that human or pipetting errors could lead to a recognizable pattern in the results. For instance, inadequate mixing of samples or reagents might consistently result in a higher or lower concentration in the third well compared to the first and second wells. Similarly, pipetting errors could lead to consistent variations in reagent and sample addition among earlier or later wells, that again produces a recognisable pattern.

To test for consistent patterns, the well values were analysed as a proportion of the average value over the triplicate. Data for this analysis was taken from both South African plasma sample analysis and plasma samples used in Chapter 3 – Assay Optimisation and Characterisation. This resulted in 41 available triplicates. However, those containing an outlier (please see the definition given in Chapter 2 – Methods, Section 1.VI ExoCounter) were removed to avoid the possibility that a more substantial issue than human error had affected the outlying well. This removed 18 triplicates, leaving a final set of 23 triplicates. The triplicates containing an outlier were tested for non-random distribution of outliers by Chi-squared test, but this was found to be insignificant, $p=0.311$.

Each well value was calculated as a proportion of the triplicate average, and the mean proportion per well number is displayed in the figure below. The mean proportion was 0.956, 1.053 and 0.991 to 3 d.p. for well 1, 2 and 3 respectively. This was tested for significance by Brown-Forsythe ANOVA test and was found insignificant ($p=0.0742$). The data was also analysed in a more qualitative manner, by looking at the patterns observed e.g. well numbers in order of smallest to largest. The frequency of each pattern was recorded and tested for non-random distribution by Chi-squared test, which was not significant ($p=0.263$). The data was also tested by Chi-squared to determine whether one well number was more likely to be the highest or lowest value than the other well numbers, but no significant association was found ($p=0.260$ and $p=0.119$ for the largest

well and smallest well respectively). These results therefore do not indicate that there is a large or consistent impact of human error on the ExoCounter assay. Of course, this may vary depending on the manual dexterity and experience of the researcher with the assay.

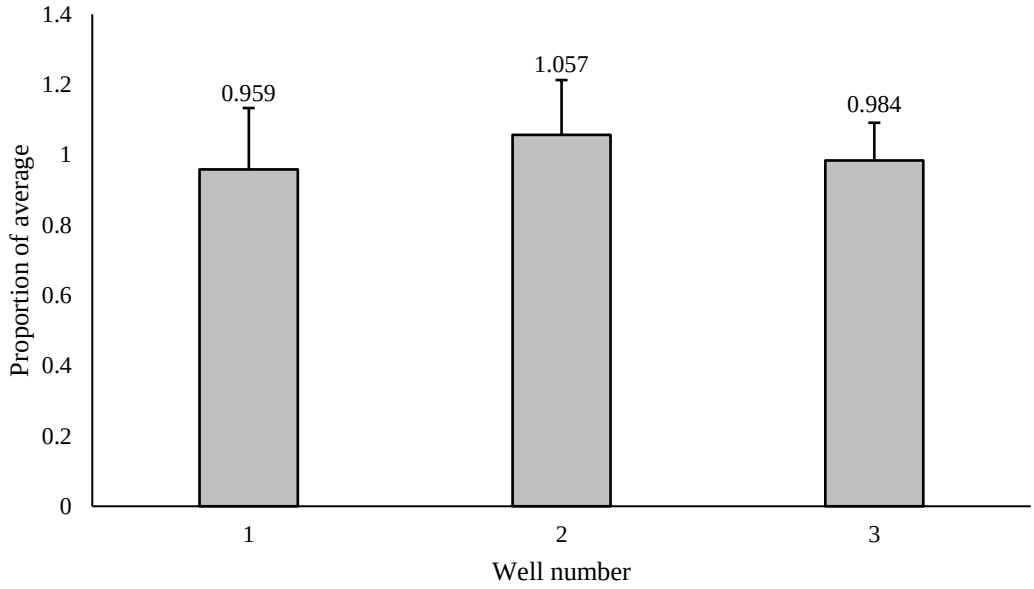

Figure 25: Graph showing the mean proportion of the average ExoCounter count per well over a triplicate. Bars represent standard deviation.

Order of values, smallest to largest	Percentage occurrence (1 d.p.)
1,2,3	20.8%
1,3,2	25%
2,1,3	0%
2,3,1	12.5%
3,1,2	16.7%
3,2,1	25%

Table 9: Quantifying the occurrence of patterns of values in triplicates.

Chapter 5 – Final Discussion

The work in this project can roughly be divided into three main sections: characterisation of the ExoCounter assay's performance, analysis of plasma samples and analysis of CSF samples. This section will discuss the data relevant to each section.

Characterisation of the ExoCounter Assay's Performance

The data obtained mostly in Chapter 3 compliments previously published evidence supporting the reliability and accuracy of the ExoCounter assay[337,338]. Parameters such as linearity, repeatability and specificity were analysed with promising results. Chapter 3 also supported published evidence that freeze-thaw cycles may affect exosome yield. This is an important consideration for further studies of biological fluids, where freezing is often necessary for storage after sample collection. Furthermore, Section 5 of Chapter 4 found no evidence of human error affecting the assay, nor any consistent pattern of outliers on the disc. This of course may vary between researchers and samples/reagents, which may affect sensitivity of the assay. It may be advisable to follow a consistent pipetting pattern so that any pipetting errors may be more easily identifiable by comparing the counts to the positions on the disc.

Spike-in experiments enabled comparisons of assay performance in different biofluids. This is a relevant issue to address if the ExoCounter is going to be used on a wide range of sample types. The initial comparison between CSF and plasma spike-in showed much higher values in the CSF samples, however there was the issue that a different aliquot of isolated exosomes was used to prevent additional freeze-thaw cycles and that this exosome aliquot was in the freezer for a longer period than the aliquot used in the CSF spike-in. When a spike-in was run on plasma and CSF using the same aliquot on the same

day to counteract these issues, the plasma spike-in had the higher counts, but the difference was much smaller. Overall, it is difficult to say how the biological fluid affects the count, and it would be advisable to investigate this further with more repetitions.

Overall, the findings relating to characterisation of the assay's performance were positive. It is recommended that researchers working with the ExoCounter continue to perform optimisation and checks of performance, particularly when working with new sample types or protocol adjustments, given the relatively new introduction of the ExoCounter assay.

Analysis of Plasma Samples

No significant difference was seen in the plasma ExoCounter values between clinical groupings. This is not necessarily surprising as large overlap is seen between clinical groupings in many other studies of placenta-derived extracellular vesicles/exosomes. The figures below show a selection of studies that also observe large overlap between normal and preeclamptic pregnancies. Although all studies used slightly different methods and sample types, the studies consistently show overlap between the preeclamptic and normal groups. Therefore, considering the small samples sizes and lack of matching for gestational age, seeing no significant difference in this project is still consistent with previous data.

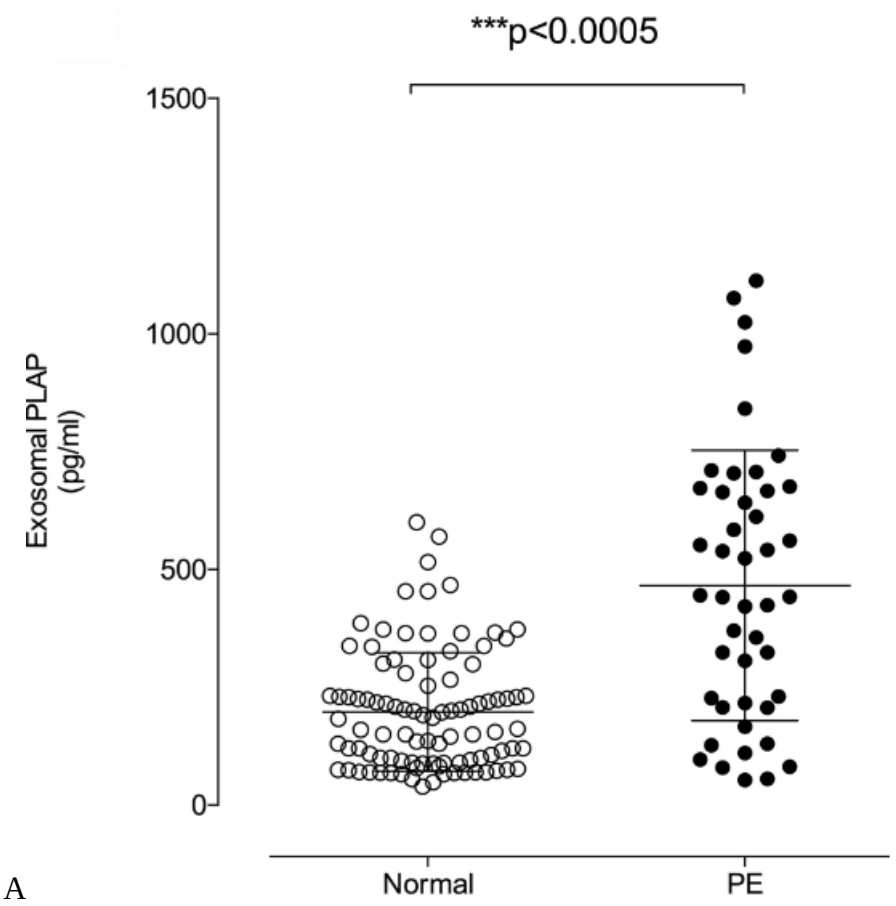
***p<0.0005
Exosomal PLAP (pg/ml)
1500
1000
500
0
Normal
PE

A

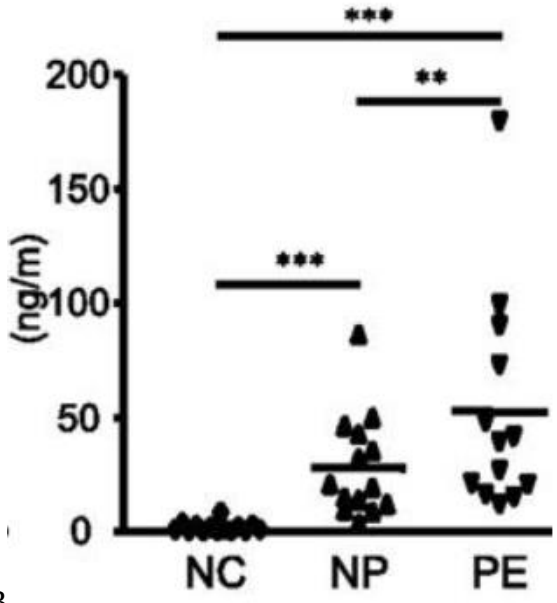
***
**
***
200
150
100
50
0
(ng/m)
NC
NP
PE

B

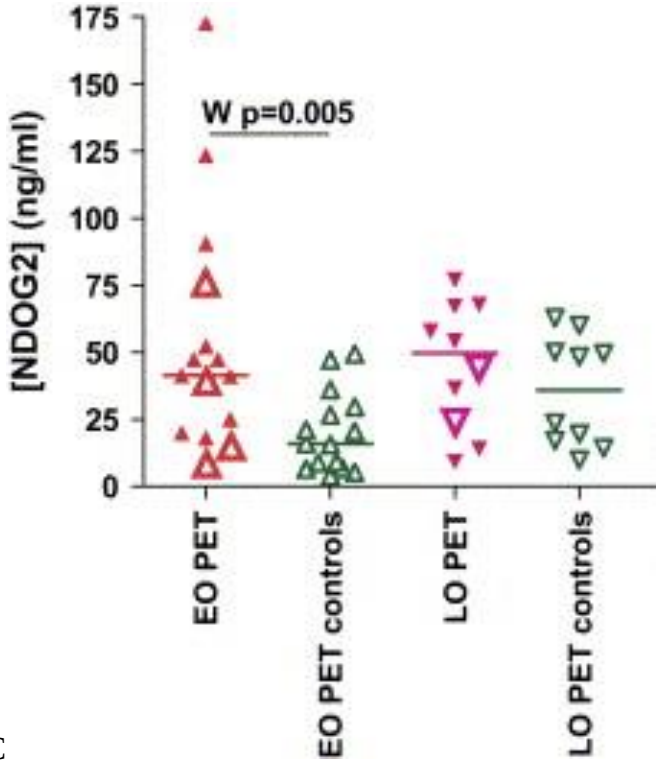
175
150
125
100
75
50
25
0
[NDOG2] (ng/ml)
W p=0.005
EO PET
EO PET controls
LO PET
LO PET controls

C

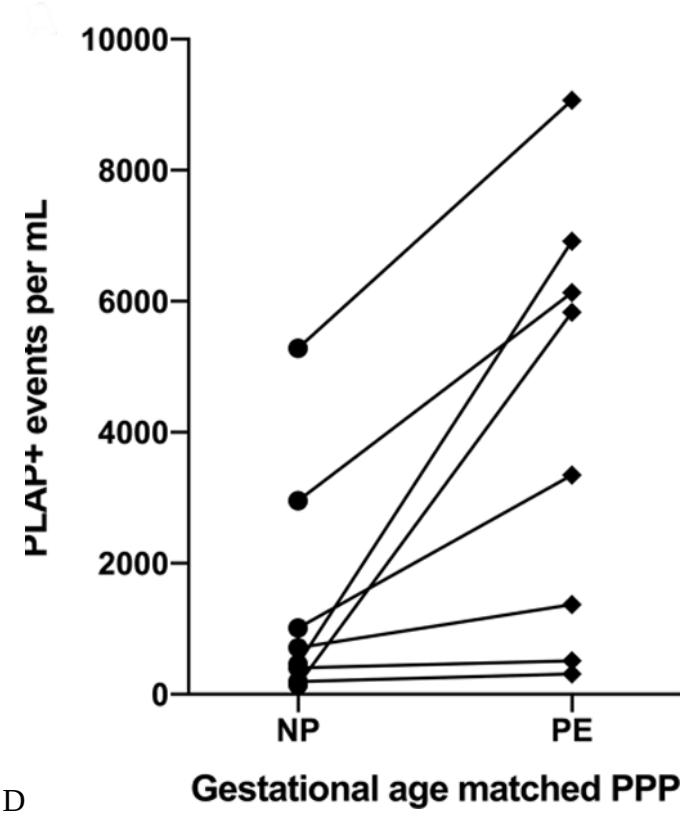
10000
8000
6000
4000
2000
0
PLAP+ events per mL
NP
PE
Gestational age matched PPP

D

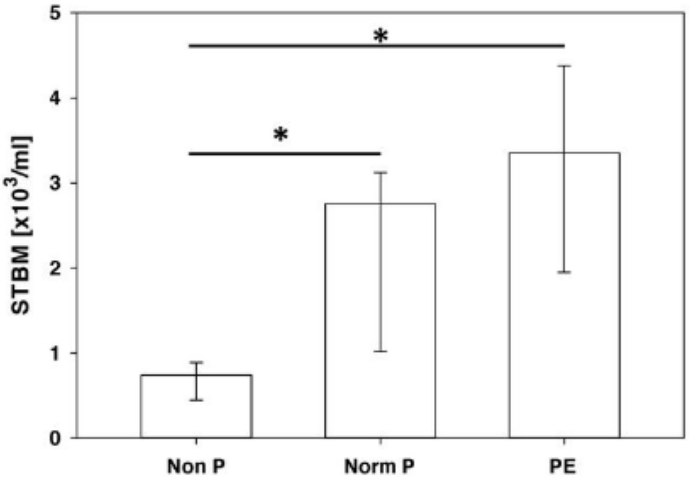

E

Figure 26: Previously published papers showing overlap between preeclamptic and non-hypertensive pregnancy counts of placenta-derived vesicles. (A); Image from Salomon et al 2017[262] *evaluating exosomal PLAP by ELISA assay in normal and preeclamptic pregnancies. Horizontal lines show mean and standard deviation. PE=preeclampsia. Samples matched by gestational age. (B); Image from Germain et al 2007*[282] *evaluating free circulating syncytiotrophoblast-derived microparticles in peripheral plasma by ELISA assay. ***, p<0.001. **, p<0.01. NC=non-pregnant control. NP=non-hypertensive pregnancy. PE=preeclampsia. Samples matched for age (+/- 4 years), parity (0, 1-3, ≥4), gestational age (+/- 13 days). (C); Image from Goswami et al 2006*[265] *evaluating NDOG2 positive vesicles by ELISA. EOPET=early onset preeclampsia. LOPET=late onset preeclmapsia. Horizontal lines represent the median. Controls (nonhypertensive pregnancy) were matched for gestational age. This figure was cropped to remove clinical groups that are not relevant to this project, such as IUGR. (D); Image from Gill et al 2019*[264] *evaluating PLAP-positive events in gestational age-matched platelet poor plasma (PPP) by flow cytometry. NP=normal pregnancy. PE = preeclampsia. (E); Image from Dragovic et al 2013*[370]*, showing total syncytiotrophoblast-derived extracellular vesicles ('STBM') in platelet-free plasma*

*from non-pregnant ('Non P'), normal ('Norm P') and preeclamptic ('PE') women, as measured by flow cytometry with fluorescent markers (e.g. NDOG2). *, $p<0.05$.*

The persistent overlap seen between preeclamptic and non-hypertensive exosome/vesicle counts has implications on the use of this parameter clinically. In terms of diagnostics, it suggests that peripheral placenta-derived exosome levels may not be a good predictive measure in isolation. Certainly, the value of this measure in ruling out preeclampsia is likely to be limited, as there are clearly many cases of preeclampsia with counts in the normal range. This is not to suggest that there is no role for placenta-derived exosome levels in early prediction or diagnostic criteria, but rather that it would likely need to be combined with other markers and parameters to have a useful effect. For example, levels of circulating PLAP+ vesicles above a certain threshold may suggest increased risk of preeclampsia within an algorithm that also includes other elements such as pre-existing risk factors, evidence of inflammatory responses, and angiogenic markers.

Other options for using preeclampsia-derived exosomes in a predictive or diagnostic capacity may focus on the established changes in cargo, as described in Chapter 1. This includes changes in nucleic acid content, lipid profile and proteins from various biological pathways[143,371]. However, when considering incorporation of exosomes into predictive/diagnostic criteria, it is important to weigh up the predictive value of exosomes against the cost, time, and capacity for large-scale measurements within a healthcare system, and this must also be compared to the predictive value and practicalities of other factors.

Moving onto the aim of understanding pathology, changes in placenta-derived exosome levels may be relevant. Preeclampsia cases with altered levels of placenta-derived exosomes may reflect placental dysfunction and stress, and/or preeclamptic exosomes

may drive inflammation and endothelial dysfunction in the periphery. Given the evidence that preeclamptic exosomes can affect systems associated with preeclampsia pathology, it is possible that they contribute to complications and symptoms of preeclampsia, and this effect may be exacerbated in pregnancies with high levels of placenta-derived exosomes in maternal circulation. It is also important to remember that there are many differentially expressed factors in preeclampsia, not just exosomes, and the relative contributions of angiogenic, inflammatory and other compounds have not been well researched.

Both in this study and the ones mentioned above, a large range is seen in preeclamptic placenta-derived exosome counts, with only some cases raised above the levels seen in normal pregnancy. Given the loose diagnostic criteria for preeclampsia, differences in clinical presentation of preeclampsia cases, and questions about whether all diagnosed preeclampsia cases are the same disease, this variation in exosome levels may reflect differences in underlying disease mechanisms. However, the range in this project was much higher than that seen in other studies, which raises the question of whether the highest values seen represent true signal. There was no evidence in this project of interference by HAMAs, however, more extensive experiments are suggested in the 'Future Work' section to rule out this possibility more definitively. It would be useful to understand what the cause of these extremely high values is, whether it's true signal or something affecting the ExoCounter assay's performance.

Unfortunately this project had limited information about the reasons for preeclampsia diagnosis, keeping in mind that preeclampsia is diagnosed as gestational hypertension and another complication, which can be renal, haematological, liver-related, neurological, pulmonary or uteroplacental in nature[115]. It would be interesting to compare levels of placenta-derived extracellular vesicles or other markers to different clusters of symptoms,

e.g. cases with primarily uteroplacental complications versus cases with primarily neurological complications, to see if markers differ.

Analysis of CSF Samples

This project did not provide evidence of placenta-derived exosomes within CSF, as no difference was found between counts in pregnant and non-pregnant CSF. While no evidence in favour of this was found, it is important to clarify that this project does not disprove the presence of placenta-derived exosomes in pregnant CSF. There are several scenarios in which placenta-derived exosomes may cross the BBB and not be detected by the ExoCounter assay:

1. Placenta-derived exosomes are present in extremely low concentrations, that are below the limit of detection for the ExoCounter assay. One paper isolated total exosomes from CSF by ultracentrifugation. The maximum protein density of the exosome-enriched pellet was 5.5 μg/ml. Based on the starting volume of CSF (200-500ml), this suggests that protein concentration of exosomes within CSF is between 0.011 and 0.0275 μg/ml, not accounting for any exosome loss during isolation[372]. In the 200μl aliquots of CSF used in this project, it can be estimated that there would be 2.2 – 5.5ng of exosomal protein. At such small volumes of protein, and not knowing what proportion of CSF exosomes would be placenta-derived, any placenta-derived exosomes may be below the limit of detection for the assay (listed as 1.16ng of exosomal protein in Kabe et al 2018), unless the influx of placenta-derived exosomes was such that they represented a large proportion of total CSF exosomes and/or increased the total exosomal protein in CSF. If the exosomes were present but at concentrations too low for the

ExoCounter's sensitivity, it is questionable whether they would be biologically relevant in such low numbers.

2. Placenta-derived exosomes are not stable when frozen in CSF, and therefore collapse before analysis by ExoCounter assay. However, this seems unlikely as other papers have successfully isolated extracellular vesicles from CSF following freeze-thaw cycles[373,374]. This could potentially be tested experimentally by spike-in of placenta-derived exosomes into CSF followed by freezing, thawing, and measurement.
3. Placenta-derived exosomes are very quickly taken up by neurological tissues, and therefore removed from the CSF.
4. Placenta-derived exosomes release cargo into BBB cells. This cargo is then repackaged and released in BBB exosomes, which would not be detected by the CD63+ PLAP+ criteria.

Despite these possibilities, the limited evidence available suggests that it is likely that placenta-derived exosomes do not reach the CNS, or only do so in negligible numbers. This conclusion is supported by murine studies and this project did not provide any evidence to the contrary. There are two main reasons that may prevent placenta-derived exosomes from reaching the CSF: placenta-derived exosomes are unable to cross the BBB, or placenta-derived exosomes do not reach the BBB in sufficient amounts as they are degraded or taken up by other tissues.

The first possibility may be achieved by selectivity of the BBB in allowing vesicles to cross. Markers on placenta-derived exosomes or another property of these vesicles may prevent passage through the BBB. This could be tested experimentally using an in vitro model of the BBB, such as a transwell assay. Of course, in vitro models of the BBB have drawbacks and are imperfect representations of the in vivo scenario, however this would

still give an estimation about the permeability of the BBB to placenta-derived vesicles[375,376].

The other possibility is that placenta-derived vesicles do not reach the BBB. This is perhaps the more likely explanation given the proven ability of other exosome types to cross the BBB, and murine evidence of placenta-derived or pregnancy-specific vesicles being preferentially taken up by other organs. Studies looking at localisation of injected placenta-derived vesicles in mice repeatedly identify lungs, kidney, and liver as areas where injected placental vesicles are detected, while some also identify various compartments of the female reproductive system e.g. cervix and uterine epithelium[313,314,377]. Localisation of vesicles to these organs may be influenced by the level of blood flow and extensive capillary networks, expression of immune cells with phagocytic receptors, as well as interactions between cell types and vesicle membrane proteins[283,313,377–379]. Indeed, this pattern of localisation (with the inclusion of the spleen) is seen in other exosome populations, supporting the idea that there is something specific about these organs that promotes exosome retention[283].

Overall, it seems quite likely based on the evidence of this project and previously published evidence that placenta-derived exosomes are not present in the CSF in biologically relevant concentrations. However, it is too early to completely rule out this possibility.

Limitations of the Project

A serious issue with the project was that the samples in the different clinical groups were not matched. Significant differences were found in the parity and gestational age between different clinical groups. This is particularly important as gestational age has been previously suggested to affect placenta-derived extracellular vesicle counts[367]. These

confounding factors make it difficult to draw a robust comparison between clinical groups. A better sample-set would use matched samples so that key parameters were roughly similar between the groups or would have stricter selection criteria so that important factors all fall within a prespecified and smaller range.

As with all human data, another issue is interindividual variation caused by uncontrolled factors. The spread of the data within clinical groupings was large, suggesting that more factors influence the counts than just clinical ones. While the patients were grouped into three clinical categories, and extensive demographic and clinical information was recorded, there are many uncontrollable factors at play that create additional noise in the data. This includes diet, daily exercise, fluid intake, activities, e.g. work, etc. Unlike in vivo studies using mice or similar models, it is not feasible or ethical to control these factors in human participants, and it is not clear how these uncontrolled factors may affect data and obscure any clinically linked patterns.

Another limitation of the project was relatively small sample numbers, which were further reduced due to HIV-related concerns and insufficient sample volumes for testing. Sample size is a consistent issue in research using human biological fluids, due to the cost, time and difficulty associated with extracting, storing, and analysing biofluids. This is particularly true for CSF, which is not as easily extracted as fluids such as urine, blood, or saliva. Small sample sizes can have the effect that interindividual variation masks larger patterns in the data. A particular point where low sample sizes was an issue was the comparison between pregnant and non-pregnant CSF. The non-pregnant CSF only had a sample size of four, due to the difficulty of obtaining this sort of sample. Therefore, it is difficult to say whether these four samples are representative of the normal spread of data in non-pregnant samples, and it would be useful to test further non-pregnant CSF samples to get a better idea of baseline values.

Future Work

The results of this project did not suggest that the ExoCounter was sensitive enough to detect any placenta-derived extracellular vesicles in CSF, and it would not be recommended to analyse this further using the same methodology. If large enough volumes of CSF could be obtained from pregnant women, it may be possible to increase the concentration of exosomes in samples by isolating exosomes and then resuspending them in a smaller volume of fluid before measurement by ExoCounter assay. This would require that a significantly larger volume than 200µl is obtained from each woman, otherwise dilution of isolated exosomes to the volumes needed for the ExoCounter would not result in an increased concentration of exosomes, particularly when accounting for pipetting errors and loss of exosomes during isolation. This method was not used in this project because the sample volumes were too low for isolation and resuspension. Another possibility could be to combine the CSF from women of the same clinical grouping to produce large enough sample volumes for isolation and resuspension, but this method has its own drawbacks. Overall, it may be useful to test for placenta-derived exosomes in CSF with an altered methodology to rule out their presence in CSF more conclusively.

The results from plasma samples were more promising and may suggest possible lines for future work. Firstly, it would be useful to repeat some aspects of this project with slightly different methodology. As explained in the Limitations section, samples were not matched for gestational age, maternal age, sex of the child etc., with the most important of these factors being gestational age, as there is previously published evidence suggesting increased placenta-derived extracellular vesicle counts with increasing gestational age[265]. For a better comparison between the three clinical groups, it would be better to take plasma samples at the same gestational age. Additionally, future work could

use plasma samples that are taken at regular intervals, providing information on how counts change with gestational age.

To better investigate the use of ExoCounter values as a predictive measure in preeclampsia/eclampsia, it would be useful to look at plasma samples taken very early in gestation. For example, a study may look at plasma taken at regular intervals in the first and second trimesters and compare that with pregnancy outcomes. As only plasma would be used, it would be easier to increase the sample size because it is more feasible to extract plasma than CSF. This study could be combined with the gestational age investigation described above, as the same measurements could be used to track changes with gestational age and identify any correlations with clinical outcomes.

Another aspect of the plasma data that could be investigated further is the effect of exosome ratios compared to absolute numbers. It has been previously published that the number of total exosomes increases significantly in the plasma in preeclampsia[232,367,368], particularly in the third trimesters. While placenta-derived exosome numbers are also reported to increase in preeclampsia, there is evidence that the increase is lesser compared to the increase in total exosome load. As a result, the proportion of placenta-derived exosomes within the total exosome load may be decreased. It is important to understand how the ExoCounter responds to changes in exosome proportions, as well as absolute numbers, as this could potentially be an issue, particularly as the first antibody used in the ExoCounter assay is often exosome-specific but does not distinguish between populations of exosomes.

A possible method of addressing this issue could be to dilute placenta-derived exosomes in non-placental exosomes in a known concentration. These diluted exosomes can then be run in different volumes, so that the absolute number of placenta-derived exosomes

changes but not the proportion within all exosomes. A second experiment could run the same absolute number of placenta-derived exosomes but diluted in different proportions of non-placental exosomes. Comparing the results from these two experiments would give an idea of the effects of proportion and absolute number on the final ExoCounter results.

It may be valuable to investigate the effects of interfering antibodies further. As explained in Chapter 4 Section 3.i, there was a large overlap between the plasma ExoCounter values in HAMA-positive and HAMA-negative samples. However, the three largest values all fell in the HAMA-positive group. As previously mentioned, HAMAs are highly heterogeneous and can target different areas of mouse immunoglobulins and come in different immunoglobulin forms, such as IgG and IgM antibodies. As a result, it is possible that some HAMA types have an effect but not others, and it was not possible to rule out the idea that HAMAs may be contributing to the highest values seen in the plasma samples. There are various methods that could be used to investigate this possibility further.

1. Addition of non-immune mouse antibodies can be used to reduce interference of HAMAs in immunoassays. Plasma samples with very high counts could be run with and without non-immune mouse antibodies. If the counts were significantly different, this may suggest that HAMAs are having an effect[359].
2. Assays, such as ELISA, which can specifically detect IgM- or IgG-type HAMAs, could be used to detect whether a specific immunoglobulin class has a different effect on ExoCounter counts[359].
3. Dilution testing on samples with suspected HAMA interference. In the absence of HAMA interference, high linearity should be observed when

increasing the dilution of plasma. However, interference by HAMAs results in reduced linearity upon dilution.

Methods such as these could be employed to estimate the likelihood of HAMA interference on the ExoCounter assay. This is an important issue to investigate further if the ExoCounter assay is to be used further in research of biofluids which may contain antibodies. It would also be useful to show experimentally if the size-exclusion aspect of the ExoCounter assay succeeds in reducing interference by non-exosomal particles, such as microvesicles. Hypothetically, the combined use of antibody-based and size-based selection is supposed to reduce interference, but there is no published experimental evidence confirming this.

Conclusion

This project was based on the following previously published evidence, which was discussed in detail in Chapter 1:

- Extensive neurological changes are observed in healthy and pathological pregnancy.
- Exosomes can cross the BBB and be taken up by the brain. Placenta-derived exosomes can increase the permeability and decrease the TEER of a BBB model, particularly when exosomes were isolated from preeclamptic pregnancies.
- Placenta-derived exosomes are taken up by different maternal organs and can affect the behaviour of other cell types in vitro and in animal models.
- The ExoCounter assay has demonstrably high sensitivity and low limits of detection, and is suitable for distinguishing different populations of exosomes, where there is an appropriate marker.

Based on this, a set of hypotheses were drawn up (as set out in Chapter 1, 'Rationale for the Project and Hypotheses'). These hypotheses were then addressed experimentally. The results of these experiments in relation to the hypotheses are summarised here:

1. Syncytiotrophoblast-derived vesicles can cross the BBB and be detected in CSF. **No evidence in favour of this.**
2. The ExoCounter assay has high sensitivity with small volumes of sample, and will be suitable for detecting syncytiotrophoblast-derived vesicles in CSF. **Evidence in favour of this.**
3. Increased BBB permeability in (pre)eclamptic pregnancy, possibly combined with increased numbers of syncytiotrophoblast-derived vesicles, leads to

increased numbers of these vesicles in (pre)eclamptic CSF. **No evidence in favour of this.**

4. Syncytiotrophoblast-derived vesicles may be biologically active in the neurological system and contribute to associated complications and changes. **Not assessed in this project.**

Evidence on the ExoCounter assay's performance included demonstrations of linearity and repeatability, evidence of minimal interference by human or pipetting error, and demonstrated dependence of the assay on intact exosome membranes. Important issues that were raised included the effects of freeze-thaw cycles on exosome counts and the comparative performance of the assay in different biological fluids, which warrants further investigation.

Analysis of plasma samples revealed a significant range of values between samples. While no evidence of interference by anti-mouse antibodies was found in this project, more research into this area is important, as interfering antibodies could be a serious issue in some sample types. No difference was seen between clinical groups, but this was complicated by small sample sizes and a lack of gestational age matching in the samples.

Further work is recommended to develop some of the ideas of this project further. This includes comparison of gestational age-matched samples to better identify differences between clinical groups, investigating the relative effects of absolute numbers of an exosome population versus their proportion in the total exosome population, and measuring plasma from early in pregnancy to assess predictive value.

Overall: the project contributed additional evidence in favour of the ExoCounter assay's high performance, while raising potential issues such as interfering antibodies (HAMAs), freeze-thaw cycles and varied performance in different biological fluids. No evidence was

found of placenta-derived exosomes in the CSF, which aligns with murine studies showing exosome localisation primarily to the liver, lungs, and kidneys. No difference was seen in plasma counts between clinical groupings, but it is difficult to account for the effects of gestational age in unmatched samples. An extremely wide range was seen in plasma sample counts, which warrants further investigation. Variation was particularly high in the preeclamptic group, and may relate to the heterogeneity of the disorder itself.

Bibliography

1. Dasgupta, K. & Jeong, J. Developmental biology of the meninges. *genesis* **57**, e23288 (2019).
2. Firat, R. B. Opening the “Black Box”: Functions of the Frontal Lobes and Their Implications for Sociology. *Frontiers in Sociology* **4**, (2019).
3. Cortés Pascual, A., Moyano Muñoz, N. & Quílez Robres, A. The Relationship Between Executive Functions and Academic Performance in Primary Education: Review and Meta-Analysis. *Front Psychol* **10**, (2019).
4. Siddiqui, S., Chatterjee, U., Kumar, D., Siddiqui, A. & Goyal, N. Neuropsychology of prefrontal cortex. *Indian J Psychiatry* **50**, 202 (2008).
5. Brownsett, S. L. E. & Wise, R. J. S. The Contribution of the Parietal Lobes to Speaking and Writing. *Cerebral Cortex* **20**, 517–523 (2010).
6. Rehman, A. & Al Khalili, Y. *Neuroanatomy, Occipital Lobe*. (2023).
7. Patel, A., Biso, G. M. N. R. & Fowler, J. B. *Neuroanatomy, Temporal Lobe*. (2022).
8. Shahid, Z., Asuka, E. & Singh, G. *Physiology, Hypothalamus*. (2022).
9. Beuriat, P.-A., Cristofori, I., Gordon, B. & Grafman, J. The shifting role of the cerebellum in executive, emotional and social processing across the lifespan. *Behavioral and Brain Functions* **18**, 6 (2022).
10. Anatomy of the Brain. *American Association Of Neurological Surgeons*.
11. Brain Basics: Know Your Brain. *National Institute of Neurological Disorders and Stroke* (2022).
12. Brain Anatomy and How the Brain Works. *John Hopkins Medicine*.
13. Saker, E. *et al.* The Human Central Canal of the Spinal Cord: A Comprehensive Review of its Anatomy, Embryology, Molecular Development, Variants, and Pathology. *Cureus* (2016) doi:10.7759/cureus.927.
14. The Johns Hopkins University. Brain Anatomy and How the Brain Works.
15. Ludwig, P. E., Reddy, V. & Varacallo, M. *Neuroanatomy, Neurons*. (2022).
16. Sharpee, T. O. Toward Functional Classification of Neuronal Types. *Neuron* **83**, 1329–1334 (2014).
17. Wen, Q. & Chklovskii, D. B. Segregation of the Brain into Gray and White Matter: A Design Minimizing Conduction Delays. *PLoS Comput Biol* **1**, e78 (2005).
18. Maldonado, K. A. & Alsayouri, K. *Physiology, Brain*. (2022).
19. Powell, E. M. & Geller, H. M. Dissection of astrocyte-mediated cues in neuronal guidance and process extension. *Glia* **26**, 73–83 (1999).
20. Christopherson, K. S. *et al.* Thrombospondins Are Astrocyte-Secreted Proteins that Promote CNS Synaptogenesis. *Cell* **120**, 421–433 (2005).

21. Schummers, J., Yu, H. & Sur, M. Tuned Responses of Astrocytes and Their Influence on Hemodynamic Signals in the Visual Cortex. *Science (1979)* **320**, 1638–1643 (2008).

22. Perea, G., Navarrete, M. & Araque, A. Tripartite synapses: astrocytes process and control synaptic information. *Trends Neurosci* **32**, 421–431 (2009).

23. Sofroniew, M. v & Vinters, H. v. Astrocytes: biology and pathology. *Acta Neuropathol* **119**, 7–35 (2010).

24. Abbott, N. J., Rönnbäck, L. & Hansson, E. Astrocyte–endothelial interactions at the blood–brain barrier. *Nat Rev Neurosci* **7**, 41–53 (2006).

25. Jäkel, S. & Dimou, L. Glial Cells and Their Function in the Adult Brain: A Journey through the History of Their Ablation. *Front Cell Neurosci* **11**, (2017).

26. Lenz, K. M. & Nelson, L. H. Microglia and Beyond: Innate Immune Cells As Regulators of Brain Development and Behavioral Function. *Front Immunol* **9**, (2018).

27. Ransohoff, R. M. & Khoury, J. el. Microglia in Health and Disease. *Cold Spring Harb Perspect Biol* **8**, a020560 (2016).

28. Parkhurst, C. N. *et al.* Microglia Promote Learning-Dependent Synapse Formation through Brain-Derived Neurotrophic Factor. *Cell* **155**, 1596–1609 (2013).

29. Wardlaw, J. M. *et al.* Perivascular spaces in the brain: anatomy, physiology and pathology. *Nat Rev Neurol* **16**, 137–153 (2020).

30. Marques, F. *et al.* The choroid plexus in health and in disease: dialogues into and out of the brain. *Neurobiol Dis* **107**, 32–40 (2017).

31. Telano, L. N. & Baker, S. *Physiology, Cerebral Spinal Fluid*. (2023).

32. Javed, K., Reddy, V. & Lui, F. *Neuroanatomy, Choroid Plexus*. (2023).

33. Wichmann, T. O., Damkier, H. H. & Pedersen, M. A Brief Overview of the Cerebrospinal Fluid System and Its Implications for Brain and Spinal Cord Diseases. *Front Hum Neurosci* **15**, (2022).

34. Orešković, D. & Klarica, M. The formation of cerebrospinal fluid: Nearly a hundred years of interpretations and misinterpretations. *Brain Res Rev* **64**, 241–262 (2010).

35. Sato, O. *et al.* BULK FLOW IN THE CEREBROSPINAL FLUID SYSTEM OF THE DOG. *Acta Neurol Scand* **51**, 1–11 (2009).

36. Pollay, M. & Curl, F. Secretion of cerebrospinal fluid by the ventricular ependyma of the rabbit. *American Journal of Physiology-Legacy Content* **213**, 1031–1038 (1967).

37. Miyajima, M. & Arai, H. Evaluation of the Production and Absorption of Cerebrospinal Fluid. *Neurol Med Chir (Tokyo)* **55**, 647–56 (2015).

38. Orešković, D. & Klarica, M. A new look at cerebrospinal fluid movement. *Fluids Barriers CNS* **11**, 16 (2014).

39. Merril, C. R., Seipp, H. W. & Luchsinger, P. C. Total CO_2, Pco_2, and pH in human spinal fluid. *J Appl Physiol* **16**, 485–487 (1961).

40. Castro, D., Patil, S. M. & Keenaghan, M. *Arterial Blood Gas*. (2022).

41. Akaishi, T. *et al.* Osmotic pressure of serum and cerebrospinal fluid in patients with suspected neurological conditions. *Neural Regen Res* **15**, 944 (2020).

42. Batlle, D., Chen, S. & Haque, S. K. Physiologic Principles in the Clinical Evaluation of Electrolyte, Water, and Acid–Base Disorders. in *Seldin and Giebisch's The Kidney* 2477–2511 (Elsevier, 2013). doi:10.1016/B978-0-12-381462-3.00074-4.

43. Millen, J. & Woollam, D. *The anatomy of the cerebrospinal fluid*. (Oxford University Press, 1962).

44. Hladky, S. B. & Barrand, M. A. Mechanisms of fluid movement into, through and out of the brain: evaluation of the evidence. *Fluids Barriers CNS* **11**, 26 (2014).

45. Davson, H. & Segal, M. *Physiology of the CSF and Blood-Brain Barriers*. (CRC Press; 1st edition, 1995).

46. Zhang, Y. *et al.* A comprehensive map and functional annotation of the normal human cerebrospinal fluid proteome. *J Proteomics* **119**, 90–99 (2015).

47. Kroksveen, A. C., Opsahl, J. A., Aye, T. T., Ulvik, R. J. & Berven, F. S. Proteomics of human cerebrospinal fluid: Discovery and verification of biomarker candidates in neurodegenerative diseases using quantitative proteomics. *J Proteomics* **74**, 371–388 (2011).

48. Schutzer, S. E. *et al.* Establishing the Proteome of Normal Human Cerebrospinal Fluid. *PLoS One* **5**, e10980 (2010).

49. Zhang, J. Proteomics of human cerebrospinal fluid – the good, the bad, and the ugly. *Proteomics Clin Appl* **1**, 805–819 (2007).

50. Reiber, H. Dynamics of brain-derived proteins in cerebrospinal fluid. *Clinica Chimica Acta* **310**, 173–186 (2001).

51. Begcevic, I., Brinc, D., Drabovich, A. P., Batruch, I. & Diamandis, E. P. Identification of brain-enriched proteins in the cerebrospinal fluid proteome by LC-MS/MS profiling and mining of the Human Protein Atlas. *Clin Proteomics* **13**, 11 (2016).

52. Guldbrandsen, A. *et al.* In-depth Characterization of the Cerebrospinal Fluid (CSF) Proteome Displayed Through the CSF Proteome Resource (CSF-PR). *Molecular & Cellular Proteomics* **13**, 3152–3163 (2014).

53. Kroksveen, A. C., Opsahl, J. A., Aye, T. T., Ulvik, R. J. & Berven, F. S. Proteomics of human cerebrospinal fluid: Discovery and verification of biomarker candidates in neurodegenerative diseases using quantitative proteomics. *J Proteomics* **74**, 371–388 (2011).

54. Knox, E. G., Aburto, M. R., Clarke, G., Cryan, J. F. & O'Driscoll, C. M. The blood-brain barrier in aging and neurodegeneration. *Mol Psychiatry* **27**, 2659–2673 (2022).

55. Alahmari, A. Blood-Brain Barrier Overview: Structural and Functional Correlation. *Neural Plast* **2021**, 1–10 (2021).

56. Daneman, R. & Prat, A. The Blood–Brain Barrier. *Cold Spring Harb Perspect Biol* **7**, a020412 (2015).

57. Armulik, A. *et al.* Pericytes regulate the blood–brain barrier. *Nature* **468**, 557–561 (2010).

58. Sobue, K. *et al.* Induction of blood–brain barrier properties in immortalized bovine brain endothelial cells by astrocytic factors. *Neurosci Res* **35**, 155–164 (1999).

59. Hayashi, Y. *et al.* Induction of various blood-brain barrier properties in non-neural endothelial cells by close apposition to co-cultured astrocytes. *Glia* **19**, 13–26 (1997).

60. Janzer, R. C. & Raff, M. C. Astrocytes induce blood–brain barrier properties in endothelial cells. *Nature* **325**, 253–257 (1987).

61. Michinaga, S. & Koyama, Y. Dual Roles of Astrocyte-Derived Factors in Regulation of Blood-Brain Barrier Function after Brain Damage. *Int J Mol Sci* **20**, 571 (2019).

62. Kang, R. *et al.* The Dual Role of Microglia in Blood-Brain Barrier Dysfunction after Stroke. *Curr Neuropharmacol* **18**, 1237–1249 (2020).

63. Erdheim J & Stumme E. . Über die Schwangerschaftsveränderung der Hypophyse. *Beitr. Pathol. Anat.* **45**, 1–17 (1909).

64. Oatridge, A. *et al.* Change in brain size during and after pregnancy: study in healthy women and women with preeclampsia. *AJNR Am J Neuroradiol* **23**, 19–26 (2002).

65. Luders, E., Kurth, F. & Sundström Poromaa, I. The neuroanatomy of pregnancy and postpartum. *Neuroimage* **263**, 119646 (2022).

66. Hoekzema, E. *et al.* Mapping the effects of pregnancy on resting state brain activity, white matter microstructure, neural metabolite concentrations and grey matter architecture. *Nat Commun* **13**, 6931 (2022).

67. Hoekzema, E. *et al.* Pregnancy leads to long-lasting changes in human brain structure. *Nat Neurosci* **20**, 287–296 (2017).

68. Chechko, N. *et al.* The expectant brain–pregnancy leads to changes in brain morphology in the early postpartum period. *Cerebral Cortex* **32**, 4025–4038 (2022).

69. Chu, T. *et al.* Pregnancy leads to changes in the brain functional network: a connectome analysis. *Brain Imaging Behav* **16**, 811–819 (2022).

70. Bakoyiannis, I. Identification of a brain structure that modulates maternal behavior during pregnancy. *Lab Anim (NY)* **51**, 101–101 (2022).

71. Topilko, T. *et al.* Edinger-Westphal peptidergic neurons enable maternal preparatory nesting. *Neuron* **110**, 1385-1399.e8 (2022).

72. Moya, J. *et al.* A review of physiological and behavioral changes during pregnancy and lactation: Potential exposure factors and data gaps. *J Expo Sci Environ Epidemiol* **24**, 449–458 (2014).

73. Augustine, R. A., Ladyman, S. R. & Grattan, D. R. From feeding one to feeding many: hormone-induced changes in bodyweight homeostasis during pregnancy. *J Physiol* **586**, 387–397 (2008).

74. Pittman, Q. J. Brain adaptations for a successful pregnancy. *J Physiol* **586**, 367–367 (2008).

75. Gadsby, R., Ivanova, D., Trevelyan, E., Hutton, J. L. & Johnson, S. The onset of nausea and vomiting of pregnancy: a prospective cohort study. *BMC Pregnancy Childbirth* **21**, 10 (2021).

76. Beat Eating Disorders. Pica. *Beat Eating Disorders*.

77. Ezzeddin, N., Zavoshy, R., Noroozi, M., Jahanihashemi, H. & Riseh, S. H. Prevalence and risk factors for pica during pregnancy in Tehran, Iran. *Eating and Weight Disorders - Studies on Anorexia, Bulimia and Obesity* **20**, 457–463 (2015).

78. Zhou, Y. *et al.* The prevalence of psychiatric symptoms of pregnant and non-pregnant women during the COVID-19 epidemic. *Transl Psychiatry* **10**, 319 (2020).

79. Slattery, D. A. & Neumann, I. D. No stress please! Mechanisms of stress hyporesponsiveness of the maternal brain. *J Physiol* **586**, 377–385 (2008).

80. Pownall, M., Hutter, R. R. C., Rockliffe, L. & Conner, M. Memory and mood changes in pregnancy: a qualitative content analysis of women's first-hand accounts. *J Reprod Infant Psychol* 1–12 (2022) doi:10.1080/02646838.2022.2052827.

81. Gałązka, I., Drosdzol-Cop, A., Naworska, B., Czajkowska, M. & Skrzypulec-Plinta, V. Changes in the Sexual Function During Pregnancy. *J Sex Med* **12**, 445–454 (2015).

82. Chang, S.-R., Chen, K.-H., Lin, H.-H. & Yu, H.-J. Comparison of Overall Sexual Function, Sexual Intercourse/Activity, Sexual Satisfaction, and Sexual Desire During the Three Trimesters of Pregnancy and Assessment of Their Determinants. *J Sex Med* **8**, 2859–2867 (2011).

83. Kuga, M., Ikeda, M., Suzuki, K. & Takeuchi, S. Changes in Gustatory Sense During Pregnancy. *Acta Otolaryngol* **122**, 146–153 (2002).

84. Choo, E. & Dando, R. The Impact of Pregnancy on Taste Function. *Chem Senses* **42**, 279–286 (2017).

85. Silvestri, R. & Aricò, I. Sleep disorders in pregnancy. *Sleep Science* **12**, (2019).

86. Davies, S. J., Lum, J. A., Skouteris, H., Byrne, L. K. & Hayden, M. J. Cognitive impairment during pregnancy: a meta-analysis. *Medical Journal of Australia* **208**, 35–40 (2018).

87. Vanston, C. M. & Watson, N. V. Selective and persistent effect of foetal sex on cognition in pregnant women. *Neuroreport* **16**, 779–782 (2005).

88. DE GROOT, R. H. M., VUURMAN, E. F. P. M., HORNSTRA, G. & JOLLES, J. Differences in cognitive performance during pregnancy and early motherhood. *Psychol Med* **36**, 1023 (2006).

89. Henry, J. F. & Sherwin, B. B. Hormones and cognitive functioning during late pregnancy and postpartum: A longitudinal study. *Behavioral Neuroscience* **126**, 73–85 (2012).

90. Brindle, P. M., Brown, M. W., Brown, J., Griffith, H. B. & Turner, G. M. Objective and subjective memory impairment in pregnancy. *Psychol Med* **21**, 647–653 (1991).

91. Orchard, E. R., Ward, P. G. D., Egan, G. F. & Jamadar, S. D. Evidence of Subjective, But Not Objective, Cognitive Deficit in New Mothers at 1-Year Postpartum. *J Womens Health* **31**, 1087–1096 (2022).

92. Schneider, Z. Cognitive performance in pregnancy. *Aust J Adv Nurs* **6**, 40–7 (1989).

93. Barda, G. *et al.* The effect of pregnancy on maternal cognition. *Sci Rep* **11**, 12187 (2021).

94. Anderson, M. V & Rutherford, M. D. Cognitive reorganization during pregnancy and the postpartum period: an evolutionary perspective. *Evol Psychol* **10**, 659–87 (2012).

95. Bower, G. H. *A brief history of memory research - The Oxford Handbook of Memory*. (Oxford University Press, 2000).

96. Miyake, A. & Shah, P. Models of Working Memory: Mechanisms of Active Maintenance and Executive Control. *Am J Psychol* **114**, (2001).

97. Cowan, N. Working Memory Underpins Cognitive Development, Learning, and Education. *Educ Psychol Rev.* **26**, 197–223 (2014).

98. Crystal, J. D. & Wilson, A. G. Prospective memory: a comparative perspective. *Behavioural processes* **112**, 88–99 (2015).

99. Ameen-Ali, K. E., Easton, A. & Eacott, M. J. Moving beyond standard procedures to assess spontaneous recognition memory. *Neurosci Biobehav Rev* **53**, 37–51 (2015).

100. Medina, J. J. The biology of recognition memory. *Psychiatr. Times* **13**, 13–16 (2008).

101. Kinsley, C. H., Meyer, E. & Rafferty, K. A. Sex Steroid Hormone Determination of the Maternal Brain: Effects Beyond Reproduction. *Mini-Reviews in Medicinal Chemistry* **12**, 1063–1070 (2012).

102. Kinsley, C. H., Franssen, R. A. & Meyer, E. A. Reproductive Experience may Positively Adjust the Trajectory of Senescence. in 317–345 (2011). doi:10.1007/7854_2011_123.

103. Hofman, A. *et al.* The Rotterdam Study: objectives and design update. *Eur J Epidemiol* **22**, 819–829 (2007).

104. Martínez-García, M., Paternina-Die, M., Desco, M., Vilarroya, O. & Carmona, S. Characterizing the Brain Structural Adaptations Across the Motherhood Transition. *Front Glob Womens Health* **2**, (2021).

105. Hillerer, K. M., Jacobs, V. R., Fischer, T. & Aigner, L. The Maternal Brain: An Organ with Peripartal Plasticity. *Neural Plast* **2014**, 1–20 (2014).

106. Bracken, M. B. Why animal studies are often poor predictors of human reactions to exposure. *J R Soc Med* **102**, 120–122 (2009).

107. Cipolla, M. J. The Adaptation of the Cerebral Circulation to Pregnancy: *Mechanisms and Consequences*. *Journal of Cerebral Blood Flow & Metabolism* **33**, 465–478 (2013).

108. Cipolla, M. J. *et al.* Pregnant serum induces neuroinflammation and seizure activity via TNFα. *Exp Neurol* **234**, 398–404 (2012).

109. Cipolla, M. J., Sweet, J. G. & Chan, S.-L. Cerebral vascular adaptation to pregnancy and its role in the neurological complications of eclampsia. *J Appl Physiol* **110**, 329–339 (2011).

110. Euser, A. G., Bullinger, L. & Cipolla, M. J. Magnesium sulphate treatment decreases blood-brain barrier permeability during acute hypertension in pregnant rats. *Exp Physiol* **93**, 254–261 (2008).

111. Fox, R., Kitt, J., Leeson, P., Aye, C. Y. L. & Lewandowski, A. J. Preeclampsia: Risk Factors, Diagnosis, Management, and the Cardiovascular Impact on the Offspring. *J Clin Med* **8**, 1625 (2019).

112. Brown, M. A. *et al.* Hypertensive Disorders of Pregnancy. *Hypertension* **72**, 24–43 (2018).

113. Simard, J. F. *et al.* Evidence of under-reporting of early-onset preeclampsia using register data. *Paediatr Perinat Epidemiol* **35**, 596–600 (2021).

114. Magee, L. A. *et al.* The 2021 International Society for the Study of Hypertension in Pregnancy classification, diagnosis & management recommendations for international practice. *Pregnancy Hypertens* **27**, 148–169 (2022).

115. Dimitriadis, E. *et al.* Pre-eclampsia. *Nat Rev Dis Primers* **9**, 8 (2023).

116. Staff, A. C. & Redman, C. W. G. The Differences Between Early- and Late-Onset Pre-eclampsia. in 157–172 (2018). doi:10.1007/978-981-10-5891-2_10.

117. Raymond, D. & Peterson, E. A Critical Review of Early-Onset and Late-Onset Preeclampsia. *Obstet Gynecol Surv* **66**, 497–506 (2011).

118. Pankiewicz, K., Szczerba, E., Maciejewski, T. & Fijałkowska, A. Non-obstetric complications in preeclampsia. *Menopausal Review* **18**, 99–109 (2019).

119. Davis, E. F. *et al.* Cardiovascular Risk Factors in Children and Young Adults Born to Preeclamptic Pregnancies: A Systematic Review. *Pediatrics* **129**, e1552–e1561 (2012).

120. Huang, C. *et al.* Maternal hypertensive disorder of pregnancy and mortality in offspring from birth to young adulthood: national population based cohort study. *BMJ* e072157 (2022) doi:10.1136/bmj-2022-072157.

121. Poon, L. C. Y., Kametas, N. A., Chelemen, T., Leal, A. & Nicolaides, K. H. Maternal risk factors for hypertensive disorders in pregnancy: a multivariate approach. *J Hum Hypertens* **24**, 104–110 (2010).

122. Arechvo, A. *et al.* Maternal race and pre-eclampsia: Cohort study and systematic review with meta-analysis. *BJOG* **129**, 2082–2093 (2022).

123. Anderson, N. H., Sadler, L. C., Stewart, A. W., Fyfe, E. M. & McCowan, L. M. E. Ethnicity, body mass index and risk of pre-eclampsia in a multiethnic New Zealand population. *Australian and New Zealand Journal of Obstetrics and Gynaecology* **52**, 552–558 (2012).

124. Zhang, S. *et al.* Racial Disparities in Economic and Clinical Outcomes of Pregnancy Among Medicaid Recipients. *Matern Child Health J* **17**, 1518–1525 (2013).

125. Gong, J., Savitz, D. A., Stein, C. R. & Engel, S. M. Maternal ethnicity and pre-eclampsia in New York City, 1995-2003. *Paediatr Perinat Epidemiol* **26**, 45–52 (2012).

126. Cappuccio, F. P., Cook, D. G., Atkinson, R. W. & Strazzullo, P. Prevalence, detection, and management of cardiovascular risk factors in different ethnic groups in south London. *Heart* **78**, 555–563 (1997).

127. Ramaraj, R. & Chellappa, P. Cardiovascular risk in South Asians. *Postgrad Med J* **84**, 518–523 (2008).

128. Conde-Agudelo, A. & Belizan, J. M. Risk factors for pre-eclampsia in a large cohort of Latin American and Caribbean women. *BJOG* **107**, 75–83 (2000).

129. Lv, L.-J. *et al.* Early-Onset Preeclampsia Is Associated With Gut Microbial Alterations in Antepartum and Postpartum Women. *Front Cell Infect Microbiol* **9**, (2019).

130. Chen, X. *et al.* Gut dysbiosis induces the development of pre-eclampsia through bacterial translocation. *Gut* **69**, 513–522 (2020).

131. Duckitt, K. & Harrington, D. Risk factors for pre-eclampsia at antenatal booking: systematic review of controlled studies. *BMJ* **330**, 565 (2005).

132. Skjærven, R., Wilcox, A. J. & Lie, R. T. The Interval between Pregnancies and the Risk of Preeclampsia. *New England Journal of Medicine* **346**, 33–38 (2002).

133. Robillard, P.-Y. *et al.* Paternity patterns and risk of preeclampsia in the last pregnancy in multiparae. *J Reprod Immunol* **24**, 1–12 (1993).

134. Mittendorf, R., Lain, K. Y., Williams, M. A. & Walker, C. K. Preeclampsia. A nested, case-control study of risk factors and their interactions. *J Reprod Med* **41**, 491–6 (1996).

135. Robillard, P.-Y. *et al.* The blurring boundaries between placental and maternal preeclampsia: a critical appraisal of 1800 consecutive preeclamptic cases. *The Journal of Maternal-Fetal & Neonatal Medicine* **35**, 2450–2456 (2022).

136. Bearblock, E., Aiken, C. E. & Burton, G. J. Air pollution and pre-eclampsia; associations and potential mechanisms. *Placenta* **104**, 188–194 (2021).

137. Perry, A., Stephanou, A. & Rayman, M. P. Dietary factors that affect the risk of pre-eclampsia. *BMJ Nutr Prev Health* **5**, 118–133 (2022).

138. Lain, K. Y. Contemporary Concepts of the Pathogenesis and Management of Preeclampsia. *JAMA* **287**, 3183 (2002).

139. Roberts, J. M. & Escudero, C. The placenta in preeclampsia. *Pregnancy Hypertens* **2**, 72–83 (2012).

140. Cindrova-Davies, T. & Sferruzzi-Perri, A. N. Human placental development and function. *Semin Cell Dev Biol* **131**, 66–77 (2022).

141. Papanikolaou, I. G. *et al.* Abnormal placentation: Current evidence and review of the literature. *European Journal of Obstetrics & Gynecology and Reproductive Biology* **228**, 98–105 (2018).

142. Albrecht, E. D. & Pepe, G. J. Regulation of Uterine Spiral Artery Remodeling: a Review. *Reproductive Sciences* **27**, 1932–1942 (2020).

143. Aplin, J. D., Myers, J. E., Timms, K. & Westwood, M. Tracking placental development in health and disease. *Nat Rev Endocrinol* **16**, 479–494 (2020).

144. Staff, A. C. *et al.* Failure of physiological transformation and spiral artery atherosis: their roles in preeclampsia. *Am J Obstet Gynecol* **226**, S895–S906 (2022).

145. Brosens, I. A., Robertson, W. B. & Dixon, H. G. The role of the spiral arteries in the pathogenesis of preeclampsia. *Obstet Gynecol Annu* **1**, 177–91 (1972).

146. Lyall, F., Robson, S. C. & Bulmer, J. N. Spiral Artery Remodeling and Trophoblast Invasion in Preeclampsia and Fetal Growth Restriction. *Hypertension* **62**, 1046–1054 (2013).

147. Wadhwani, P., Saha, P. K., Kalra, J. K., Gainder, S. & Sundaram, V. A study to compare maternal and perinatal outcome in early vs. late onset preeclampsia. *Obstet Gynecol Sci* **63**, 270–277 (2020).

148. Burton, G. J., Woods, A. W., Jauniaux, E. & Kingdom, J. C. P. Rheological and Physiological Consequences of Conversion of the Maternal Spiral Arteries for Uteroplacental Blood Flow during Human Pregnancy. *Placenta* **30**, 473–482 (2009).

149. Cronqvist, T. *et al.* Syncytiotrophoblast derived extracellular vesicles transfer functional placental miRNAs to primary human endothelial cells. *Sci Rep* **7**, 4558 (2017).

150. Phipps, E. A., Thadhani, R., Benzing, T. & Karumanchi, S. A. Pre-eclampsia: pathogenesis, novel diagnostics and therapies. *Nat Rev Nephrol* **15**, 275–289 (2019).

151. Donthi, D. *et al.* An Objective Histopathological Scoring System for Placental Pathology in Pre-Eclampsia and Eclampsia. *Cureus* (2020) doi:10.7759/cureus.11104.

152. Roberts, J. M. & Escudero, C. The placenta in preeclampsia. *Pregnancy Hypertension: An International Journal of Women's Cardiovascular Health* **2**, 72–83 (2012).

153. Thilaganathan, B. Pre-eclampsia and the cardiovascular-placental axis. *Ultrasound in Obstetrics & Gynecology* **51**, 714–717 (2018).

154. Thilaganathan, B. & Kalafat, E. Cardiovascular System in Preeclampsia and Beyond. *Hypertension* **73**, 522–531 (2019).

155. Ness, R. B., Markovic, N., Harger, G. & Day, R. Barrier Methods, Length of Preconception Intercourse, and Preeclampsia. *Hypertens Pregnancy* **23**, 227–235 (2004).

156. Hernández-Valencia, M., Saldaña Quezada, L., Alvarez Muñoz, M. & Valdez Martínez, E. [Barrier family planning methods as risk factor which predisposes to preeclampsia]. *Ginecol Obstet Mex* **68**, 333–8 (2000).

157. Mills, J. L., Klebanoff, M. A., Graubard, B. I., Carey, J. C. & Berendes, H. W. Barrier contraceptive methods and preeclampsia. *JAMA* **265**, 70–3 (1991).

158. Trupin, L. S., Simon, L. P. & Eskenazi, B. Change in Paternity. *Epidemiology* **7**, 240–244 (1996).

159. Cormick, G., Betrán, A. P., Ciapponi, A., Hall, D. R. & Hofmeyr, G. J. Inter-pregnancy interval and risk of recurrent pre-eclampsia: systematic review and meta-analysis. *Reprod Health* **13**, 83 (2016).

160. González-Comadran, M. *et al.* The impact of donor insemination on the risk of preeclampsia: a systematic review and meta-analysis. *European Journal of Obstetrics & Gynecology and Reproductive Biology* **182**, 160–166 (2014).

161. Luo, Z.-C. *et al.* The effects and mechanisms of primiparity on the risk of pre-eclampsia: a systematic review. *Paediatr Perinat Epidemiol* **21**, 36–45 (2007).

162. Koelman, C. A. *et al.* Correlation between oral sex and a low incidence of preeclampsia: a role for soluble HLA in seminal fluid? *J Reprod Immunol* **46**, 155–166 (2000).

163. Saito, S. & Sakai, M. Th1/Th2 balance in preeclampsia. *J Reprod Immunol* **59**, 161–173 (2003).

164. Sasaki, Y. *et al.* Proportion of peripheral blood and decidual CD4+ CD25bright regulatory T cells in pre-eclampsia. *Clin Exp Immunol* **149**, 139–145 (2007).

165. Lynch, A. M. *et al.* Alternative complement pathway activation fragment Bb in early pregnancy as a predictor of preeclampsia. *Am J Obstet Gynecol* **198**, 385.e1-385.e9 (2008).

166. Liu, X. *et al.* Trophoblast-Derived Extracellular Vesicles Promote Preeclampsia by Regulating Macrophage Polarization. *Hypertension* **79**, 2274–2287 (2022).

167. Hausvater, A. *et al.* The association between preeclampsia and arterial stiffness. *J Hypertens* **30**, 17–33 (2012).

168. Pant, V., Yadav, B. K. & Sharma, J. A cross sectional study to assess the sFlt-1:PlGF ratio in pregnant women with and without preeclampsia. *BMC Pregnancy Childbirth* **19**, 266 (2019).

169. Maynard, S. E. *et al.* Excess placental soluble fms-like tyrosine kinase 1 (sFlt1) may contribute to endothelial dysfunction, hypertension, and proteinuria in preeclampsia. *Journal of Clinical Investigation* **111**, 649–658 (2003).

170. Ahmad, S. & Ahmed, A. Elevated Placental Soluble Vascular Endothelial Growth Factor Receptor-1 Inhibits Angiogenesis in Preeclampsia. *Circ Res* **95**, 884–891 (2004).

171. Suwaki, N. *et al.* Hypoadiponectinemia and circulating angiogenic factors in overweight patients complicated with pre-eclampsia. *Am J Obstet Gynecol* **195**, 1687–1692 (2006).

172. Levine, R. J. *et al.* Serum sFlt1 concentration during preeclampsia and mid trimester blood pressure in healthy nulliparous women. *Am J Obstet Gynecol* **194**, 1034–1041 (2006).

173. Palmer, K. R., Tong, S. & Kaitu'u-Lino, T. J. Placental-specific sFLT-1: role in pre-eclamptic pathophysiology and its translational possibilities for clinical prediction and diagnosis. *Mol Hum Reprod* (2016) doi:10.1093/molehr/gaw077.

174. Thadhani, R. *et al.* Pilot Study of Extracorporeal Removal of Soluble Fms-Like Tyrosine Kinase 1 in Preeclampsia. *Circulation* **124**, 940–950 (2011).

175. Thadhani, R. *et al.* Removal of Soluble Fms-Like Tyrosine Kinase-1 by Dextran Sulfate Apheresis in Preeclampsia. *Journal of the American Society of Nephrology* **27**, 903–913 (2016).

176. Steegers, E. A., von Dadelszen, P., Duvekot, J. J. & Pijnenborg, R. Pre-eclampsia. *The Lancet* **376**, 631–644 (2010).

177. Ness, R. B. & Roberts, J. M. Heterogeneous causes constituting the single syndrome of preeclampsia: A hypothesis and its implications. *Am J Obstet Gynecol* **175**, 1365–1370 (1996).

178. Myatt, L. & Roberts, J. M. Preeclampsia: Syndrome or Disease? *Curr Hypertens Rep* **17**, 83 (2015).

179. Jhee, J. H. *et al.* Prediction model development of late-onset preeclampsia using machine learning-based methods. *PLoS One* **14**, e0221202 (2019).

180. Phipps, E. A., Thadhani, R., Benzing, T. & Karumanchi, S. A. Pre-eclampsia: pathogenesis, novel diagnostics and therapies. *Nat Rev Nephrol* **15**, 275–289 (2019).

181. Gilbert, J. S. *et al.* Recombinant Vascular Endothelial Growth Factor 121 Infusion Lowers Blood Pressure and Improves Renal Function in Rats With PlacentalIschemia-Induced Hypertension. *Hypertension* **55**, 380–385 (2010).

182. Bergmann, A. *et al.* Reduction of circulating soluble Flt-1 alleviates preeclampsia-like symptoms in a mouse model. *J Cell Mol Med* **14**, 1857–1867 (2009).

183. Li, Z. *et al.* Recombinant Vascular Endothelial Growth Factor 121 Attenuates Hypertension and Improves Kidney Damage in a Rat Model of Preeclampsia. *Hypertension* **50**, 686–692 (2007).

184. Spradley, F. T. *et al.* Placental Growth Factor Administration Abolishes Placental Ischemia-Induced Hypertension. *Hypertension* **67**, 740–747 (2016).

185. Makris, A. *et al.* Placental Growth Factor Reduces Blood Pressure in a Uteroplacental Ischemia Model of Preeclampsia in Nonhuman Primates. *Hypertension* **67**, 1263–1272 (2016).

186. Turanov, A. A. *et al.* RNAi modulation of placental sFLT1 for the treatment of preeclampsia. *Nat Biotechnol* **36**, 1164–1173 (2018).

187. Beaufils, M., Donsimoni, R., Uzan, S. & Colau, J. C. PREVENTION OF PRE-ECLAMPSIA BY EARLY ANTIPLATELET THERAPY. *The Lancet* **325**, 840–842 (1985).

188. Askie, L. M., Duley, L., Henderson-Smart, D. J. & Stewart, L. A. Antiplatelet agents for prevention of pre-eclampsia: a meta-analysis of individual patient data. *The Lancet* **369**, 1791–1798 (2007).

189. Davenport, M. H. *et al.* Prenatal exercise for the prevention of gestational diabetes mellitus and hypertensive disorders of pregnancy: a systematic review and meta-analysis. *Br J Sports Med* **52**, 1367–1375 (2018).

190. Woo Kinshella, M. *et al.* Calcium for pre-eclampsia prevention: A systematic review and network meta-analysis to guide personalised antenatal care. *BJOG* **129**, 1833–1843 (2022).

191. Tita, A. T. *et al.* Treatment for Mild Chronic Hypertension during Pregnancy. *New England Journal of Medicine* **386**, 1781–1792 (2022).

192. *Chesley's Hypertensive Disorders in Pregnancy*. (Elsevier, 2009). doi:10.1016/B978-0-12-374213-1.X0001-8.

193. Miller, E. C. & Vollbracht, S. Neurology of Preeclampsia and Related Disorders: an Update in Neuro-obstetrics. *Curr Pain Headache Rep* **25**, 40 (2021).

194. Hasegawa, J. *et al.* Maternal Death Due to Stroke Associated With Pregnancy-Induced Hypertension. *Circulation Journal* **79**, 1835–1840 (2015).

195. Gibbs, C. E. & Locke, W. E. Maternal deaths in Texas, 1969 to 1973. A report of 501 consecutive maternal deaths from the Texas Medical Association's Committee on Maternal Health. *Am J Obstet Gynecol* **126**, 687–92 (1976).

196. Judy, A. E. *et al.* Systolic Hypertension, Preeclampsia-Related Mortality, and Stroke in California. *Obstetrics & Gynecology* **133**, 1151–1159 (2019).

197. Hibbard, L. T. Maternal mortality due to acute toxemia. *Obstetrics and gynecology* **42**, 263–70 (1973).

198. Michinaga, S. & Koyama, Y. Pathogenesis of Brain Edema and Investigation into Anti-Edema Drugs. *Int J Mol Sci* **16**, 9949–9975 (2015).

199. Richards, A., Graham, D. & Bullock, R. Clinicopathological study of neurological complications due to hypertensive disorders of pregnancy. *J Neurol Neurosurg Psychiatry* **51**, 416–421 (1988).

200. Sonneveld, M. J. *et al.* Cerebral perfusion pressure in women with preeclampsia is elevated even after treatment of elevated blood pressure. *Acta Obstet Gynecol Scand* **93**, 508–511 (2014).

201. van Veen, T. R. *et al.* Cerebral Autoregulation in Normal Pregnancy and Preeclampsia. *Obstetrics & Gynecology* **122**, 1064–1069 (2013).

202. van Veen, T. R. *et al.* Cerebral autoregulation in different hypertensive disorders of pregnancy. *Am J Obstet Gynecol* **212**, 513.e1-513.e7 (2015).

203. Zatik, J. *et al.* Assessment of cerebral hemodynamics during roll over test in healthy pregnant women and those with pre-eclampsia. *BJOG* **108**, 353–358 (2001).

204. Bergman, L. *et al.* Evidence of Neuroinflammation and Blood–Brain Barrier Disruption in Women with Preeclampsia and Eclampsia. *Cells* **10**, 3045 (2021).

205. Johnson, A. C. *et al.* Inhibition of blood-brain barrier efflux transporters promotes seizure in pregnant rats: Role of circulating factors. *Brain Behav Immun* **67**, 13–23 (2018).

206. Spradley, F. T. Targeting inflammation to reduce seizure severity in an experimental model of eclampsia. *Hypertension Research* **43**, 350–353 (2020).

207. León, J. *et al.* Disruption of the Blood-Brain Barrier by Extracellular Vesicles From Preeclampsia Plasma and Hypoxic Placentae: Attenuation by Magnesium Sulfate. *Hypertension* **78**, 1423–1433 (2021).

208. Wang, K. *et al.* Association of Preeclampsia with Incident Dementia and Alzheimer's Disease among Women in the Framingham Offspring Study. *J Prev Alzheimers Dis* (2022) doi:10.14283/jpad.2022.62.

209. Basit, S., Wohlfahrt, J. & Boyd, H. A. Pre-eclampsia and risk of dementia later in life: nationwide cohort study. *BMJ* k4109 (2018) doi:10.1136/bmj.k4109.

210. Schliep, K. C. *et al.* Hypertensive disorders of pregnancy and subsequent risk of Alzheimer's disease and other dementias. *Alzheimer's & Dementia: Diagnosis, Assessment & Disease Monitoring* **15**, (2023).

211. Siepmann, T. *et al.* Long-term cerebral white and gray matter changes after preeclampsia. *Neurology* **88**, 1256–1264 (2017).

212. Aukes, A. *et al.* Long-term cerebral imaging after pre-eclampsia. *BJOG* **119**, 1117–1122 (2012).

213. Kitt, J., Frost, A. & Leeson, P. Preeclampsia and the Brain—A Long-term View. *JAMA Netw Open* **4**, e215364 (2021).

214. Bergman, L. *et al.* Cognitive impairment in preeclampsia complicated by eclampsia and pulmonary edema after delivery. *Acta Obstet Gynecol Scand* **100**, 1280–1287 (2021).

215. Fields, J. A. *et al.* Preeclampsia and cognitive impairment later in life. *Am J Obstet Gynecol* **217**, 74.e1-74.e11 (2017).

216. Mielke, M. M. *et al.* Impaired Cognition and Brain Atrophy Decades After Hypertensive Pregnancy Disorders. *Circ Cardiovasc Qual Outcomes* **9**, (2016).

217. Dayan, N., Kaur, A., Elharram, M., Rossi, A. M. & Pilote, L. Impact of Preeclampsia on Long-Term Cognitive Function. *Hypertension* **72**, 1374–1380 (2018).

218. Doyle, L. & Wang, M. Overview of Extracellular Vesicles, Their Origin, Composition, Purpose, and Methods for Exosome Isolation and Analysis. *Cells* **8**, 727 (2019).

219. Teng, F. & Fussenegger, M. Shedding Light on Extracellular Vesicle Biogenesis and Bioengineering. *Advanced Science* **8**, (2021).

220. Kalluri, R. & LeBleu, V. S. The biology **,** function **,** and biomedical applications of exosomes. *Science (1979)* **367**, (2020).

221. Sivanantham, A. & Jin, Y. Impact of Storage Conditions on EV Integrity/Surface Markers and Cargos. *Life* **12**, 697 (2022).

222. Gelibter, S. *et al.* The impact of storage on extracellular vesicles: A systematic study. *J Extracell Vesicles* **11**, (2022).

223. Doyle, L. & Wang, M. Overview of Extracellular Vesicles, Their Origin, Composition, Purpose, and Methods for Exosome Isolation and Analysis. *Cells* **8**, 727 (2019).

224. Caruso, S. & Poon, I. K. H. Apoptotic Cell-Derived Extracellular Vesicles: More Than Just Debris. *Front Immunol* **9**, (2018).

225. Battistelli, M. & Falcieri, E. Apoptotic Bodies: Particular Extracellular Vesicles Involved in Intercellular Communication. *Biology (Basel)* **9**, 21 (2020).

226. Shehzad, A., Islam, S. U., Shahzad, R., Khan, S. & Lee, Y. S. Extracellular vesicles in cancer diagnostics and therapeutics. *Pharmacol Ther* **223**, 107806 (2021).

227. Kalluri, R. & McAndrews, K. M. The role of extracellular vesicles in cancer. *Cell* **186**, 1610–1626 (2023).

228. Li, N. *et al.* Recent Advances of Using Exosomes as Diagnostic Markers and Targeting Carriers for Cardiovascular Disease. *Mol Pharm* **20**, 4354–4372 (2023).

229. Muthu, S., Bapat, A., Jain, R., Jeyaraman, N. & Jeyaraman, M. Exosomal therapy—a new frontier in regenerative medicine. *Stem Cell Investig* **8**, 7–7 (2021).

230. Sandfeld-Paulsen, B. *et al.* Exosomal proteins as prognostic biomarkers in non-small cell lung cancer. *Mol Oncol* **10**, 1595–1602 (2016).

231. Melo, S. A. *et al.* Glypican-1 identifies cancer exosomes and detects early pancreatic cancer. *Nature* **523**, 177–182 (2015).

232. Kupper, N. & Huppertz, B. The endogenous exposome of the pregnant mother: Placental extracellular vesicles and their effect on the maternal system. *Mol Aspects Med* **87**, 100955 (2022).

233. Hessvik, N. P. & Llorente, A. Current knowledge on exosome biogenesis and release. *Cellular and Molecular Life Sciences* **75**, 193–208 (2018).

234. Otegui, M. & Reyes, F. C. Endosomes in Plants. *Nature Education* (2010).

235. van Niel, G. *et al.* The Tetraspanin CD63 Regulates ESCRT-Independent and -Dependent Endosomal Sorting during Melanogenesis. *Dev Cell* **21**, 708–721 (2011).

236. Stuffers, S., Sem Wegner, C., Stenmark, H. & Brech, A. Multivesicular Endosome Biogenesis in the Absence of ESCRTs. *Traffic* **10**, 925–937 (2009).

237. Theos, A. C. *et al.* A Lumenal Domain-Dependent Pathway for Sorting to Intralumenal Vesicles of Multivesicular Endosomes Involved in Organelle Morphogenesis. *Dev Cell* **10**, 343–354 (2006).

238. Moreno-Gonzalo, O., Fernandez-Delgado, I. & Sanchez-Madrid, F. Post-translational add-ons mark the path in exosomal protein sorting. *Cellular and Molecular Life Sciences* **75**, 1–19 (2018).

239. Wei, H. *et al.* Regulation of exosome production and cargo sorting. *Int J Biol Sci* **17**, 163–177 (2021).

240. Termini, C. M. & Gillette, J. M. Tetraspanins Function as Regulators of Cellular Signaling. *Front Cell Dev Biol* **5**, (2017).

241. Zhang, J. *et al.* Exosome and Exosomal MicroRNA: Trafficking, Sorting, and Function. *Genomics Proteomics Bioinformatics* **13**, 17–24 (2015).

242. Goldie, B. J. *et al.* Activity-associated miRNA are packaged in Map1b-enriched exosomes released from depolarized neurons. *Nucleic Acids Res* **42**, 9195–9208 (2014).

243. Mincheva-Nilsson, L. & Baranov, V. The Role of Placental Exosomes in Reproduction. *American Journal of Reproductive Immunology* **63**, 520–533 (2010).

244. Burkova, E. E., Sedykh, S. E. & Nevinsky, G. A. Human Placenta Exosomes: Biogenesis, Isolation, Composition, and Prospects for Use in Diagnostics. *Int J Mol Sci* **22**, 2158 (2021).

245. Balasundaram, P. & Farhana, A. *Immunology at the Maternal-Fetal Interface*. (2023).

246. Bai, K. *et al.* Placenta-Derived Exosomes as a Modulator in Maternal Immune Tolerance During Pregnancy. *Front Immunol* **12**, (2021).

247. Suryawanshi, H. *et al.* A single-cell survey of the human first-trimester placenta and decidua. *Sci Adv* **4**, (2018).

248. ISHIDA, Y. *et al.* Maternal peripheral blood natural killer cells incorporate placenta-associated microRNAs during pregnancy. *Int J Mol Med* **35**, 1511–1524 (2015).

249. Nardi, F. da S. *et al.* High levels of circulating extracellular vesicles with altered expression and function during pregnancy. *Immunobiology* **221**, 753–760 (2016).

250. Bai, K. *et al.* Human placental exosomes induce maternal systemic immune tolerance by reprogramming circulating monocytes. *J Nanobiotechnology* **20**, 86 (2022).

251. Corthay, A. How do Regulatory T Cells Work? *Scand J Immunol* **70**, 326–336 (2009).

252. Powell, R. M. *et al.* Decidual T Cells Exhibit a Highly Differentiated Phenotype and Demonstrate Potential Fetal Specificity and a Strong Transcriptional Response to IFN. *The Journal of Immunology* **199**, 3406–3417 (2017).

253. Kahn, D. A. & Baltimore, D. Pregnancy induces a fetal antigen-specific maternal T regulatory cell response that contributes to tolerance. *Proceedings of the National Academy of Sciences* **107**, 9299–9304 (2010).

254. Rowe, J. H., Ertelt, J. M., Aguilera, M. N., Farrar, M. A. & Way, S. S. Foxp3+ Regulatory T Cell Expansion Required for Sustaining Pregnancy Compromises Host Defense against Prenatal Bacterial Pathogens. *Cell Host Microbe* **10**, 54–64 (2011).

255. Rowe, J. H., Ertelt, J. M., Xin, L. & Way, S. S. Pregnancy imprints regulatory memory that sustains anergy to fetal antigen. *Nature* **490**, 102–106 (2012).

256. Shi, L., Chen, S., Yang, L. & Li, Y. The role of PD-1 and PD-L1 in T-cell immune suppression in patients with hematological malignancies. *J Hematol Oncol* **6**, 74 (2013).

257. Gerosa, M., Schioppo, T. & Meroni, P. L. Challenges and treatment options for rheumatoid arthritis during pregnancy. *Expert Opin Pharmacother* **17**, 1539–1547 (2016).

258. Cronqvist, T. *et al.* Syncytiotrophoblast derived extracellular vesicles transfer functional placental miRNAs to primary human endothelial cells. *Sci Rep* **7**, 4558 (2017).

259. Salomon, C. *et al.* A Gestational Profile of Placental Exosomes in Maternal Plasma and Their Effects on Endothelial Cell Migration. *PLoS One* **9**, e98667 (2014).

260. Salomon, C. *et al.* Extravillous trophoblast cells-derived exosomes promote vascular smooth muscle cell migration. *Front Pharmacol* **5**, (2014).

261. Komaki, M. *et al.* Exosomes of human placenta-derived mesenchymal stem cells stimulate angiogenesis. *Stem Cell Res Ther* **8**, 219 (2017).

262. Salomon, C. *et al.* Placental Exosomes as Early Biomarker of Preeclampsia: Potential Role of Exosomal MicroRNAs Across Gestation. *J Clin Endocrinol Metab* **102**, 3182–3194 (2017).

263. Pillay, P., Maharaj, N., Moodley, J. & Mackraj, I. Placental exosomes and pre-eclampsia: Maternal circulating levels in normal pregnancies and, early and late onset pre-eclamptic pregnancies. *Placenta* **46**, 18–25 (2016).

264. Gill, M. *et al.* Placental Syncytiotrophoblast-Derived Extracellular Vesicles Carry Active NEP (Neprilysin) and Are Increased in Preeclampsia. *Hypertension* **73**, 1112–1119 (2019).

265. Goswami, D. *et al.* Excess syncytiotrophoblast microparticle shedding is a feature of early-onset pre-eclampsia, but not normotensive intrauterine growth restriction. *Placenta* **27**, 56–61 (2006).

266. Schuster, J., Cheng, S., Padbury, J. & Sharma, S. Placental extracellular vesicles and pre-eclampsia. *American Journal of Reproductive Immunology* **85**, (2021).

267. Tannetta, D. S., Dragovic, R. A., Gardiner, C., Redman, C. W. & Sargent, I. L. Characterisation of Syncytiotrophoblast Vesicles in Normal Pregnancy and Pre-Eclampsia: Expression of Flt-1 and Endoglin. *PLoS One* **8**, e56754 (2013).

268. Baig, S. *et al.* Lipidomic analysis of human placental Syncytiotrophoblast microvesicles in adverse pregnancy outcomes. *Placenta* **34**, 436–442 (2013).

269. Bisson, C. *et al.* Preeclampsia pathophysiology and adverse outcomes during pregnancy and postpartum. *Front Med (Lausanne)* **10**, (2023).

270. Li, H. *et al.* Differential Proteomic Analysis of Syncytiotrophoblast Extracellular Vesicles from Early-Onset Severe Preeclampsia, using 8-Plex iTRAQ Labeling Coupled with 2D Nano LC-MS/MS. *Cellular Physiology and Biochemistry* **36**, 1116–1130 (2015).

271. Lam, K. K. W. *et al.* Glycodelin-A Protein Interacts with Siglec-6 Protein to Suppress Trophoblast Invasiveness by Down-regulating Extracellular Signal-regulated Kinase (ERK)/c-Jun Signaling Pathway. *Journal of Biological Chemistry* **286**, 37118–37127 (2011).

272. Chang, X. *et al.* Exosomes From Women With Preeclampsia Induced Vascular Dysfunction by Delivering sFlt (Soluble Fms-Like Tyrosine Kinase)-1 and sEng (Soluble Endoglin) to Endothelial Cells. *Hypertension* **72**, 1381–1390 (2018).

273. Ermini, L. *et al.* A Single Sphingomyelin Species Promotes Exosomal Release of Endoglin into the Maternal Circulation in Preeclampsia. *Sci Rep* **7**, 12172 (2017).

274. Gebara, N., Correia, Y., Wang, K. & Bussolati, B. Angiogenic Properties of Placenta-Derived Extracellular Vesicles in Normal Pregnancy and in Preeclampsia. *Int J Mol Sci* **22**, 5402 (2021).

275. Motta-Mejia, C. *et al.* Placental Vesicles Carry Active Endothelial Nitric Oxide Synthase and Their Activity is Reduced in Preeclampsia. *Hypertension* **70**, 372–381 (2017).

276. Bavishi, C., Messerli, F. H., Kadosh, B., Ruilope, L. M. & Kario, K. Role of neprilysin inhibitor combinations in hypertension: insights from hypertension and heart failure trials. *Eur Heart J* **36**, 1967–1973 (2015).

277. Sahli, S. *et al.* A New Class of Inhibitors for the Metalloprotease Neprilysin Based on a Central Imidazole Scaffold. *Helv Chim Acta* **88**, 707–730 (2005).

278. Matsubara, K. The Potential for Exosomes in the Prevention and Treatment of Preeclampsia. *Hypertension Research in Pregnancy* **11**, HRP2023-002 (2023).

279. Gu, M. *et al.* Influence of placental exosomes from early onset preeclampsia women umbilical cord plasma on human umbilical vein endothelial cells. *Front Cardiovasc Med* **9**, (2022).

280. VanWijk, M. J. *et al.* Isolated microparticles, but not whole plasma, from women with preeclampsia impair endothelium-dependent relaxation in isolated myometrial arteries from healthy pregnant women. *Am J Obstet Gynecol* **187**, 1686–1693 (2002).

281. Gupta, A., Smith, P., Bournazos, S. & Ravetch, J. V. A novel mouse strain optimized for chronic human antibody administration. *Proceedings of the National Academy of Sciences* **119**, (2022).

282. Germain, S. J., Sacks, G. P., Soorana, S. R., Sargent, I. L. & Redman, C. W. Systemic Inflammatory Priming in Normal Pregnancy and Preeclampsia: The Role of Circulating Syncytiotrophoblast Microparticles. *The Journal of Immunology* **178**, 5949–5956 (2007).

283. Heidarzadeh, M. *et al.* Exosomal delivery of therapeutic modulators through the blood–brain barrier; promise and pitfalls. *Cell Biosci* **11**, 142 (2021).

284. Banks, W. A. *et al.* Transport of Extracellular Vesicles across the Blood-Brain Barrier: Brain Pharmacokinetics and Effects of Inflammation. *Int J Mol Sci* **21**, 4407 (2020).

285. Morad, G. *et al.* Cdc42-Dependent Transfer of mir301 from Breast Cancer-Derived Extracellular Vesicles Regulates the Matrix Modulating Ability of Astrocytes at the Blood–Brain Barrier. *Int J Mol Sci* **21**, 3851 (2020).

286. Abdelsalam, M., Ahmed, M., Osaid, Z., Hamoudi, R. & Harati, R. Insights into Exosome Transport through the Blood–Brain Barrier and the Potential Therapeutical Applications in Brain Diseases. *Pharmaceuticals* **16**, 571 (2023).

287. Zhou, F. *et al.* Small Extracellular Vesicles in Milk Cross the Blood-Brain Barrier in Murine Cerebral Cortex Endothelial Cells and Promote Dendritic Complexity in the Hippocampus and Brain Function in C57BL/6J Mice. *Front Nutr* **9**, (2022).

288. Li, C. *et al.* Overcoming the blood-brain barrier: Exosomes as theranostic nanocarriers for precision neuroimaging. *Journal of Controlled Release* **349**, 902–916 (2022).

289. Ramos-Zaldívar, H. M. *et al.* Extracellular vesicles through the blood–brain barrier: a review. *Fluids Barriers CNS* **19**, 60 (2022).

290. Banks, W. A. *et al.* Transport of Extracellular Vesicles across the Blood-Brain Barrier: Brain Pharmacokinetics and Effects of Inflammation. *Int J Mol Sci* **21**, 4407 (2020).

291. Hornung, S., Dutta, S. & Bitan, G. CNS-Derived Blood Exosomes as a Promising Source of Biomarkers: Opportunities and Challenges. *Front Mol Neurosci* **13**, (2020).

292. Shi, M. *et al.* CNS tau efflux via exosomes is likely increased in Parkinson's disease but not in Alzheimer's disease. *Alzheimer's & Dementia* **12**, 1125–1131 (2016).

293. Shi, M. *et al.* Plasma exosomal α-synuclein is likely CNS-derived and increased in Parkinson's disease. *Acta Neuropathol* **128**, 639–650 (2014).

294. Chen, C. C. *et al.* Elucidation of Exosome Migration Across the Blood–Brain Barrier Model In Vitro. *Cell Mol Bioeng* **9**, 509–529 (2016).

295. Banks, W. A., Niehoff, M. L., Ponzio, N. M., Erickson, M. A. & Zalcman, S. S. Pharmacokinetics and modeling of immune cell trafficking: quantifying differential influences of target tissues versus lymphocytes in SJL and lipopolysaccharide-treated mice. *J Neuroinflammation* **9**, 714 (2012).

296. Hervé, F., Ghinea, N. & Scherrmann, J.-M. CNS Delivery Via Adsorptive Transcytosis. *AAPS J* **10**, 455–472 (2008).

297. Vorbrodt, A. W. & Trowbridge, R. S. Ultrastructural study of transcellular transport of native and cationized albumin in cultured sheep brain microvascular endothelium. *J Neurocytol* **20**, 998–1006 (1991).

298. Kay, R. R. Macropinocytosis: Biology and mechanisms. *Cells & Development* **168**, 203713 (2021).

299. Kaksonen, M. & Roux, A. Mechanisms of clathrin-mediated endocytosis. *Nat Rev Mol Cell Biol* **19**, 313–326 (2018).

300. Godlee, C. & Kaksonen, M. From uncertain beginnings: Initiation mechanisms of clathrin-mediated endocytosis. *Journal of Cell Biology* **203**, 717–725 (2013).

301. Matsumoto, J. *et al.* Transmission of α-synuclein-containing erythrocyte-derived extracellular vesicles across the blood-brain barrier via adsorptive mediated transcytosis: another mechanism for initiation and progression of Parkinson's disease? *Acta Neuropathol Commun* **5**, 71 (2017).

302. Chan, B. D. *et al.* Exosomes in Inflammation and Inflammatory Disease. *Proteomics* **19**, (2019).

303. Rempe, R. G., Hartz, A. M. & Bauer, B. Matrix metalloproteinases in the brain and blood–brain barrier: Versatile breakers and makers. *Journal of Cerebral Blood Flow & Metabolism* **36**, 1481–1507 (2016).

304. Chan, B. D. *et al.* Exosomes in Inflammation and Inflammatory Disease. *Proteomics* **19**, (2019).

305. Selmaj, I., Mycko, M. P., Raine, C. S. & Selmaj, K. W. The role of exosomes in CNS inflammation and their involvement in multiple sclerosis. *J Neuroimmunol* **306**, 1–10 (2017).

306. Begum, G. *et al.* Selective knockout of astrocytic Na^+/H^+ exchanger isoform 1 reduces astrogliosis, BBB damage, infarction, and improves neurological function after ischemic stroke. *Glia* **66**, 126–144 (2018).

307. Mathew, B., Mansuri, M. S., Williams, K. R. & Nairn, A. C. Exosomes as Emerging Biomarker Tools in Neurodegenerative and Neuropsychiatric Disorders—A Proteomics Perspective. *Brain Sci* **11**, 258 (2021).

308. Perets, N. *et al.* Golden Exosomes Selectively Target Brain Pathologies in Neurodegenerative and Neurodevelopmental Disorders. *Nano Lett* **19**, 3422–3431 (2019).

309. Tucureanu, M. M. *et al.* Lipopolysaccharide-induced inflammation in monocytes/macrophages is blocked by liposomal delivery of G_i-protein inhibitor. *Int J Nanomedicine* **Volume 13**, 63–76 (2017).

310. Zhang, N. *et al.* Role of Exosomes in Brain Diseases. *Front Cell Neurosci* **15**, (2021).

311. Si, Q., Wu, L., Pang, D. & Jiang, P. Exosomes in brain diseases: Pathogenesis and therapeutic targets. *MedComm (Beijing)* **4**, (2023).

312. Morales-Prieto, D. M. *et al.* Small Extracellular Vesicles from Peripheral Blood of Aged Mice Pass the Blood-Brain Barrier and Induce Glial Cell Activation. *Cells* **11**, 625 (2022).

313. Nguyen, S. L. *et al.* Integrins mediate placental extracellular vesicle trafficking to lung and liver in vivo. *Sci Rep* **11**, 4217 (2021).

314. Tong, M. *et al.* Placental Nano-vesicles Target to Specific Organs and Modulate Vascular Tone In Vivo. *Human Reproduction* **32**, 2188–2198 (2017).

315. Clark, K. *et al.* Placental Mesenchymal Stem Cell-Derived Extracellular Vesicles Promote Myelin Regeneration in an Animal Model of Multiple Sclerosis. *Cells* **8**, 1497 (2019).

316. Barzegar, M. *et al.* Human placental mesenchymal stem cells improve stroke outcomes via extracellular vesicles-mediated preservation of cerebral blood flow. *EBioMedicine* **63**, 103161 (2021).

317. Zhang, Y., Zhong, Y., Zou, L. & Liu, X. Significance of Placental Mesenchymal Stem Cell in Placenta Development and Implications for Preeclampsia. *Front Pharmacol* **13**, (2022).

318. Salomon, C. *et al.* Exosomal Signaling during Hypoxia Mediates Microvascular Endothelial Cell Migration and Vasculogenesis. *PLoS One* **8**, e68451 (2013).

319. Tafti, D., Ehsan, M. & Xixis, K. L. *Multiple Sclerosis*. (2023).

320. Vigh, J. P. *et al.* Transendothelial Electrical Resistance Measurement across the Blood–Brain Barrier: A Critical Review of Methods. *Micromachines (Basel)* **12**, 685 (2021).

321. Srinivasan, B. *et al.* TEER Measurement Techniques for In Vitro Barrier Model Systems. *SLAS Technol* **20**, 107–126 (2015).

322. ThermoFisher Scientific. Transmission Electron Microscopy vs Scanning Electron Microscopy. *Materials Science Learning Center*.

323. University of Warwick - Department of Physics. Transmission Electron Microscopy (TEM). *University of Warwick - Department of Physics* (2010).

324. Koritzinsky, E. H., Street, J. M., Star, R. A. & Yuen, P. S. T. Quantification of Exosomes. *J Cell Physiol* **232**, 1587–1590 (2017).

325. Akers, J. C. *et al.* Comparative Analysis of Technologies for Quantifying Extracellular Vesicles (EVs) in Clinical Cerebrospinal Fluids (CSF). *PLoS One* **11**, e0149866 (2016).

326. Théry, C., Amigorena, S., Raposo, G. & Clayton, A. Isolation and Characterization of Exosomes from Cell Culture Supernatants and Biological Fluids. *Curr Protoc Cell Biol* **30**, (2006).

327. Introduction to Nanoparticle Tracking Analysis (NTA) - Measurement Principle of ZetaView®. *Particle Metrix GmbH*.

328. Kurian, T. K., Banik, S., Gopal, D., Chakrabarti, S. & Mazumder, N. Elucidating Methods for Isolation and Quantification of Exosomes: A Review. *Mol Biotechnol* **63**, 249–266 (2021).

329. Filipe, V., Hawe, A. & Jiskoot, W. Critical Evaluation of Nanoparticle Tracking Analysis (NTA) by NanoSight for the Measurement of Nanoparticles and Protein Aggregates. *Pharm Res* **27**, 796–810 (2010).

330. Lai, J. J. *et al.* Exosome Processing and Characterization Approaches for Research and Technology Development. *Advanced Science* **9**, (2022).

331. Serrano-Pertierra, E. *et al.* Extracellular Vesicles: Current Analytical Techniques for Detection and Quantification. *Biomolecules* **10**, 824 (2020).

332. Boyd, R. D., Pichaimuthu, S. K. & Cuenat, A. New approach to inter-technique comparisons for nanoparticle size measurements; using atomic force microscopy, nanoparticle tracking analysis and dynamic light scattering. *Colloids Surf A Physicochem Eng Asp* **387**, 35–42 (2011).

333. Hoo, C. M., Starostin, N., West, P. & Mecartney, M. L. A comparison of atomic force microscopy (AFM) and dynamic light scattering (DLS) methods to characterize nanoparticle size distributions. *Journal of Nanoparticle Research* **10**, 89–96 (2008).

334. Thermo Fisher Scientific. Extracellular Vesicle Detection with Flow Cytometry.

335. Gao, J. *et al.* Recent developments in isolating methods for exosomes. *Front Bioeng Biotechnol* **10**, (2023).

336. Sidhom, K., Obi, P. O. & Saleem, A. A Review of Exosomal Isolation Methods: Is Size Exclusion Chromatography the Best Option? *Int J Mol Sci* **21**, 6466 (2020).

337. Jiang, S. *et al.* ExoCounter Assays Identify Women Who May Develop Early-Onset Preeclampsia From 12.5 µL First-Trimester Serum by Characterizing Placental Small Extracellular Vesicles. *Hypertension* **80**, 1439–1451 (2023).

338. Kabe, Y. *et al.* Development of a Highly Sensitive Device for Counting the Number of Disease-Specific Exosomes in Human Sera. *Clin Chem* **64**, 1463–1473 (2018).

339. Maia et al. Population Analysis of Extracellular Vesicles in Microvolumes of Biofluids. *bioRxiv* (2020).

340. Yokoi, A. *et al.* Mechanisms of nuclear content loading to exosomes. *Sci Adv* **5**, (2019).

341. Sunderland, C. A., Davies, J. O. & Stirrat, G. M. Immunohistology of normal and ovarian cancer tissue with a monoclonal antibody to placental alkaline phosphatase. *Cancer Res* **44**, 4496–502 (1984).

342. Alkaline phosphatase, placental. *The Human Protein Atlas*.

343. Aldridge, G. M., Podrebarac, D. M., Greenough, W. T. & Weiler, I. J. The use of total protein stains as loading controls: An alternative to high-abundance single-protein controls in semi-quantitative immunoblotting. *J Neurosci Methods* **172**, 250–254 (2008).

344. Ferguson, R. E. *et al.* Housekeeping proteins: A preliminary study illustrating some limitations as useful references in protein expression studies. *Proteomics* **5**, 566–571 (2005).

345. Moritz, C. P. Tubulin or Not Tubulin: Heading Toward Total Protein Staining as Loading Control in Western Blots. *Proteomics* **17**, 1600189 (2017).

346. Thacker, J. S., Yeung, D. H., Staines, W. R. & Mielke, J. G. Total protein or high-abundance protein: Which offers the best loading control for Western blotting? *Anal Biochem* **496**, 76–78 (2016).

347. Fosang, A. J. & Colbran, R. J. Transparency Is the Key to Quality. *Journal of Biological Chemistry* **290**, 29692–29694 (2015).

348. Pillai-Kastoori, L., Schutz-Geschwender, A. R. & Harford, J. A. A systematic approach to quantitative Western blot analysis. *Anal Biochem* **593**, 113608 (2020).

349. Schilde, L. M. *et al.* Protein variability in cerebrospinal fluid and its possible implications for neurological protein biomarker research. *PLoS One* **13**, e0206478 (2018).

350. Hsieh, E., Hsiao, C. & Liu, J. Statistical methods for evaluating the linearity in assay validation. *J Chemom* **23**, 56–63 (2009).

351. *International Conference on HarmonizationTripartite Guideline Q2A: Test on Validation of Analytical Procedures*. (1995).

352. Xu, L. *et al.* Blood cell-derived extracellular vesicles: diagnostic biomarkers and smart delivery systems. *Bioengineered* **12**, 7929–7940 (2021).

353. Brennan, K. *et al.* A comparison of methods for the isolation and separation of extracellular vesicles from protein and lipid particles in human serum. *Sci Rep* **10**, 1039 (2020).

354. Body mass index (BMI). *NHS Inform* (2023).

355. Akokuwebe, M. E. & Idemudia, E. S. Prevalence and Socio-Demographic Correlates of Body Weight Categories Among South African Women of Reproductive Age: A Cross-Sectional Study. *Front Public Health* **9**, (2021).

356. The Editors of Encyclopaedia Britannica. Coloured. *Britannica* (2023).

357. Luo, Z.-C. *et al.* The effects and mechanisms of primiparity on the risk of pre-eclampsia: a systematic review. *Paediatr Perinat Epidemiol* **21**, 36–45 (2007).

358. *WHO recommendations for Prevention and treatment of pre-eclampsia and eclampsia*. (2011).

359. Klee, G. G. Human Anti-Mouse Antibodies. *Arch Pathol Lab Med* **124**, 921–923 (2000).

360. Šolcová, M., Trefil, L., Rajdl, D., Potočová, I. & Racek, J. False positive result of human chorionic gonadotropin caused by human anti-mouse antibodies. *Biochem Med (Zagreb)* **33**, 82–86 (2023).

361. Campos Munoz, A., Jain, N. K. & Gupta, M. *Albumin Colloid*. (2023).

362. Gojnic, M. *et al.* Plasma albumin level as an indicator of severity of preeclampsia. *Clin Exp Obstet Gynecol* **31**, 209–10 (2004).

363. Chen, H., Tao, F., Fang, X. & Wang, X. Association of hypoproteinemia in preeclampsia with maternal and perinatal outcomes: A retrospective analysis of high-risk women. *Journal of Research in Medical Sciences* **21**, 98 (2016).

364. Motulsky, H. J. & Brown, R. E. Detecting outliers when fitting data with nonlinear regression – a new method based on robust nonlinear regression and the false discovery rate. *BMC Bioinformatics* **7**, 123 (2006).

365. GraphPad by Dotmatics. Comparing the Grubbs' and ROUT method of identifying outliers. *GraphPad Knowledgebase*.

366. GraphPad. How it works: ROUT method. *GraphPad Statistics Guide*.

367. Li, Z. *et al.* Quantification of placental extracellular vesicles in different pregnancy status via single particle analysis method. *Clinica Chimica Acta* **539**, 266–273 (2023).

368. Menon, R. *et al.* Protein Profile Changes in Circulating Placental Extracellular Vesicles in Term and Preterm Births: A Longitudinal Study. *Endocrinology* **161**, (2020).

369. Sarker, S. *et al.* Placenta-derived exosomes continuously increase in maternal circulation over the first trimester of pregnancy. *J Transl Med* **12**, 204 (2014).

370. Dragovic, R. A., Southcombe, J. H., Tannetta, D. S., Redman, C. W. G. & Sargent, I. L. Multicolor Flow Cytometry and Nanoparticle Tracking Analysis of Extracellular Vesicles in the Plasma of Normal Pregnant and Pre-eclamptic Women1. *Biol Reprod* **89**, (2013).

371. Pillay, P., Moodley, K., Moodley, J. & Mackraj, I. Placenta-derived exosomes: potential biomarkers of preeclampsia. *Int J Nanomedicine* **Volume 12**, 8009–8023 (2017).

372. Street, J. M. *et al.* Identification and proteomic profiling of exosomes in human cerebrospinal fluid. *J Transl Med* **10**, 5 (2012).

373. Akers, J. C. *et al.* Optimizing preservation of extracellular vesicular miRNAs derived from clinical cerebrospinal fluid. *Cancer Biomarkers* **17**, 125–132 (2016).

374. Krušić Alić, V. *et al.* Extracellular Vesicles from Human Cerebrospinal Fluid Are Effectively Separated by Sepharose CL-6B—Comparison of Four Gravity-Flow Size Exclusion Chromatography Methods. *Biomedicines* **10**, 785 (2022).

375. Erickson, M. A., Wilson, M. L. & Banks, W. A. In vitro modeling of blood–brain barrier and interface functions in neuroimmune communication. *Fluids Barriers CNS* **17**, 26 (2020).

376. Williams-Medina, A., Deblock, M. & Janigro, D. In vitro Models of the Blood–Brain Barrier: Tools in Translational Medicine. *Front Med Technol* **2**, (2021).

377. Kang, M., Blenkiron, C. & Chamley, L. W. The biodistribution of placental and fetal extracellular vesicles during pregnancy following placentation. *Clin Sci* **137**, 385–399 (2023).

378. National Cancer Institute. Classification & Structure of Blood Vessels. *SEER Training Modules*.

379. Calzia, E., Iványi, Z. & Radermacher, P. Determinants of Blood Flow and Organ Perfusion. in *Functional Hemodynamic Monitoring* 19–32 (Springer-Verlag). doi:10.1007/3-540-26900-2_3.